NEW MEXICO INSTITUTE OF MINING AND TECHNOLOGY

A PRELIMINARY INVESTIGATION OF THE DISSOLUTION KINETICS OF STRONTIANITE AND WITHERITE

by

John L. Sonderegger, II

In Partial Fulfillment of the Requirements
for the Degree of Doctor of Philosophy
in Geoscience

May, 1974

TABLE OF CONTENTS

LIST OF FIGURES AND TABLES

ABSTRACT

A preliminary investigation of the dissolution kinetics of strontianite and witherite in aqueous solutions indicates that dissolution rates are controlled by reactions at mineral surface. Dissolution rates were not effected by changes in stirring rates; activation energies calculated for strontianite and witherite are 8.4 and 10.0 kilocalories, respectively.

At pH values of less than 4.0, the dissolution rate for strontianite is a linear function of pH; the dissolution reaction is interpreted to be first order with respect to a_{H^+} and to consist of the protonation of the CO_3^{2-} lattice anion and desorption as HCO_3^-. Experiments with different partial pressures of CO_2 indicate that H_2CO_3 has a catalytic effectiveness approximately 1% of that of the hydrogen ion. The effect of P_{CO_2} is interpreted to be dependent upon surface adsorption and is expressed using the Langmuir adsorption isotherm.

Forward reaction rates determined far from equilibrium are used to calculate back reaction rates. These data are consistent with a controlling mechanism which is first order with respect to Sr^{2+} or HCO_3^-. The rate limiting step is interpreted to be the adsorption or deprotonation of HCO_3^-.

LIST OF SYMBOLS

a - a constant

a_i - activity of the i^{th} species

$\overset{o}{a}_i$ - effective ion diameter of the i^{th} species

α - an empirical coefficient

A - coefficient or species

A_k - the k^{th} negatively charged species in solution

b - a constant

β - an empirical exponent

B - coefficient or species

C_i - concentration of the i^{th} species

$\in i$ - the i^{th} positively charged species in solution

δ - thickness of the diffusion layer

δ_p - thickness of the product diffusion layer

δ_r - thickness of the reactant diffusion layer

$+\delta$ - a positive charge

$-\delta$ - a negative charge

D_i - diffusion coefficient of the i^{th} species

E_a - activation energy

f_T - a temperature dependent function

F - a species

g_T - a temperature dependent function

G - a species

$G_{H_2CO_3}$ - structure factor for carbonic acid

h_T - a temperature dependent function

i - integer index for chemical species

I - stoichiometric ionic strength

$\bar{I}$ - true ionic strength

j - integer index for reactant species

k_1 - a rate constant

k_2 - a rate constant

k - a constant or rate constant

k_f - a forward rate constant

k_b - a backward rate constant

K - equilibrium constant

l - integer index for product species

m_i - molality of the $i^{\underline{th}}$ species

M_{H_2O} - mass of water

n_i - number of moles of the $i^{\underline{th}}$ species

N_i - mole fraction of the $i^{\underline{th}}$ gas species

θ - fraction of the surface area covered by an adsorbed gas

P_i - partial pressure of the $i^{\underline{th}}$ gas species

P_{tot} - total gas pressure

R - the gas constant

$\underline{R}$ - the overal (observed) reaction rate

$\underline{R}_f$ - the forward reaction rate

$\underline{R}_b$ - the backward reaction rate

$\underline{R}_T$ - the overall reaction rate

$\underline{R}_T'$ - the net overall reaction rate - a function of P_{CO_2}

R_i - reaction order of the $i^{\underline{th}}$ species

R_o - overall reaction order

s - subscript to denote saturation value

S - surface area

t - time, or subscript to denote value at time = t

T - absolute temperature

$\bar{v}_i$ - velocity coefficient of the $i^{\underline{th}}$ species

ν_i - stoichiometric coefficient of the $i^{\underline{th}}$ species

V - volume

ACKNOWLEDGEMENTS

I would like to thank the members of my committee, Dr.s Vernon G. LeFebre, Richard E. Beane, and Kay R. Brower, for their continued interest in this research and for their stimulating questions. Dr. Brower's laboratory expertise greatly aided in achieving the goals of this research.

Laboratory space was kindly provided by Dr.s G. W. Gross and D. D. Rabinowitz.

Support for the laboratory investigation was provided by the Geoscience Department through a Research Assistantship.

Finally, I would like to thank my wife Brenda for her patience throughout my academic wanderings.

INTRODUCTION

Geochemists have been interested in the history of the elements and the paths they take in the "rock cycle" for many years (Rankama and Sahama, 1950). The growth of computer technology has facilitated this type of research (cf. Horn and Adams, 1966) and the interest in such models is evidenced by the texts of Garrels and Mackenzie (1971) and Berner (1971). At present, the models available (Helgeson, 1968; Helgeson, Garrels and Mackenzie, 1969) have outstripped available kinetic data and time is treated in arbitrary units of reaction progress. Many investigators are now involved with quantitatively describing the kinetic parameters which effect mineral dissolution and precipitation (Lagache, 1965; Wollast, 1967; Campbell and Nancollas, 1969; Luce, 1969; Bovington and Jones, 1970a, 1970b; Little and Nancollas, 1970; Bailey and Reesman, 1971; Liu and Nancollas, 1971; Sayles and Fyfe, 1973). Recent work on carbonate precipitation and dissolution (Gaines and Heffner, 1973; Mitterer and Carter, 1973; Walls, 1973; Berner and Morse, 1974; Plummer and Mackenzie, 1974) has been largely restricted to studies of calcium and magnesium carbonates.

Strontianite and witherite are not common sedimentary minerals, but their occurrence is believed to control the strontium and barium concentration of ground waters in Missouri (Carpenter and Miller, 1969). This preliminary investigation was undertaken to determine the dissolution

kinetics of these minerals so that the minerals might be included in models relating to the change of ground water composition with time. Constant and variable volume batch reactors were used to study thermodynamically open systems subjected to a constant gas flow. The dissolution of these minerals was studied at temperatures of 30, 40, and 50° C in order to determine their activation energies. Strontianite dissolution was investigated at varying pH and partial pressure of carbon dioxide conditions to determine their effect upon carbonate mineral dissolution. The experimental rate data provide information about activation energies, the extent of acid catalysis, mineral solubility products, and the rate limiting step.

REVIEW OF PRINCIPLES

Introduction

Kinetics is the branch of chemistry concerned with systems whose chemical compositions change as a function of time. The approach to a kinetic investigation is initially empirical, with the goal of describing mathematically the effect of conditions of state, namely temperature and pressure, and composition upon the rate of reaction. A mathematical representation, commonly termed the rate law, may suggest a molecular interpretation of the rate controlling process. At present there are no general models, rules, or laws which are applicable to all reactions (Benson, 1960; Gardiner, 1969; and Levenspiel, 1972). Consequently, generalizations about conditions not actually investigated are unreliable since the relative contributions of concurrent processes may differ in the regions not investigated (Gardiner, 1969).

Components, Phases, and Systems

Many chemistry texts have developed the concept of chemical equilibrium as the result of equal but opposing reaction rates, and have based the law of mass action on a theory of reaction kinetics. However, the only valid approach to derive the equilibrium relationship for a reaction is based upon thermodynamics or statistical mechanics (Frost, 1941). Because the thermodynamic definition of equilibrium

is used in this paper, the necessary conditions to define the system must be considered.

The number of components in a system may be defined as (Findlay, 1951):

> "the smallest number of independently variable constituents by means of which the composition of each phase participating in the state of equilibrium can be expressed in the form of a chemical equation."

A phase may be defined as a physically distinct and mechanically separable portion of the system of interest (Findlay, 1951).

A system is the part of the objective world which is the subject of thermodynamic study (Lewis and Randall, 1923). Three types of systems are generally recognized and are isolated, closed, and open. An isolated system may not exchange energy or matter with regions outside the system boundaries. A closed system may exchange energy but not matter with regions outside the system boundaries. An open system may exchange both energy and matter with regions outside the system boundaries. Homogeneous systems consist of only one phase, while heterogeneous systems consist of two or more phases.

Activities and Activity Coefficients

The activity of the $i^{\underline{th}}$ species, a_i, is defined as

$$a_i = \frac{f_i}{f_i^o} \tag{1}$$

where f_i is the fugacity of the $i^{\underline{th}}$ species and f_i^o is the

standard or reference state fugacity of the $i^{\underline{th}}$ species (Klotz, 1964). By definition, the activities of pure liquids and solids at the reference conditions have a value of unity. The activity of an ideal gas, a_i, is defined as

$$a_i = N_i P_{tot} / 1 \text{ atm.} \qquad (2)$$

where N_i is the mole fraction of the $i^{\underline{th}}$ gas in a gas mixture, and P_{tot} is the total gas pressure in atmospheres (Garrels and Christ, 1965). For most gases in the pressure range from zero to one atmosphere, the deviation from the Ideal Gas Law is very small and activity, fugacity, and partial pressure are almost equal (Denbigh, 1966).

The activity of aqueous species is based upon a reference state of one mole of that species at infinite dilution (Klotz, 1964). This hypothetical reference state results from a linear extrapolation of the Henry's Law behavior of the species from the very dilute region to a one molal concentration. The correction for the non-ideal behavior of the aqueous species is accomplished by the use of an individual molal activity of coefficient, γ_i, such that

$$a_i = \gamma_i m_i \qquad (3)$$

where a_i is the activity of the $i^{\underline{th}}$ species and m_i is the true molality of the $i^{\underline{th}}$ species.

This study utilized the extended Debye-Hückel equation which was modified by the addition of an empirical term to account for short range interactions between the ions and the solvent (Robinson and Stokes, 1965) and has the form

$$\log \gamma_i = \frac{-A(z_i)^2(\bar{I})^{\frac{1}{2}}}{1 + \overset{o}{a}_i B(\bar{I})^{\frac{1}{2}}} + bI \qquad (4)$$

where A and B are the Debye-Huckel parameters, $\overset{o}{a}_i$ is the effective diameter of the $i^{\underline{th}}$ species, z_i is the charge of the $i^{\underline{th}}$ species, b is an adjustable parameter for fitting experimental data, and $\bar{I}$ is the true ionic strength (Helgeson, 1969) defined as

$$\bar{I} = \tfrac{1}{2} \sum_i m_i (z_i)^2 \qquad (5)$$

for all species in solution. A value of 0.2 was used in equation (4) for b which is the same value used by Liu and Nancollas [1971 (Liu, 1972, personal comm.)].

For neutral complexes and dissolved gases, the activity coefficient can be approximated by the relationship

$$\log \gamma_i = k_{i,s} I \qquad (6)$$

where $k_{i,s}$ is the salting coefficient for the $i^{\underline{th}}$ species in the $s^{\underline{th}}$ supporting electrolyte solution (Garrels and Christ, 1965) and I is the stoichiometric ionic strength which may be defined as

$$I = \tfrac{1}{2} \sum_i C_i (z_i)^2 \qquad (7)$$

where C_i is the number of moles of the $i^{\underline{th}}$ species per kilogram of solvent. The stoichiometric ionic strength is calculated by assuming the absence of ion pairs (cation-anion complexes).

Partial Equilibrium

Partial equilibrium describes a system which is in equilibrium with respect to at least one process and is out of equilibrium with respect to at least one process (Barton,

Bethke, and Toulmin, 1963). Garrels (1959) noted that reactions among dissolved species are generally quite rapid relative to reactions between dissolved and solid species. Consequently, for irreversible geochemical reactions such as mineral dissolution, partial equilibrium has commonly been assumed to consist of equilibrium within the aqueous phase and between the aqueous phase and the solid product phases, combined with heterogeneous disequilibrium between the aqueous phase and reacting solid phases. This assumption of partial equilibrium has been used with success by several investigators (Helgeson, 1968; Helgeson, Garrels and Mackenzie, 1969; Brown, 1970; Helgeson, 1971) to model the dissolution of various silicate minerals.

Nomenclature

For a reaction such as

$$aA + bB = fF + gG \tag{8}$$

the reaction rate, $\underline{R}$, is traditionally defined as

$$\underline{R} = \frac{dC_A}{-adt} = \frac{dC_B}{-bdt} = \frac{dC_F}{fdt} = \frac{dC_G}{gdt} \tag{9}$$

where C_A, C_B, C_F, and C_G are the concentrations of the subscripted species, -a, -b, f, and g are the stoichiometric coefficients, and t is time (Benson, 1960). The stoichiometric coefficients of the $i^{\underline{th}}$ species, ν_i, is the number of moles of species $\underline{i}$ in the equation as written and is negative for reactants and positive for products.

The rate limiting step of a reaction may be controlled

by only some of the species involved in the overall reaction. The molecularity, or number of molecules, of a particular species involved in the rate limiting step may sometimes be determined by expressing the reaction rate as

$$\underline{R} = \frac{dC_A}{-adt} = k(C_A)^{\alpha}(C_B)^{\beta}(C_F)^{\gamma}(C_G)^{\delta} \qquad (10)$$

where k is an empirical rate constant and α, β, γ, and δ are empirically determined values, usually integers, which represent the molecularity of the species A, B, F, and G in the rate limiting step. The reaction order for the overall reaction is defined (Benson, 1960) as the sum of the exponents in equation (10) for all species which are found to effect the reaction rate. Thus, for the reaction expressed by equation (8), assuming that all species are kinetically active, the overall reaction order, R_o, is expressed by

$$R_o = \alpha + \beta + \gamma + \delta \qquad (11)$$

In homogeneous systems, the overall reaction order is rarely greater than two.

The overall reaction order should not be confused with the individual reaction order, R_i, with respect to the $\underline{i^{th}}$ species, which is the empirical exponent for the concentration of that species (Benson, 1960) as expressed in equation (10). Thus, the reaction order with respect to A is α and with respect to F is γ.

Types of Reaction Vessels

The three basic types of reaction vessels commonly employed in kinetic studies are the batch reactor, the

tubular or "plug-flow" reactor, and the backmix reactor (Levenspiel, 1972). A batch reactor contains the reaction products, and measurements are made of the concentration of one or more constituents as a function of time. Batch reactors may be divided into the subclasses of constant volume or variable volume reactors, both of which were used in this study. The reaction rate for constant volume batch reactors may be expressed as

$$\underline{R} = dC_i / {}_i dt \tag{12}$$

where $\underline{R}_i$ is the reaction rate with respect to the $i^{\underline{th}}$ species, C_i is the concentration of the $i^{\underline{th}}$ constituent, ${}_i$ is the stoichiometric coefficient of the $i^{\underline{th}}$ species, and t is time (Levenspiel, 1972).

The reaction rate for a variable volume batch reactor must include a term to compensate for the volume change and may be expressed as

$$\underline{R}_i = \frac{dC_i}{\nu_i dt} + \left(\frac{C_i}{V} \frac{dV}{\nu_i dt}\right) \tag{13}$$

where V is the reactor volume and the other terms are as described above (Levenspiel, 1972).

Molecular Equilibrium

The Gibbs free energy of a solid-aqueous system with fixed temperature and pressure is, by definition, a minimum value at equilibrium. If the system is not perturbed in any manner, the activities of all species remain constant; however, the individual atoms composing the species are free

to transfer from one species to another provided that an equal number of atoms of the same element transfer in the opposite direction at the same rate. The molecular or microscopic view of equilibrium is that for any equation the rates for the forward and reverse directions of the reaction are identical

The Principle of Mass Action

Between 1864 and 1879, Guldberg and Waage published a series of papers dealing with reaction kinetics and equilibrium conditions. Their principle or "law" of mass action, a generalization drawn from experimental results, is that the forward and reverse reaction rates are respectively proportional to the concentrations of the reactant and product species each raised to the power of the coefficient for that species in the chemical equation. The principle of mass action may be written

$$\underline{R} = k_f \prod_j (a_j)^{-\nu_j} - k_b \prod_l (a_l)^{\nu_l} \qquad (14)$$

where k_f is the forward rate constant, a_j is the activity of the $j^{\underline{th}}$ reactant species, ν_j is the stoichiometric coefficient of the $j^{\underline{th}}$ species, k_b is the backward rate constant, a_l is the activity of the $l^{\underline{th}}$ product species, and ν_l is the stoichiometric coefficient of the $l^{\underline{th}}$ product species (Anderson and Boyd, 1971). At equilibrium, the forward reaction rate must be equal to the backward reaction rate,

$$k_f \prod_j (a_j)^{-\nu_j} = k_b \prod_1 (a_1)^{\nu_1} \qquad (15)$$

For the equilibrium condition, rearrangement of equation (15) yields

$$\prod_1 (a_1)^{\nu_1} / \prod_j (a_j)^{-\nu_j} = k_f/k_b = K \qquad (16)$$

where K is the thermodynamic equilibrium constant.

Rate Laws for Mineral Dissolution

The dissolution rate of a mineral in an aqueous solution may be expressed in terms of the rate of change of the concentrations of species involved in the reaction. Usually the species measured is in the aqueous phase and is derived from the mineral. The general case for the congruent dissolution of a mineral, N_aX_b, dissolving in water may be represented as

$$N_aX_b = aN^{z_N} + bX^{z_X} \qquad (17)$$

where N^{z_N} and X^{z_X} are ions in solution having the respective charges of z_N and z_X. The dissolution rate, $\underline{R}$, may then be expressed as

$$\underline{R} = dm_N{}^{z_N}/adt = k(m_N{}^{z_N}{}_s - m_N{}^{z_N}{}_t)^n \qquad (18)$$

where k is the reaction rate constant, $m_N{}^{z_N}{}_s$ is the molality of N^{z_N} at saturation, $m_N{}^{z_N}{}_t$ is the molality of N^{z_N} at time t, and n is an empirical constant.

For reactions such as dissolution reactions occurring at a phase boundary, the reaction rate may be controlled by either the diffusion of reactants and products to and from the phase boundary or by the reaction occurring at the interface (Benson, 1960). Diffusion controlled reactions are usually explained by the Nernst theory which may be expressed, for one dimensional transport, as

$$\frac{dn_i}{dt} = \bar{v}_i \frac{dn_i}{dx} \tag{19}$$

in which n_i is the number of molecules of the $i^{\underline{th}}$ species in solution, dn_i/dx is the concentration gradient, and $\bar{v}_i$ is the individual ion velocity expressed as

$$\bar{v}_i = dx/dt = D_i S/V \tag{20}$$

where D_i is the temperature dependent individual ion diffusion coefficient, S is the surface area, and V is the solution volume (Moelwyn-Hughes, 1947). The concentration gradient may be rewritten as

$$dn_i/dx = (n_{i_s} - n_{i_t})/\delta \tag{21}$$

where n_{i_s} is the number of moles of the $i^{\underline{th}}$ species at saturation, n_{i_t} is the number of moles of the $i^{\underline{th}}$ species in solution at time t, and δ is the thickness of the diffusion layer (Berner, 1971).

In geochemical literature, molality is a common basis for expressing the concentration of a species in solution.

The molality of the $i^{\underline{th}}$ species, m_i, may be expressed as

$$m_i = k'n_i/V \tag{22}$$

where k' is the temperature dependent constant for converting pure water volume to mass.

First Order Reactions

For first order reactions, the empirical constant, n, is equal to unity and equation (18) reduces to

$$dm_i/\nu_i dt = k(m_{i_s} - m_{i_t}) \tag{23}$$

where m_{i_s} is the molality of the $i^{\underline{th}}$ species at saturation, m_{i_t} is the molality of the $i^{\underline{th}}$ species at time t, and k is the rate constant described by

$$k = k'D_iS/\delta \tag{24}$$

Equation (23) is the molal rate law for the diffusion controlled reactions according to the Nernst theory and is a simple first order rate law. The assumptions involved in the formulation of the theory are (Moelwyn-Hughes, 1947; Plummer, 1972):

1) The chemical reaction at the mineral surface occurs very rapidly and creates a saturated layer of the product species at the interface.
2) The chemical composition of the aqueous phase beyond the diffusion layer is uniform and is called the "bulk solution".

3) The concentration gradients of product and reactant species are linear and restricted to thin layers. For product species, the effective diffusion layer thickness, δ_p, is simply equal to the perpendicular distance between the saturated layer and the "bulk solution". Reactant species have an effective diffusion layer thickness, δ_r, equal to the sum of the saturated layer and the product diffusion layer.

4) The thickness of the diffusion layer is a function of the rate of stirring and the geometry of the system.

Because the reaction rate should vary as a function of the stirring rate, a qualitative test for diffusion control of first order reactions consists of comparing the reaction rates of stirred and unstirred experiments. If the reaction rate is not effected by stirring, then the reaction must be chemically controlled.

If equation (23) is rearranged and integrated, it yields

$$(1/\nu_i) \log (m_{i_s} - m_{i_t}) = kt + C \qquad (25)$$

where t is the time since the experiment started and C is the integration constant. If the $i^{\underline{th}}$ species is absent at t = 0 then C must equal the logarithm of molality of the $i^{\underline{th}}$ species at saturation. The molality of the $i^{\underline{th}}$ species at saturation may be determined analytically from experiments

which approach equilibrium from both undersaturated and supersaturated conditions, or by calculating the equilibrium composition of the aqueous phase. Plotting log ($m_{i_s} - m_{i_t}$) against time, t, yields a straight line for a first order reactions and the rate constant, k, is the slope of this straight line.

Reactions Other Than First Order

For reactions which are not first order with respect to the species considered, equation (18) may be used to represent the experimental data if the value of the exponential term, n, is determined empirically. The value of n may be determined by graphical analysis if equation (18) is rewritten as

$$\log (dm_N{}^{z_N}/adt) = n \log [k(m_N{}^{z_N}{}_s - m_N{}^{z_N}{}_t)] \qquad (26)$$

where n is defined by the slope of a straight line connecting the data points when plotted as log ($dm_N{}^{z_N}/adt$) versus log ($m_N{}^{z_N}{}_s - m_N{}^{z_N}{}_t$) (Benson, 1960; Plummer, 1972).

Other Common Empirical Rate Laws

The rate of mineral reactions with an aqueous phase can often be expressed by the general kinetic relationship

$$dm_i/dt = k_i t^{\omega} \qquad (27)$$

where m_i is the molality of the $i^{\underline{th}}$ species, t is time in arbitrary units, k_i is the rate constant for the change in molality of the $i^{\underline{th}}$ species, and ω is an empirical exponent

(Helgeson, 1971). For the dissolution of various silicate minerals, the values $\omega = 0$, $-\frac{1}{2}$, and -1 provide satisfactory agreement with the experimental data (Helgeson, 1971). The rate laws for $\omega = 0$, $-\frac{1}{2}$, and -1 are linear, parabolic, and logarithmic and may be tested by plotting the molality of the species of interest against t, $t^{\frac{1}{2}}$, and $\log t$, respectively.

The affinity model, developed by Prigogine, Outer, and Herbo (1948) for gas reactions in the vicinity of equilibrium, has been successfully applied to dissolution reactions of some carbonate minerals (Sonderegger, in prep.). The model is empirical in nature and may only be applied close to equilibrium where the reaction rate is directly proportional to the Gibbs free energy of the dissolution reaction. Under this restriction, the affinity model may be used to predict the equilibrium state from the dissolution rate data (cf. Prigogine, 1967).

The Langmuir Adsorption Isotherm

Gas phase reactions catalyzed by elementary reactions occurring at an interface, such as the walls of a reaction vessel, are frequently found to have reaction rates which vary with the surface area of the vessel. Investigations of gas adsorption at solid surfaces has led to the recognition of several basic types of adsorption-pressure relationships. The mathematical relationship between the amount of a gas adsorbed by the solid phase of interest and the gas pressure

at constant temperature is called an adsorption isotherm. In cases where chemisorption occurs at the interface, the Langmuir adsorption isotherm is generally the best equation for representing the experimental data (Maron and Prutton, 1958). Figure 1 schematically represents the relationship between gas pressure and the amount of gas adsorbed at the surface for a Type I isotherm. Chemisorption reactions appear to be restricted to this type of isotherm (Maron and Prutton, 1958).

The Langmuir adsorption isotherm equation may be expressed as

$$\theta = bP/(1 + bP) \qquad (28)$$

where θ is the fraction of the experimental surface covered by adsorbed gas, b is an empirical constant, and P is the partial pressure of the gas (Maron and Prutton, 1958). The amount of gas adsorbed per unit area or per unit mass of absorbent, y, should be proportional to the fraction of the surface covered and may be represented as

$$y = k_1 \theta = k_1 bP/(1 + bP) = aP/(1 + bP) \qquad (29)$$

where k_1 is the proportionality constant and $a = k_1 b$ (Maron and Prutton, 1958). Rearrangement of equation (29) yields:

$$P/y = (1/a) + (b/a)P \qquad (30)$$

If the reaction of interest is compatible with the Langmuir adsorption isotherm, a plot of P/y versus P should yield a straight line with slope of b/a and an intercept of 1/a.

Figure 1. Diagram depicting the relationship be-
the amount of gas adsorbed on a solid surface versus
the pressure of the gas. This is a type I adsorption
isotherm and is usually related to a chemical reaction
creating an activated species.

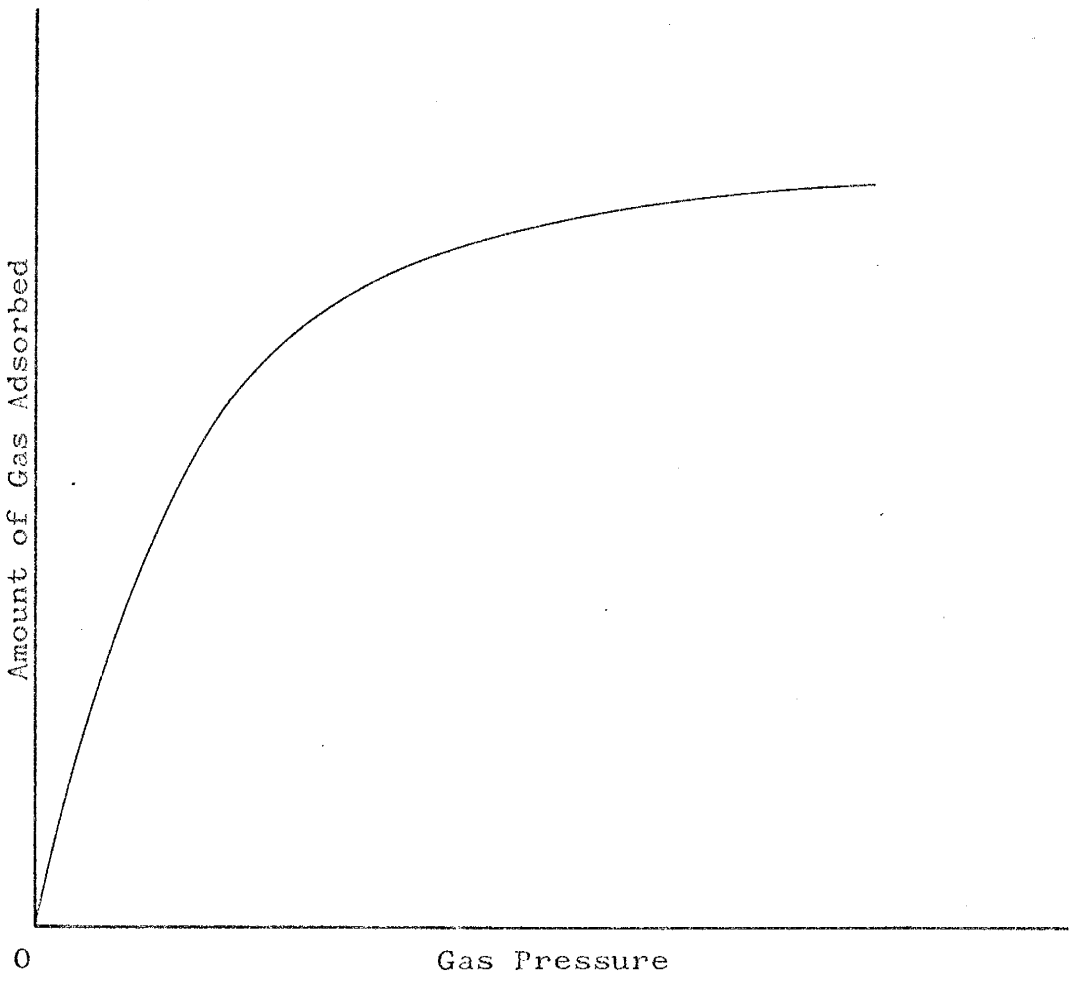
Amount of Gas Adsorbed
0
Gas Pressure

If variables such as total pressure, temperature, and pH are held constant, the change in the dissolution rate of the mineral in question may be related to the changing partial pressures of the gases in the gaseous phase. An assumption that the reaction rate is related to the fraction of the mineral surface which has adsorbed the gas phase permits the application of the Langmuir adsorption isotherm to dissolution kinetics. This assumption, a simplified approximation of the actual processes occurring at the mineral surface, allows an initial investigation of the role of specific gases on mineral dissolution. Such studies are of particular interest when the gas involved hydrates to form a weak (associated) acid, such as carbonic acid, which may catalyze the mineral dissolution reaction.

Activation Energies

For experimental data within a limited temperature range, the activation energy of a reaction may be calculated from the Arrhenius equation:

$$k_T = Ae^{(-E_a/RT)} \qquad (31)$$

where A is an empirical pre-exponential factor, E_a is the activation energy, R is the gas constant, T is the temperature in degrees Kelvin, and k_T is the temperature dependent reaction rate constant (Gardiner, 1969).

For first order dissolution reactions which may be expressed as

$$dm_i / \nu_i dt = k_T m_{i_t} \quad (23')$$

the relationship between the rate constant, k_T, and the time to half saturation, $t_{\frac{1}{2}}$, is (Benson, 1960; Plummer, 1972)

$$k_T = \ln (2)/t_{\frac{1}{2}} \quad (32)$$

If equation (31) is rewritten in the form

$$\ln (k_T) = \ln (A) - (E_a/RT) \quad (33)$$

it is clear that a plot of $\ln (k_T)$ versus $1/T$ should yield a straight line with a slope of $-E_a/R$ and an intercept of $\ln (A)$ if the Arrhenius equation is applicable to the experimental data.

Activation energies provide another method of testing whether or not a dissolution reaction is diffusion controlled. The activation energy of a diffusion controlled dissolution reaction should be 4.5 kilocalories (Liu and Nancollas, 1971). Reactions having considerably larger activation energies must be controlled by some mechanism other than diffusion of the aqueous species between the bulk solution and the mineral surface.

Comparison of Graphical Data

The previous sections have briefly discussed the use of various graphic techniques. The primary purpose of these plots is screening the experimental data to determine which rate laws are most applicable.

Kinetic rate laws are based upon assumed mechanisms and the mathematical expression of these laws requires the use of small integers or ratios of small integers as the exponential factors (Benson, 1960). Consequently, the use of a high order polynomial series to regress the experimental data defeats the goal of determining a satisfactory mechanism to explain the kinetic behavior of a reaction. Instead, a general preliminary practice is to plot the logarithm of the reaction rate against the logarithm of the expression for the mechanism being tested (cf. Levenspiel, 1972). When plotted in this manner, if the experimental data approximates a straight line, the slope of the straight line defines the molecularity of the hypothetical mechanism. The next step in a data analysis is to plot the reaction rate versus the expression raised to the power of its molecularity. If this second plot yields a linear relationship, the experimental data are compatible with the proposed mechanism.

EXPERIMENTAL PROCEDURES

Introduction

The experimental apparatus and methods employed in a kinetic investigation should be designed so that all experimental parameters can be conveniently varied by the investigator. This chapter describes the apparatus and methods used in the investigation of strontianite, $SrCO_3$, and witherite, $BaCO_3$, dissolution as a function of temperature at approximately a 0.8 atmosphere partial pressure of carbon dioxide gas, P_{CO_2}. Strontianite dissolution was also investigated at different P_{CO_2} values, and as a function of pH under an N_2 atmosphere in an attempt to evaluate the effect of P_{CO_2} and pH upon the dissolution kinetics.

Sample Preparation

The samples of strontianite from the Westphalia mining district, Germany, and witherite from the Settingstones Mine, Northumberland, England, were obtained from Ward's Natural Science Establishment. Both samples were reportedly from vein deposits and were processed in the following manner:

1) All gangue minerals and a portion of the outside of the vein were removed using a hammer and chisel.
2) The sample was broken into approximately half inch pieces with a hammer.
3) The sample was crushed in a tool steel piston

style sample crusher.

4) The sample was spread on white paper and impurities, mainly galena, sphalerite, and iron hydroxide coatings, were removed by hand.

5) The sample was seived using brass 30 mesh and nylon 100 and 200 mesh screens.

6) The -30 +100 mesh and -100 +200 mesh fractions were visually re-examined to remove impurities using a high intensity lamp and a biology pick.

7) The samples from step 6) were washed first with 0.1 N reagent grade hydrochloric acid, then with four rinses of distilled water followed by drying in a vacuum.

8) The samples were split using a small vibrating sample splitter and sealed in glassine paper packets for storage prior to use.

Reaction Vessel Design

The reaction vessel used is cylindrical in shape and was constructed from Lucite. The base is permanently attached and sealed while the top is removable and has a natural gum rubber gasket. The inside diameter is 11.3 centimeters and the height is 15.3 centimeters. A liter of water occupies about 2/3 of the available volume. The sample was added to the aqueous phase using a glass funnel inserted through a hole in the top of the reaction vessel.

Stirring was provided by an ovoid Teflon coated

magnetic spin bar within the vessel which was placed upon a variable-speed magnetic stirring unit. The ovoid shape was used to minimize grinding of the sample.

Commercially prepared nitrogen and carbon dioxide gases with purities of greater than 99% were used in this study. The gas or gas mixture was introduced into the aqueous phases through a vertical glass tube which has a sintered glass plug at the bottom. Such "bubbling tubes" greatly aid in rapidly saturating the fluid phase with the gas phase because an increased interphase contact area results from the large number of small gas bubbles produced by passage of the gas through the sintered glass. The gases were passed into a one liter Erlenmeyer flask containing 900 milliliters of water for presaturation of the gas phase with water vapor prior to introduction into the reaction vessel.

Gas mixtures of CO_2 and N_2 were provided by the use of capillary tubes and Erlenmeyer flasks (see figure 2). The capillary tubes were calibrated by the volume of water which the particular gas displaced per unit time under a fixed tank pressure. Both gases were then passed into a large Erlenmeyer flask for mixing and then introduced into the reaction vessel as discussed previously.

The heat source for the experiments consisted of a 100 watt standard frosted glass light bulb for 30° C and a 150 watt infrared bulb for 40 and 50° C. A thermistor probe extended into the aqueous phase from the top of the reaction vessel and was calibrated with an alcohol thermometer having

Figure 2. Schematic diagram of the system for delivering the gas phase to the reaction vessel: A = gas tanks; B = small flask; C = capillary tube; D = mixing flask; E = saturation flask; F = reaction vessel.

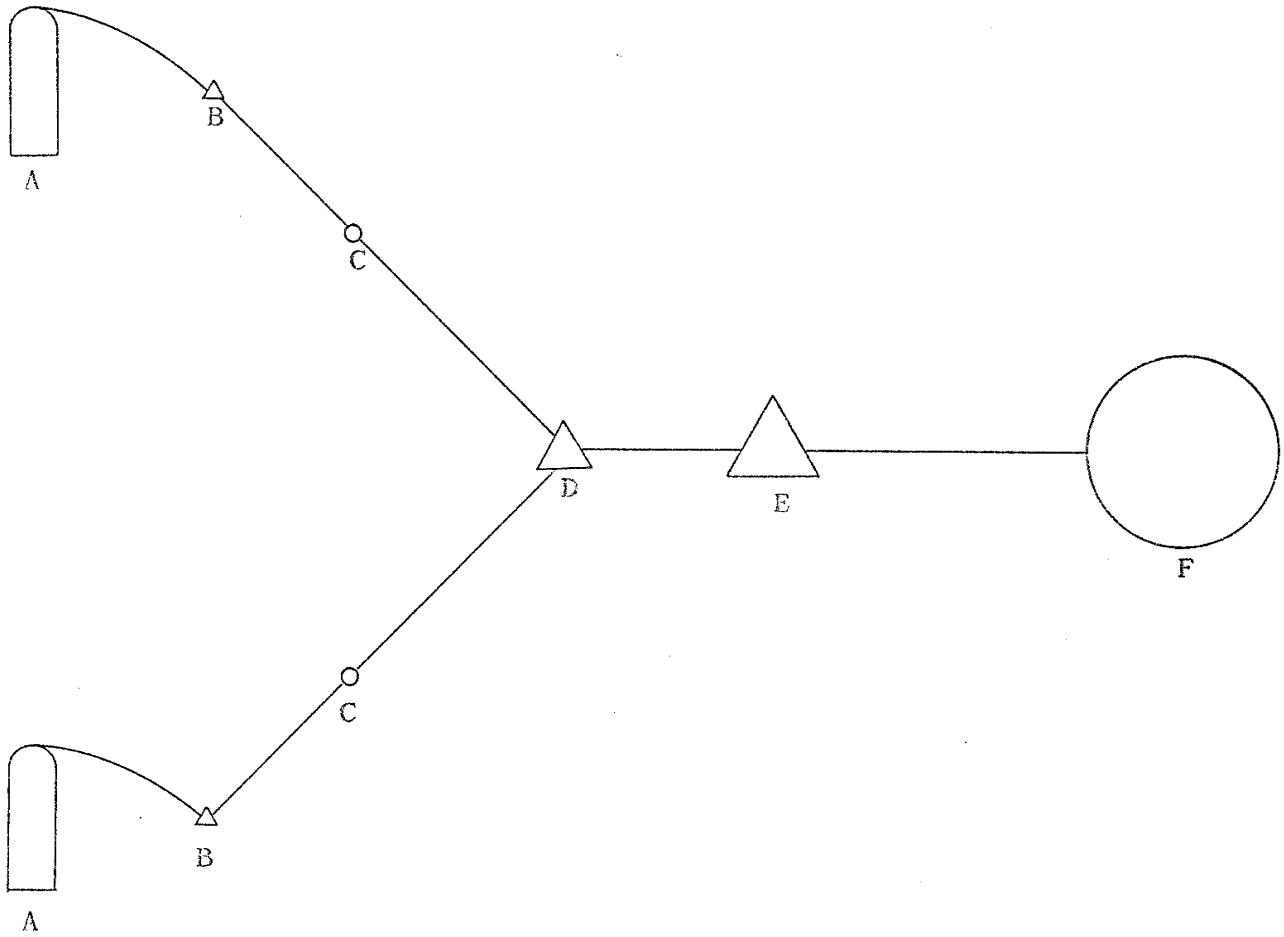
A
B
C
D
E
F
C
B
A

0.2 degree divisions which was inserted in the same manner.

Instrumentation

Two variables, pH and resistance, were monitored to determine the reaction progress. The pH was measured with a Beckman model 39013 combination electrode and a Corning model 12 pH meter. Buffers with pH values of 4.015 and 6.995 at 30° C were used to calibrate the pH meter and electrode. Instrumental drift during an experiment generally was less than ±0.02 pH units as determined using buffer solutions before and after an experimental run; however, a confidence limit of ±0.05 pH units is used to compensate for any additional errors which might have existed during the experiments.

Resistivity was measured with a conductivity cell, cell constant = 0.9828, and a Heathkit impedance bridge. Both the electrode and the conductivity cell were inserted into the reaction vessel through holes in the top of the cell with bored rubber stoppers to hold them in place.

Time Measurements

A large centrally located wall clock with a second hand was used to monitor the time.

Data Smoothing

Data smoothing was required to provide pH values for times between measurements. The data were smoothed by hand

with a flexible curve to prevent bias of the data in the direction of a kinetic model paralleling the mathematical expression of a curve fitting equation.

Calculation of Partial Pressures

In experimental systems the gas phase being bubbled through the reaction vessel must be saturated with the solvent to prevent loss of the solvent to the gas phase. At pressures of one atmosphere or less the fugacity coefficients of most gases are very close to unity and the fugacity of the i^{th} gas, f_i, may be expressed by the ideal gas law

$$f_i = N_i P_{tot} = P_i \qquad (34)$$

Where N_i is the mole fraction of the i^{th} gas in the gas mixture, P_{tot} is the total pressure, and P_i is the partial pressure of the i^{th} gas (Denbigh, 1966). When considering a system with a fixed overpressure, an aqueous phase, and one gas being bubbled through the aqueous phase, the partial pressure of the gas being bubbled through the reaction vessel may be expressed as

$$P_i = P_{tot} - P_{H_2O} \qquad (35)$$

where P_{H_2O} is the vapor pressure of water at the temperature of interest (Maron and Prutton, 1958). Equations (34) and (35) were used in calculating the partial pressure of carbon dioxide in this study.

The vapor pressures of water at 30, 40, and 50° C are 0.0419, 0.0728, and 0.135 atmospheres, respectively.

The average barometric pressure in Socorro, New Mexico, where the experiments were conducted, is approximately 650 millimeters of mercury or 0.855 atmospheres. With a total pressure of 0.855 atmospheres, the calculated carbon dioxide partial pressures at 30, 40, and 50° C were 0.813, 0.782, and 0.720 atmospheres respectively. However, the vessel into which the gas was first bubbled to saturate it with water vapor was at the ambient room temperature which ranged from 28 to 31° C. The effective P_{CO_2} for experiments run at 40 and 50° C must have ranged between 0.78 and 0.81 atmospheres and 0.72 and 0.81 atmospheres, respectively. Comparison of the calculated total strontium content with the strontium concentration determined by atomic absorption indicates that using either P_{CO_2} value results in a calculated strontium content which is within the region of analytical error. The saturation values for $m_{Sr^{2+}}$ were determined from affinity plots, so corrections of $m_{Sr^{2+}}$ for differing P_{CO_2} values would also shift these saturation values. Consequently, the data employed are internally consistent, with only the K_{sp} value possibly being in error by more than two or three percent. A value of $P_{CO_2} = 0.81$ was used for the calculations at 30, 40, and 50° C.

Calculation of Species' Concentrations

The activities and molalities of all species in solution were calculated using the method outlined by Garrels and Christ (1965, p. 76-83) with the aid of a computer

program, CATCALC, written for the dissolution of carbonate minerals under a fixed partial pressure of carbon dioxide (see Appendix A). The measured variable, pH, and the constraint of electrical neutrality permit an iterative solution of a series of simultaneous equations despite the fact that carbon dioxide is not conserved in the system of interest.

The equations necessary for these calculations are:

$$K_w = a_{H^+} a_{OH^-} \tag{36}$$

$$K_0 = a_{H_2CO_3}/P_{CO_2} \tag{37}$$

$$K_1 = (a_{H^+} a_{HCO_3^-})/a_{H_2CO_3} \tag{38}$$

$$K_2 = (a_{H^+} a_{CO_3^{2-}})/a_{HCO_3^-} \tag{39}$$

$$K_\beta = (a_{Me^{2+}} a_{HCO_3^-})/a_{MeHCO_3^+} \tag{40}$$

$$K_\gamma = (a_{Me^{2+}} a_{CO_3^{2-}})/a_{MeCO_3^o} \tag{41}$$

and

$$\sum_i \in_i z_i = \sum_k A_k z_k \tag{42}$$

where Me is the alkaline earth of interest, $\in_i$ is the $i^{\underline{th}}$ positively charged aqueous species, and A_k is the $k^{\underline{th}}$ negatively charged aqueous species. This results in a system of seven equations and nine variables of which the two independent variables, pH and P_{CO_2}, are known.

The only assumptions employed in the calculations, that equilibrium is maintained by all gaseous and aqueous species and that activities of unity are assigned to the

solid phase and water, have been shown to contribute negligible error (Helgeson, 1967). The sequence of steps employed in the calculation are:

1) Calculate the activities of H_2CO_3, HCO_3^-, CO_3^{2-}, and OH^-.
2) Assume all activity coefficients are unity.
3) Determine the molalities of the negative species and H^+.
4) Sum of the molalities of the negative species times their charge.
5) Sum of anion equivalents minus hydrogen ion molality equals sum of cation equivalents.
6) Compute the ratio of Me^{2+} to $MeHCO_3^+$.
7) Assign molalities to Me^{2+} and $MeHCO_3^o$.
8) Calculate activity and molality of $MeCO_3^o$.
9) Compute ionic strength and activity coefficients of all species.
10) Return to step 3) and repeat the calculations.

Calculation of Reaction Rate

The systems investigated were maintained at a fixed partial pressure of carbon dioxide. Consequently, the concentrations of carbonate species depended upon contributions to or withdrawals from the gas phase as well as the quantity resulting from carbonate mineral dissolution. Similarly, the pH was internally controlled by the carbon dioxide partial pressure (cf. Garrels and Christ, 1965, Capt. 3, cases 1 and 4),

or externally controlled by acid titration. The only component which was conserved in the aqueous phase was the respective alkaline earth oxide, SrO or BaO. The reaction rate, as used in this study is defined as

$$\underline{R} = dm_{Me}{}^{2+}/dt \qquad (43)$$

where Me^{2+} is either Sr^{2+} or Ba^{2+} depending uon the mineral being dissolved.

EXPERIMENTAL RESULTS

Introduction

The experimental data for the dissolution of strontinite and witherite may be divided into three subgroups:

1) The effect of pH on strontianite dissolution at 40° C with continuous removal of carbon dioxide by a stream of nitrogen.
2) The effect of various partial pressures of carbon dioxide on strontianite dissolution at 40° C and pH = 4.5.
3) The dissolution of strontianite and witherite at 30, 40, and 50° C with a fixed carbon dioxide partial pressure of 0.81.

By holding all variables except pH or P_{CO_2} constant, the effect of pH and P_{CO_2} upon strontianite dissolution can be determined. The laboratory dissolution of strontianite and witherite under a fixed partial pressure of carbon dioxide approximates geologic conditions where connection with the soil atmosphere is maintained or where a high P_{CO_2} is maintained by connection with a gas reservoir. An example of a high P_{CO_2} reservoir is the Madera Limestone aquifer in the Ladron Mountains, New Mexico (Titus, 1974, personal comm.). The results of this study include the determination of activation energies and solubility products for strontianite and witherite dissolution and an interpretation of the mechanism which limits their dissolution rate.

The Effect of pH

The rate of strontianite dissolution was investigated under a nitrogen atmosphere at pH values of 1.5, 2.5, 3.5, 4.5, 5.5, and 6.5. In order to maintain approximately the same degree of undersaturation for each of the experiments, nitrogen gas was bubbled through the system to remove the carbonic acid resulting from strontianite dissolution. Each experiment was run for one hour and the acid consumption for the period from 20 to 40 minutes was used to calculate the rate of acid addition at the experimental pH. The reaction rate was expressed by the number of moles of HCl added per minute to maintain the predetermined pH. The reaction rate varied over three orders of magnitude while the hydrogen ion activity was varied over five orders of magnitude as shown in figure 3.

To compare these results with the results of the temperature dependent strontianite dissolution, the reaction rate must be expressed in terms of $(dm_{Sr^{2+}}/dt)$. These strontianite dissolution reactions were conducted by titrating hydrochloric acid into the system to maintain the desired pH and carbon dioxide was removed by the stream of nitrogen gas. Therefore, the reaction may be written as

$$SrCO_3 + 2\ H^+ = Sr^{2+} + CO_{2(g)} + H_2O \qquad (44)$$

and the reaction rate, $\underline{R}$ is

Figure 3. Plot of the logarithm of the number of moles of hydrochloric acid added per minute to maintain the desired pH for strontianite dissolution. For pH values of 1.5, 2.5, and 3.5, the data are linear. At higher pH values, the change in the rate of acid addition is much less. Nitrogen gas was continuously bubbled through the reaction vessel.

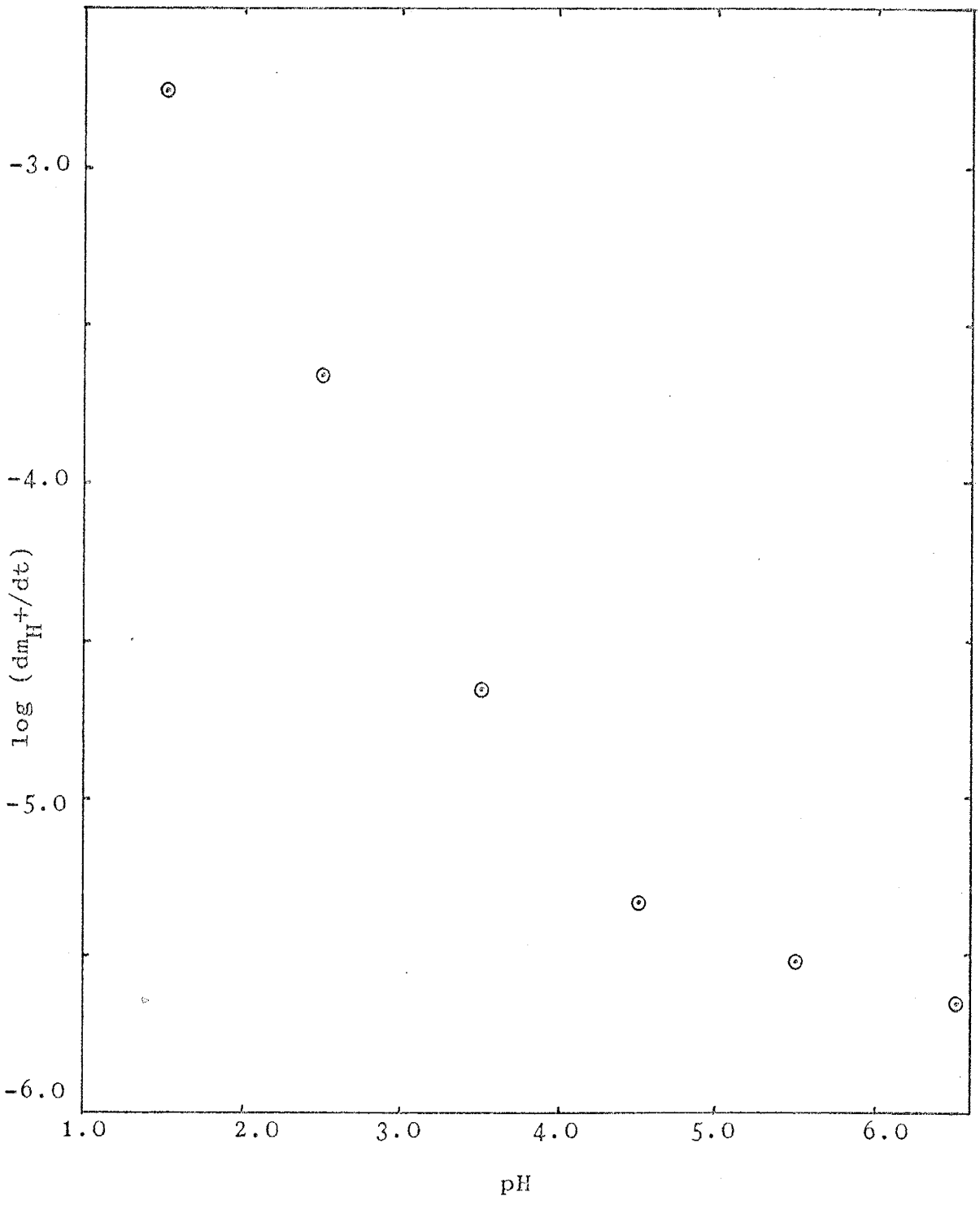
-3.0
-4.0
-5.0
-6.0
log (dm_{H^+}/dt)
1.0
2.0
3.0
4.0
5.0
6.0
pH

$$\underline{R} = (dm_{Sr}2+/dt) = \tfrac{1}{2}(dm_{H}+/dt) \qquad (45)$$

Figure 4 is a plot of the calculated log $\underline{R}$ versus pH for strontianite dissolution at 40° C under a continuously renewed N_2 atmosphere. The hydrogen ion activity decreases away from the origin, a common convention for presenting pH dependent data in the geologic literature. The data suggest that two separate contributions to the dissolution rate exist. Under low pH conditions, the dissolution rate appears to be controlled by a process which is approximately first order with respect to hydrogen ion activity because the slope of a line connecting the first three data points is approximately minus one (-0.92). At higher pH conditions, pH greater than 4.0, some other condition becomes the rate limiting factor. This second concurrent mechanism does not appear to be independent of pH, but has a small empirical exponential coefficient which is shown by the slope of a line connecting the data points at pH's of 5.5 and 6.5. The data may be represented by an equation of the form

$$\underline{R} = k_1(a_{H}+)^{0.92} + k_2(a_{H}+)^{0.13} \qquad (46)$$

where $k_1 = 2.05 \times 10^{-2}$ and $k_2 = 8.65 \times 10^{-6}$ and the exponents come from the slopes of the straight lines in figure 4. However, the last term may only be applicable to pH values up to 6.5.

While the nature of the second term in equation (46) has not been determined, two regions characterized by different rate limiting mechanisms have been shown to exist.

Figure 4. Plot of the logarithm of the reaction rate versus pH for strontianite dissolution. The reaction rate was calculated using equation (45). The slope for the low pH region is -0.92. This may be interpreted as the rate controlling step being first order with respect to a_{H^+}. Carbonate species were removed by a continuous stream of nitrogen gas.

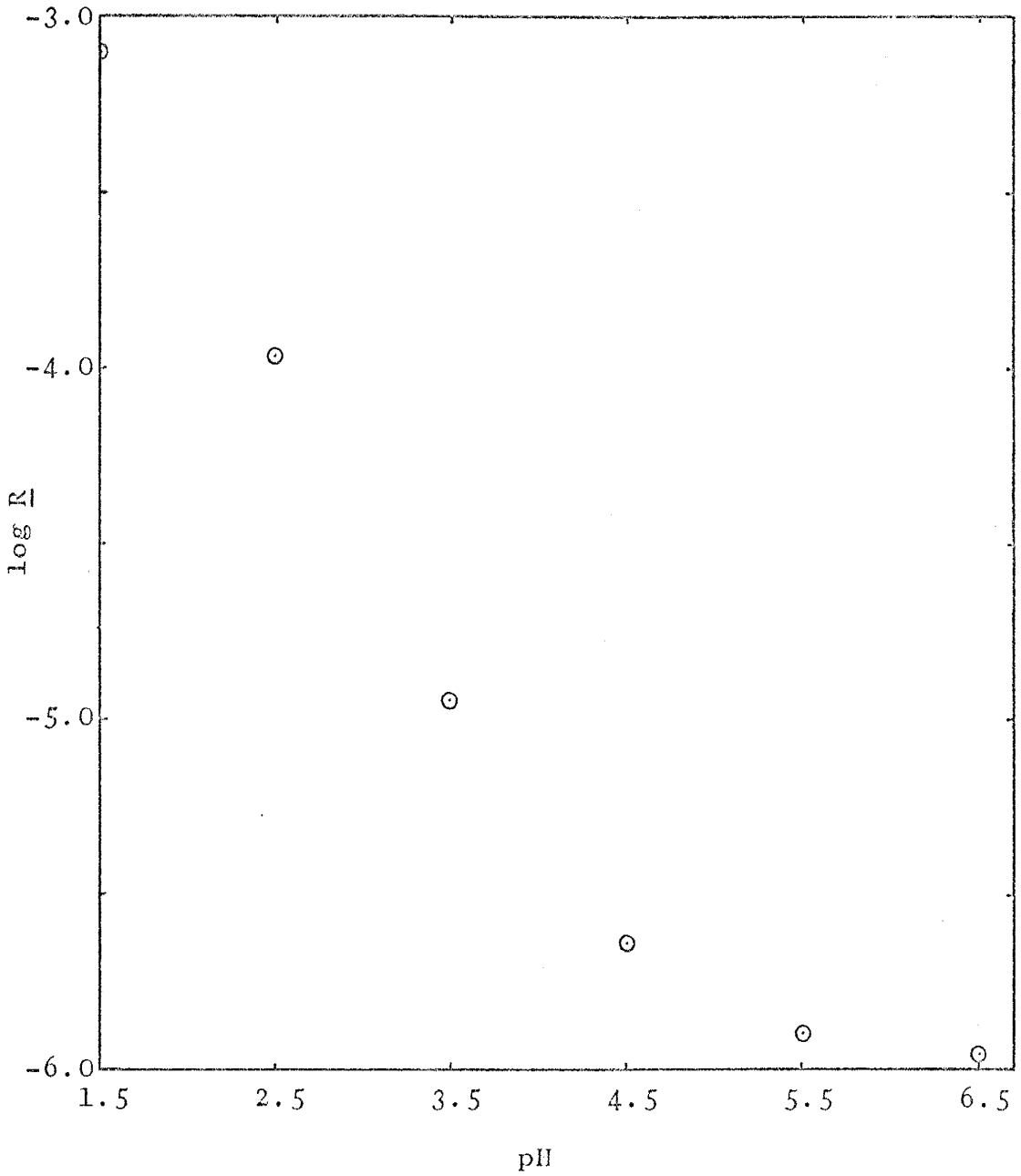
-3.0
-4.0
-5.0
-6.0
log R
1.5
2.5
3.5
4.5
5.5
6.5
pH

The strontianite dissolution rate is, within experimental error, a first order function of hydrogen ion activity at pH values less than 4.0; however, at higher pH values another mechanism, possibly a reaction involving water at the mineral surface, controls the reaction rate. Because this aspect of the experimental work was conducted under a continuously renewed nitrogen atmosphere, carbon dioxide resulting from mineral dissolution was removed from the system. Consequently, the system remained extremely undersaturated.

The extend of undersaturation is demonstrated by the molality product, $(m_{Sr^{2+}} \ m_{CO_3^{2-}})$, of strontianite at the end of 40 minutes. Assuming a P_{CO_2} value of 0.81, the molality product ranged from a low of $10^{-13.6}$ at a pH of 1.5 to a high of $10^{-11.2}$ at a pH of 6.5. Thus, neglecting activity coefficients and assuming the maximum P_{CO_2} rather than a value very close to zero, the molality product still yields a value which is only 1.3% of the solubility product. At the termination point of these experimental runs, the dissolution of strontianite was less than 2% completed. Therefore, it is reasonable to assume that any back reaction has not yet become significant (Benson, 1960; Gardiner, 1969).

Effect of P_{CO_2}

The effect of carbon dioxide partial pressure upon strontianite dissolution was investigated by streaming mixtures of carbon dioxide and nitrogen gases at 40° C.

The P_{CO_2} conditions studied were 0.0, 0.2, 0.4, and 0.8 atmospheres. Each experimental run had an initial pH of 4.02 to provide identical starting pH values which required acid addition for the P_{CO_2} values of 0.0, 0.2, and 0.4 atmospheres. The pH was maintained at 4.50 ± 0.03 by titrating 0.094 normal hydrochloric acid into the reaction vessel. The time period from 20 to 40 minutes after the start of the experiment was used to calculate the rate of acid addition. At a pH of 4.5, H_2CO_3 is the dominant carbonate species in solution and the dissolution reaction may be written as

$$SrCO_3 + 2\ H^+ = Sr^{2+} + H_2CO_3 \qquad (47)$$

for the experimental conditions. Once the pH of 4.5 has been established, the reaction rate may be expressed as

$$\begin{aligned} \underline{R} &= (dm_{Sr^{2+}}/dt) + (m_{Sr^{2+}}/M_{H_2O})(dM_{H_2O}/dt) \\ &= \tfrac{1}{2}[(dm_{H^+}/dt) + (m_{H^+}/M_{H_2O})(dM_{H_2O}/dt)] \end{aligned} \qquad (48)$$

where M_{H_2O} is the mass of liquid water.

Figure 5 is a plot of the amount of acid added per minute to maintain a pH of 4.5 as a function of the mole percent of carbon dioxide in the gas phase being introduced into the system. Figure 6 is a plot of P_{CO_2} versus the reaction rate calculated from equation (48). The partial pressure of carbon dioxide was calculated from the relationship

Figure 5. Plot of the raw data for strontianite dissolution at 40° C and pH = 4.5. The rate is the number of milliliters of 0.094 N hydrochloric acid added per minute to maintain the pH. The term % CO_2 is the percentage of carbon dioxide in the CO_2-N_2 gas mixture.

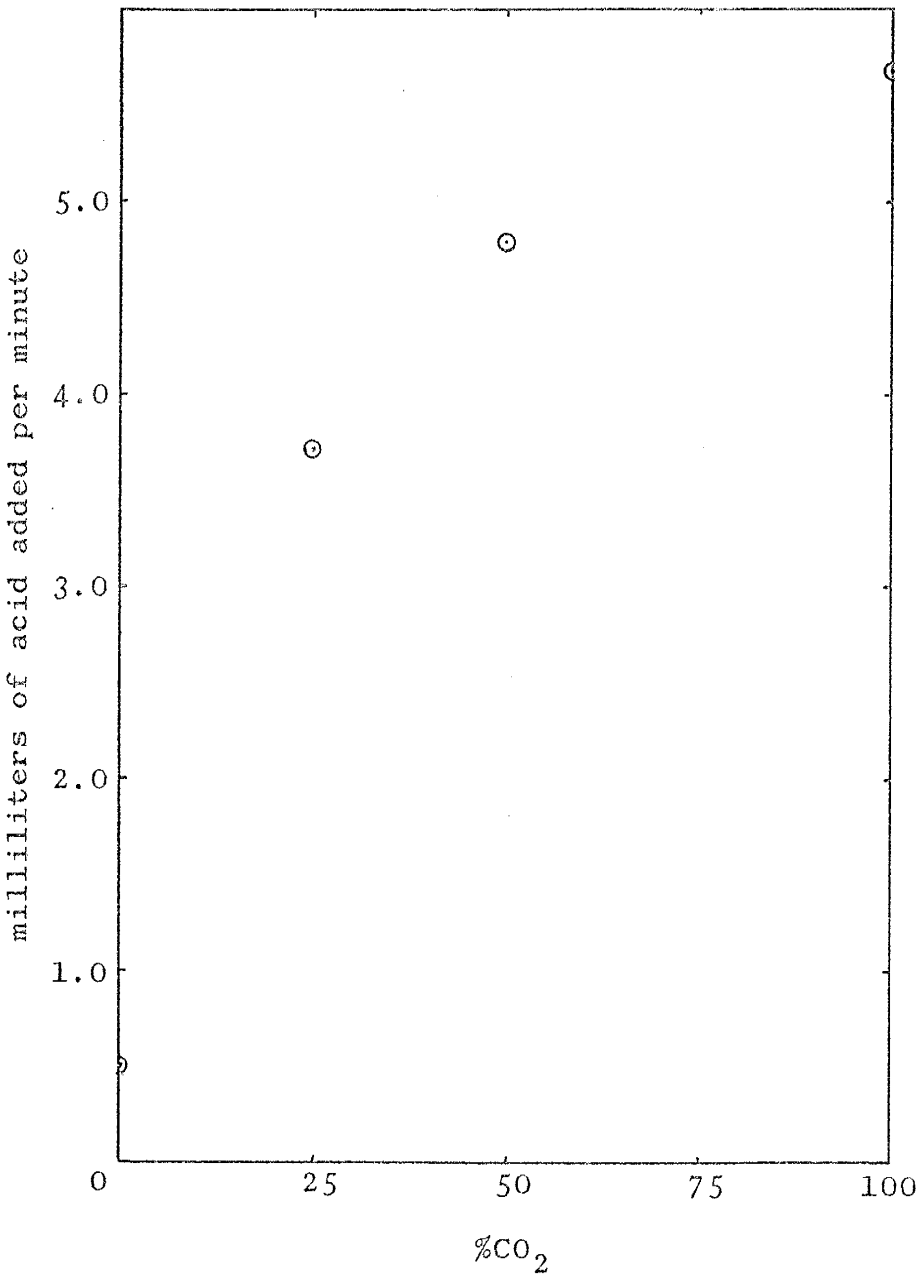
5.0
4.0
3.0
2.0
1.0
0
25
50
75
100
milliliters of acid added per minute
%CO2

Figure 6. Plot of the dissolution rate of strontianite, calculated using equation (48), versus P_{CO_2} for strontianite dissolution at 40° C and pH = 4.5.

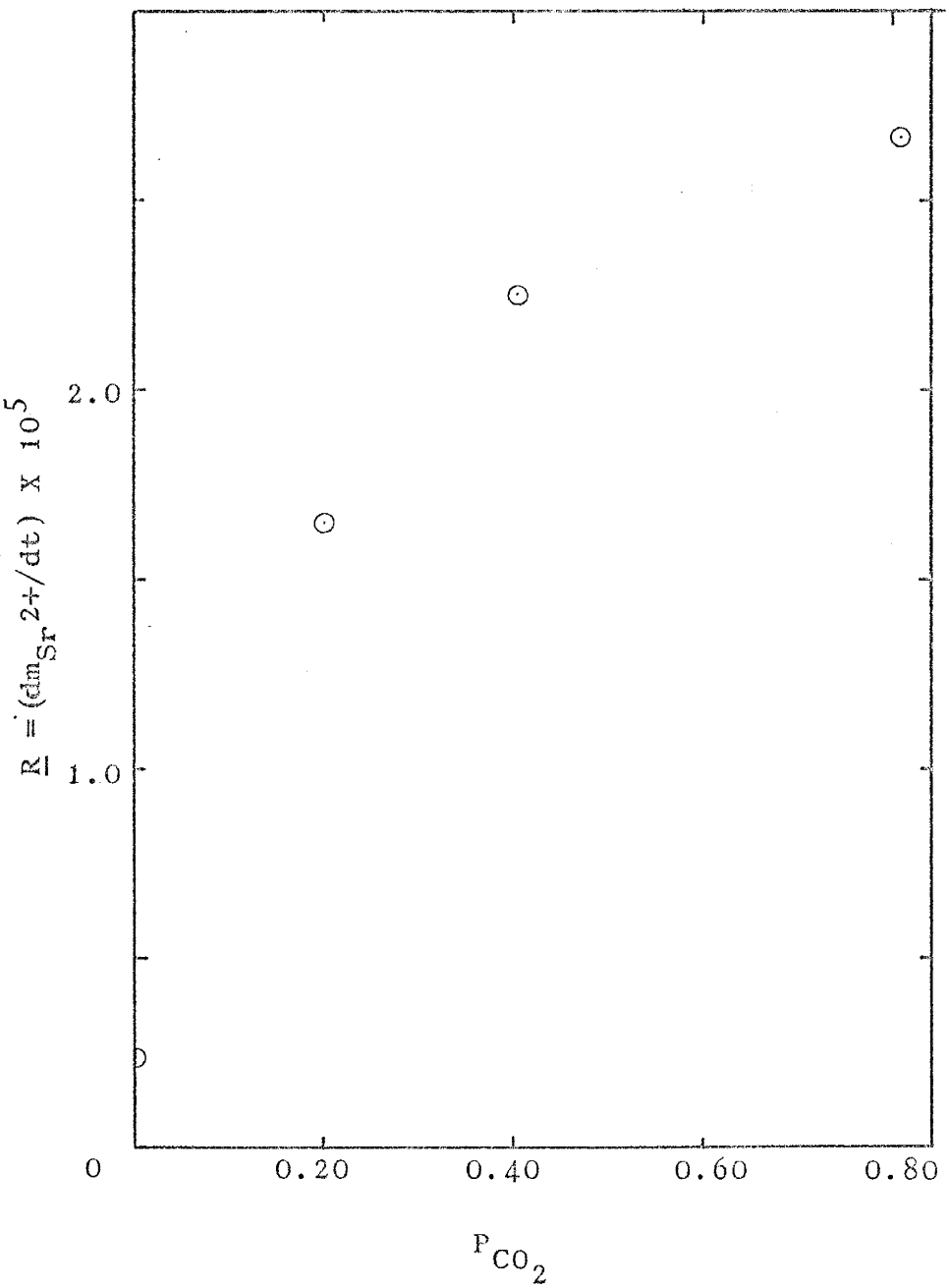
$R = (dm_{Sr^{2+}}/dt) \times 10^5$
2.0
1.0
0
0.20
0.40
0.60
0.80
P_{CO_2}

$$P_{CO_2} = N_{CO_2}(P_{tot} - P_{H_2O}) \quad (49)$$

where N_{CO_2} is the mole fraction of carbon dioxide in the CO_2-N_2 mixture. It can be seen from figure 6 that the relationship between the dissolution rate of strontianite and P_{CO_2} is definitely non-linear. Therefore, it was assumed that the reaction rate was dependent upon the degree of surface adsorption of either $CO_{2(aq)}$ or H_2CO_3 and the data were analyzed to see if an adsorption isotherm was compatible with the experimental values.

Application of the Langmuir adsorption isotherm to this study was accomplished by evaluating the change in reaction rate as a function of P_{CO_2}, assuming concurrent contributions to the reaction rate, using the relationship

$$\underline{R}_T = f_T(a_{H^+}) + g_T(P_{CO_2}) + h_T \quad (50)$$

where, at the temperature of interest, $\underline{R}_T$ is the observed reaction rate, f_T is a rate function describing the effect of hydrogen ion activity, g_T is a rate function describing the effect of carbon dioxide pressure, and h_T is a rate function of any additional unknown variables. If all known variables except the partial pressure of carbon dioxide are held constant, the function g_T may be expressed as

$$g_T(P_{CO_2}) = \underline{R}_T - \underline{R}_{T,P_{CO_2}=0} = \underline{R}'_T \quad (51)$$

where $\underline{R}_{T,P_{CO_2}=0}$ is the experimental reaction rate determined by bubbling 100% nitrogen gas through the reaction

vessel. Setting y in equation (30) equal to $\underline{R}_T'$ permitted a test of the hypothesis that the reaction rate might be controlled by an adsorption mechanism.

Figure 7 is a plot of $P_{CO_2}/\underline{R}_T'$ versus P_{CO_2}. The linearity of the points demonstrates that the kinetic effect of the partial pressure of carbon dioxide on strontianite dissolution is satisfactorily represented by the Langmuir adsorption isotherm, a Type I isotherm. This strongly suggests, but does not prove conclusively, that the rate limiting step is related to an adsorption mechanism.

The dissolution of strontianite with P_{CO_2} values of 0.0, 0.2, 0.4, and 0.8 atmospheres was conducted at an artificially maintained pH of 4.5. For this reason, none of the reactions proceeded as far as one percent of completion. Consequently, the reaction rate is only applicable to conditions far from equilibrium where the back reaction should be insignificant (Gardiner, 1969).

Effect of Temperature

Strontianite Dissolution

Strontianite dissolution with a carbon dioxide partial pressure of 0.81 atmosphere, was investigated at temperatures of 30, 40, and 50° C to determine the activation energy of the dissolution reaction and to investigate the kinetics as the reaction proceeds toward equilibrium. Minor fluctuations in barometric pressure were not considered

Figure 7. Plot of P_{CO_2}/R_T' versus P_{CO_2} for strontianite dissolution at 40° C and pH = 4.5. This plot is used to test the applicability of the Langmuir adsorption isotherm. The linearity of the data points demonstrates that R_T', the CO_2 contribution to the reaction rate, is proportional to θ, the fraction of the mineral surface covered by the adsorbed gas.

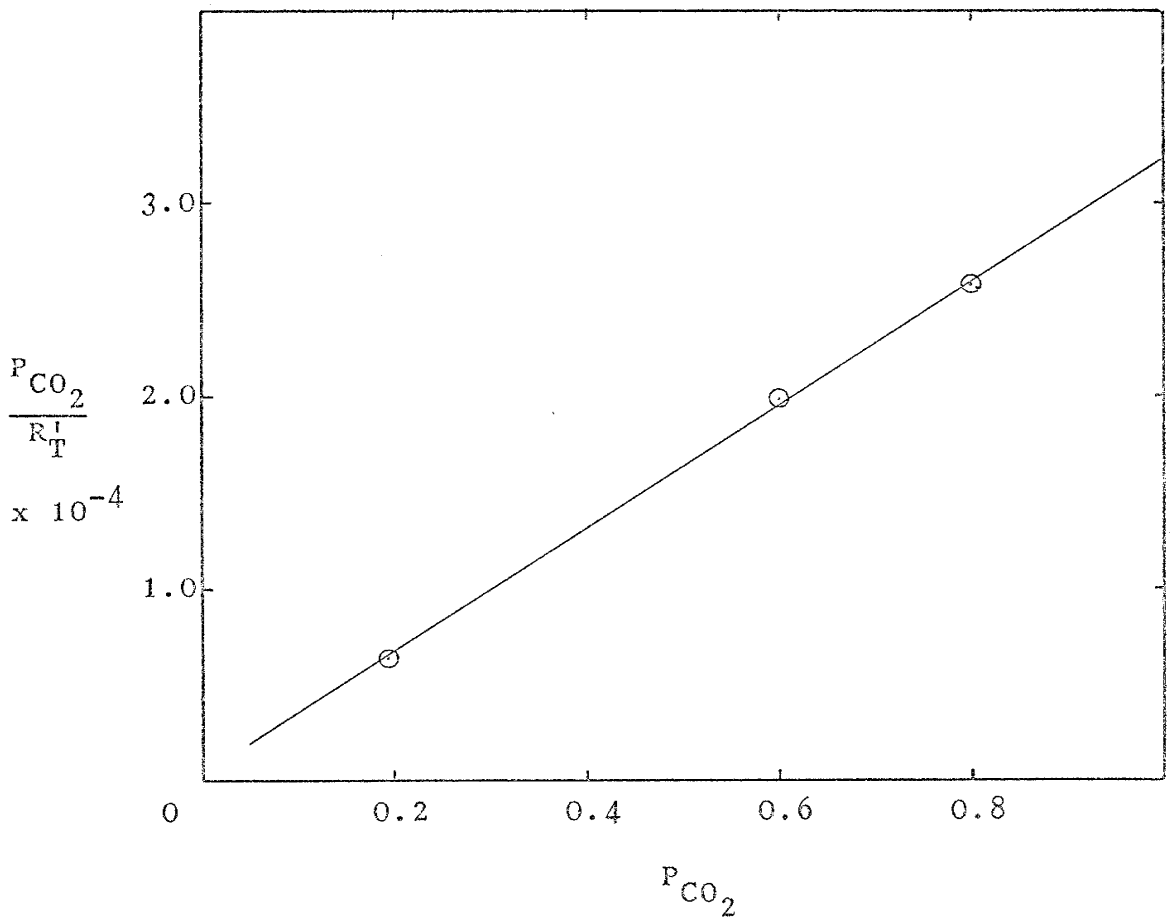
$\frac{P_{CO_2}}{R_T'}$
x 10^{-4}
3.0
2.0
1.0
0
0.2
0.4
0.6
0.8
P_{CO_2}

significant (cf. Garrels, Thompson, and Siever, 1960) and were not monitored. The experimental system was left open to the atmosphere to provide a fixed overpressure on the system.

The research required a fairly large amount of strontinite and the only size fraction used was the -30 +100 mesh split (sample between mesh sizes 0.589 mm and 0.149 mm). The sample was homogenized and passed repeatedly through a sample splitter to provide 16 aliquots. Fourteen of the splits were used for these experiments. The mean sample weight was 18.716 grams with a standard deviation of 0.208 grams.

The experimentally determined parameters, pH and specific resistivity, were monitored to define the reaction progress. Empirical resistivity values were obtained by titrating a 0.0841 molal solution of strontium hydroxide into distilled water under a carbon dioxide partial pressure within the range of 0.78 to 0.81 atmospheres at 40^{o} C. The break in the slope of a plot of resistivity against volume of titrant added suggests saturation with respect to $SrCO_3$ was achieved when 3.46×10^{-3} moles of $Sr(OH)_2$ had been added (pH = 5.81), but a definite precipitate was not formed until 4.44×10^{-3} moles had been added (pH = 5.91).

The molal solubility and solubility product values used for subsequent calculations were estimated by the affinity method of Prigogine, Outer, and Herbo (1948) to be: 3.42×10^{-3} moles of Sr^{2+} per kilogram H_2O at 30^{o} C (pK_{sp} =

9.37, equilibrium pH = 5.75); 3.22×10^{-3} moles of Sr^{2+} per kilogram H_2O at 40° C (pK_{sp} = 9.32, equilibrium pH = 5.81); and 3.05×10^{-3} moles of Sr^{2+} per kilogram H_2O at 50° C (pK_{sp} = 9.28, equilibrium pH = 5.83).

The reproducibility of the experimental data is demonstrated in figure 8 where four experimental runs at 40° c are plotted. Agreement during the first 200 minutes is excellent. From 200 to 400 minutes the divergence of experimental points is greater but well within the range of experimental error discussed earlier. Stirred and unstirred experiments proceeded at the same rate.

The molalities of all aqueous species and the activities of all aqueous species other than H^+ were calculated using the computer program CATCALC as discussed on pages 29 and 30. Appendix B contains a listing of the equilibrium constants used in the calculations. Comparison of the calculated strontium concentrations with atomic absorption analyses of samples taken at the end of the experiment are in complete agreement within the analytical limits of the equipment (± 10%) under routine conditions. The atomic absorption analyses are not consistently higher or lower than the values determined from CATCALC; thus, systematic error in the program constants is probably minimal or compensating.

The rate of mineral reaction with an aqueous phase can often be expressed by the general kinetic relationship

$$dm_i/dt = k_i t^{\omega} \qquad (27)$$

Figure 8. Plot of pH versus time in minutes for strontianite dissolution at 40° C and 0.81 atmosphere P_{CO_2}. The purpose of the plot is to demonstrate the reproducibility of the data.

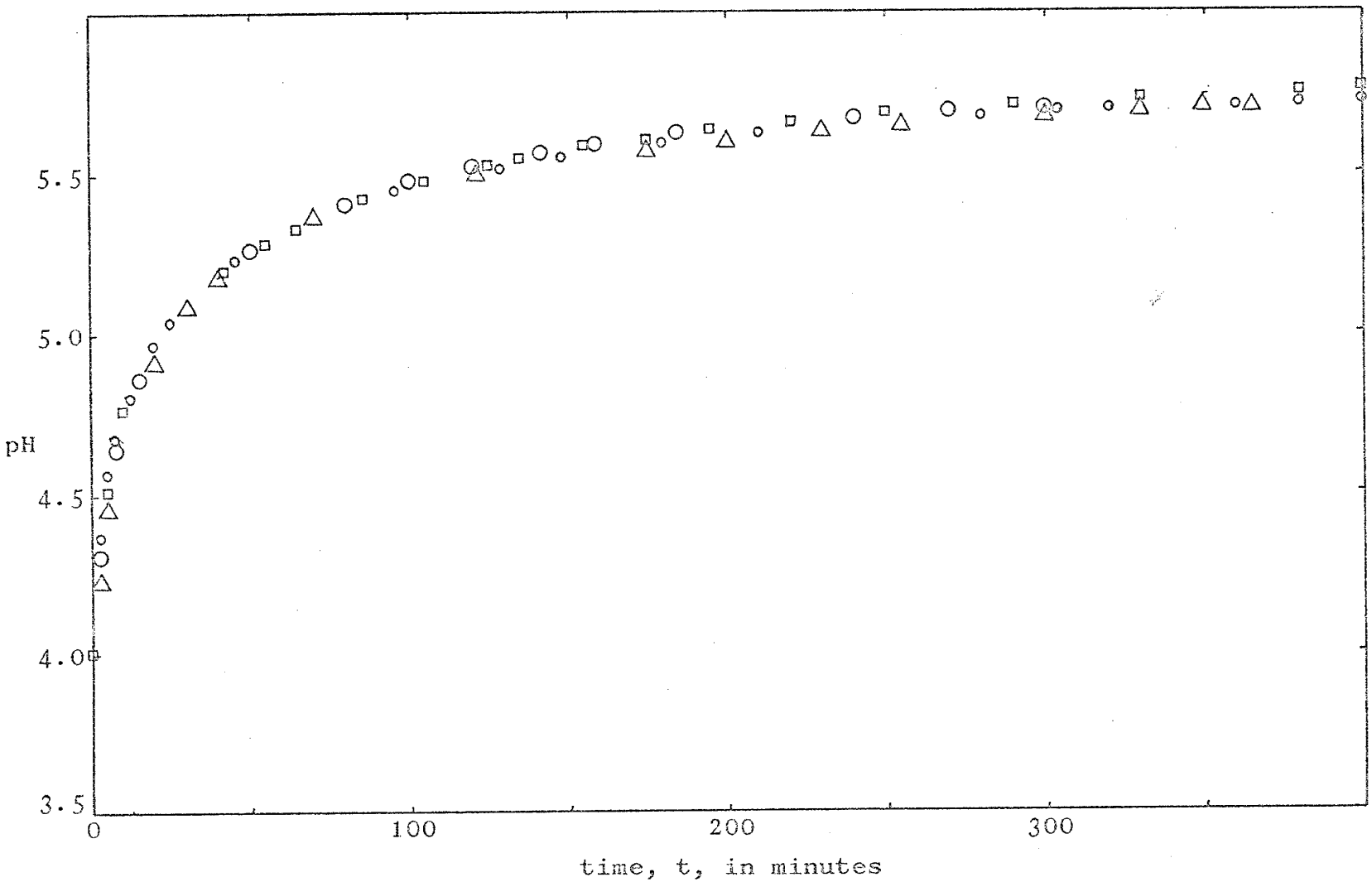
5.5
5.0
pH
4.5
4.0
3.5
0
100
200
300
time, t, in minutes

Figures 9, 10, and 11 are plots of linear ($\omega = 0$), parabolic ($\omega = -\frac{1}{2}$), and logarithmic ($\omega = -1$) rate laws for strontianite dissolution at 30, 40, and 50° C. If a rate law is applicable, its figure should show a linear relationship between m_{Sr}^{2+} and time, the square root of time, or the logarithm of time. The plot of m_{Sr}^{2+} versus time, figure 9, is obviously non-linear so the linear rate law need not be considered further. The plot of m_{Sr}^{2+} versus the square root of time, figure 10, approximates a straight line relationship, especially at 30° C; therefore, the parabolic rate law requires additional evaluation. The plot of m_{Sr}^{2+} versus the logarithm of time, figure 11, shows distinct curvature so the logarithmic rate law is not applicable.

The data were next tested to determine if equation (26) could adequately represent the experimental data. Figure 12 is a plot of log $\underline{R}$ versus log $(m_{Sr}^{2+}{}_{s} - m_{Sr}^{2+}{}_{t})$ and shows that the experimental data for 30° C deviates excessively and possibly systematically from the expected behavior. The data for 40 and 50° C approximate a first order reaction having an average value for n of 1.1. Consequently, equation (25) should be used to evaluate a possible first order reaction mechanism.

Figure 13, a plot of log $(m_{Sr}^{2+}{}_{s} - m_{Sr}^{2+}{}_{t})$ versus time since the start of the experiment, provides a test of the first order hypothesis. Because the experimental data plot in nearly straight lines, it is apparent that the experimental data are essentially compatible with a first order

Figure 9. Plot of the molality of Sr^{2+} in solution versus time for strontianite dissolution under 0.81 atmosphere P_{CO_2}. The experimental temperatures are 30, 40, and 50° C. The time since the start of the reaction is expressed in minutes. A reaction obeying the linear rate law would be represented by a straight line.

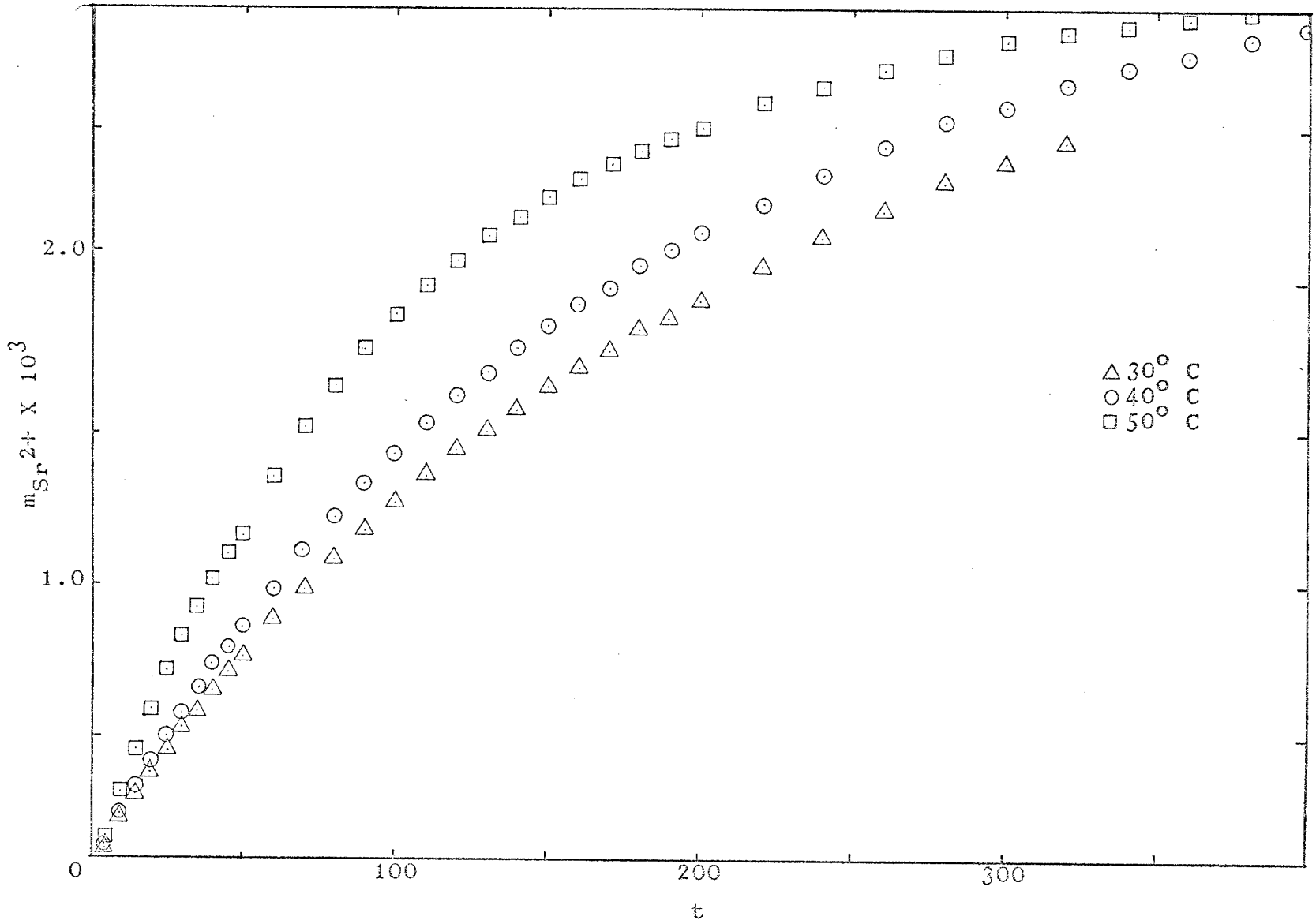
2.0
1.0
0
100
200
300
t
$m_{Sr^{2+}} \times 10^3$
△ 30° C
○ 40° C
□ 50° C

Figure 10. Plot of the molality of Sr^{2+} in solution versus the square root of time for strontianite dissolution under 0.81 atmosphere P_{CO_2}. The experimental temperatures are 30, 40, and 50° C. Time, t, is in minutes since the start of the reaction. A reaction obeying the parabolic rate law would be represented by a straight line. The lines marked A, B, and C result from regression of all of the 30° C data, the first 200 minutes of the 50° C data, and all of the 50° C data, respectively.

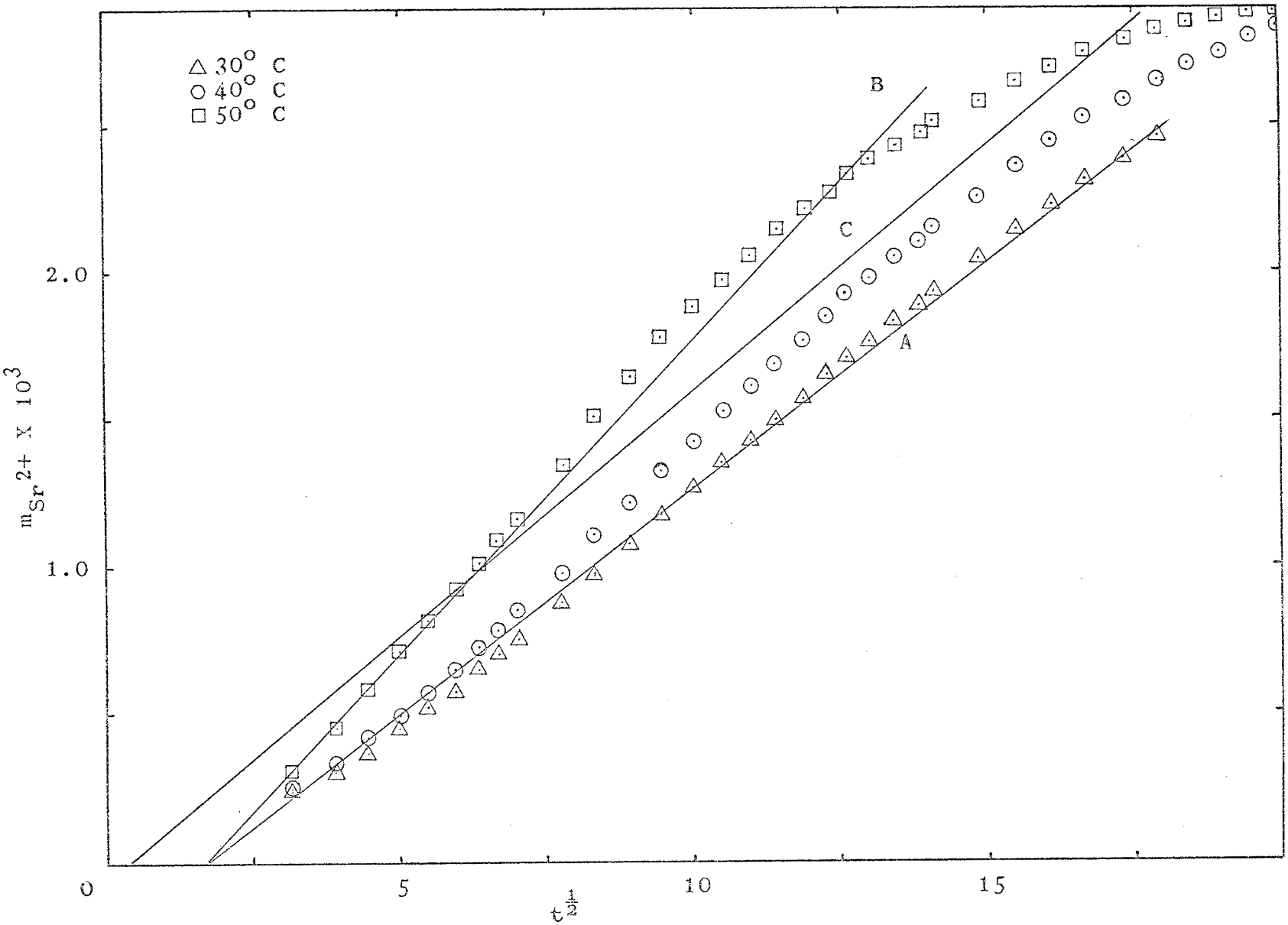
△ 30° C
○ 40° C
□ 50° C
B
C
A
2.0
1.0
0
5
10
15
$m_{Sr^{2+}} \times 10^3$
$t^{\frac{1}{2}}$

Figure 11. Semilog plot of the molality of Sr^{2+} in solution versus time, in minutes, since the reaction started. The dissolution of strontianite was studied under 0.81 atmosphere of P_{CO_2} at temperatures of 30, 40, and 50° C. A dissolution reaction which obeys the logarithmic rate law would be represented by a straight line.

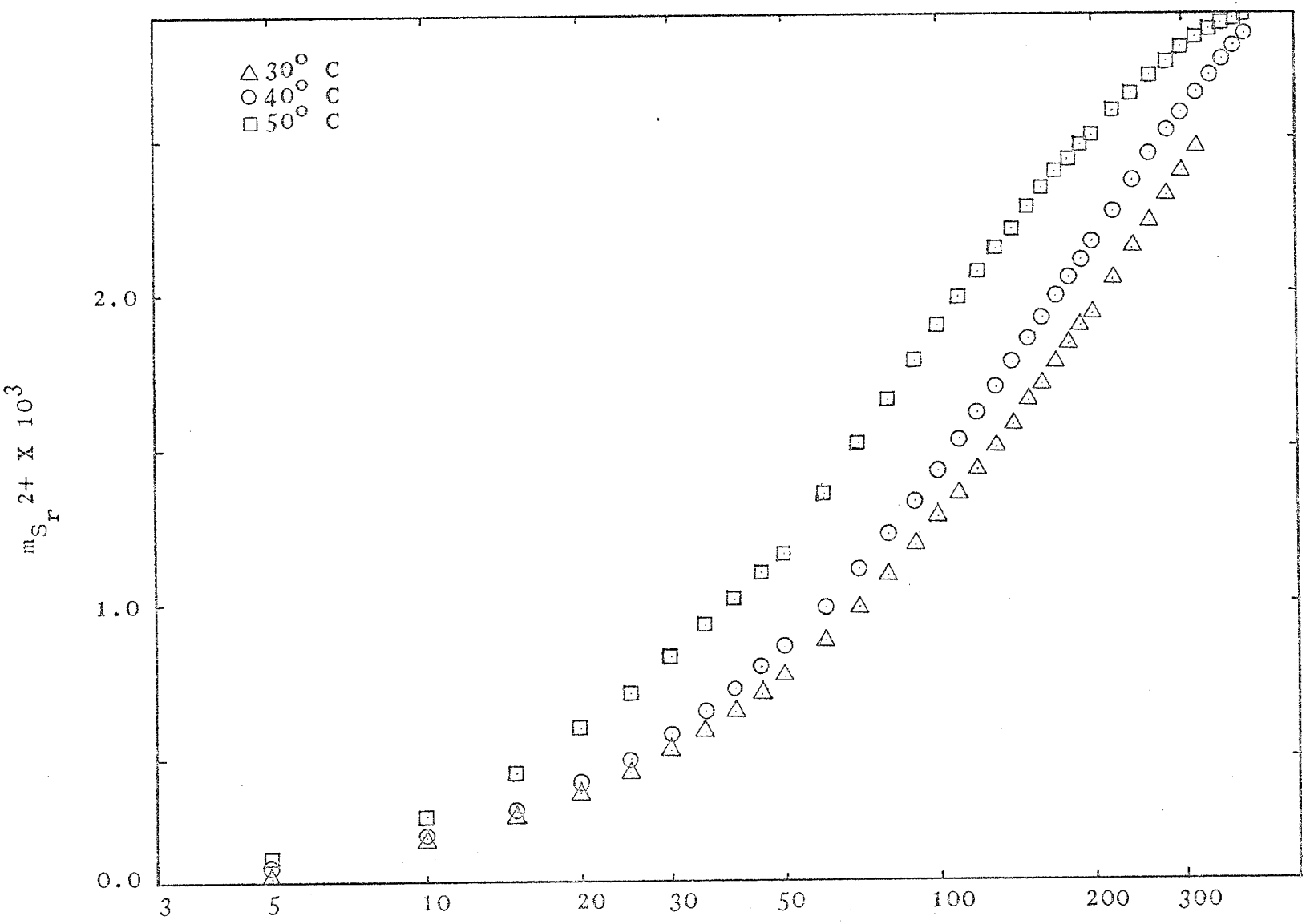
△ 30° C
○ 40° C
□ 50° C
$m_{Sr}{}^{2+} \times 10^3$
0.0
1.0
2.0
3
5
10
20
30
50
100
200
300

Figure 12. Plot of log $\underline{R}$ versus log ($m_{Sr^{2+}_s} - m_{Sr^{2+}_t}$) for strontianite dissolution under 0.81 atmosphere P_{CO_2} at temperatures of 30, 40, and 50° C. This type of plot is used to graphically evaluate n in equation (18). The values of n are 1.28 at 30° C, 1.05 at 40° C, and 1.16 at 50° C. The best fit between the experimental data and the postulated kinetic equation is obtained at 50° C.

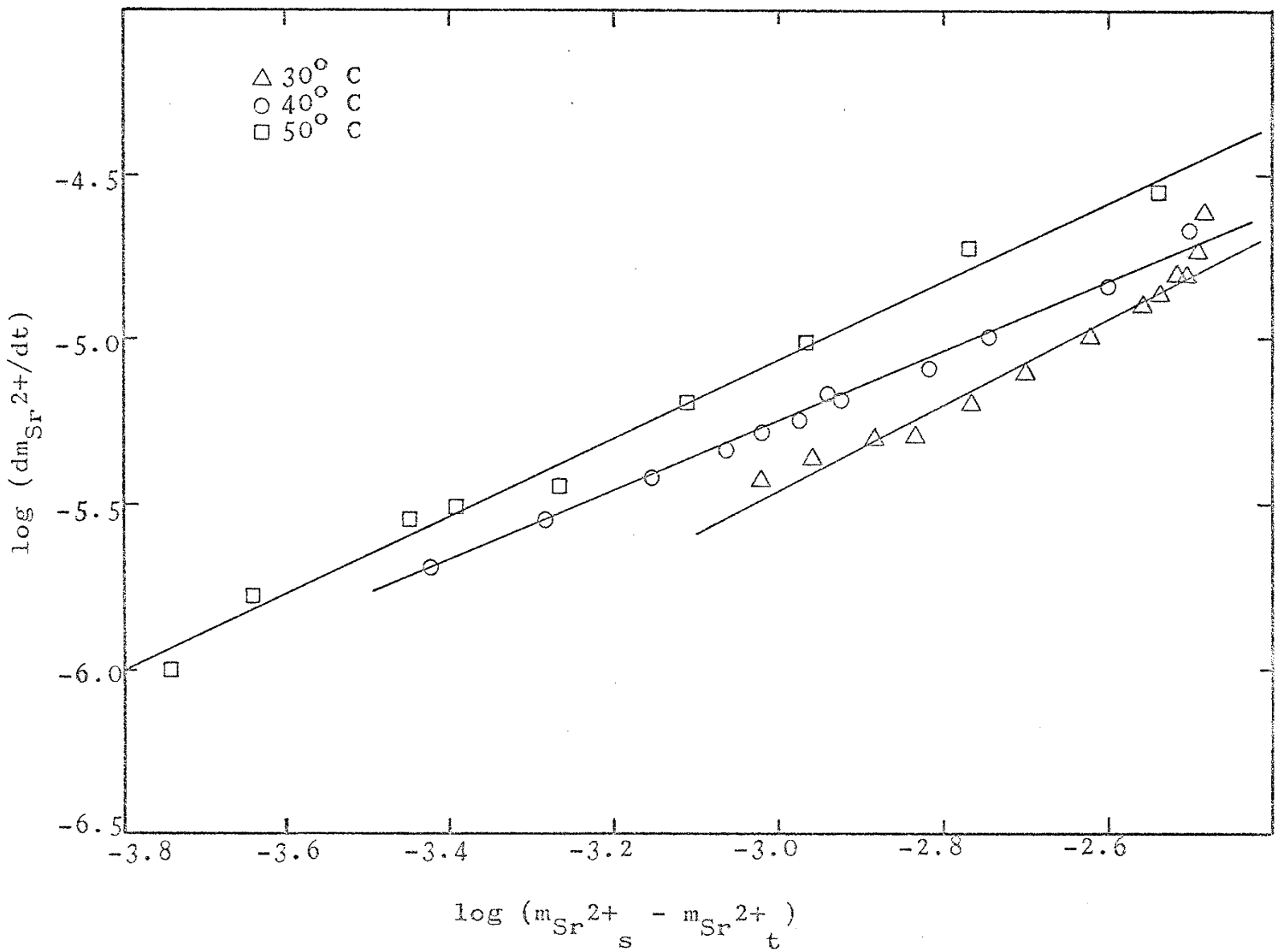
△ 30° C
○ 40° C
□ 50° C
-4.5
-5.0
-5.5
-6.0
-6.5
-3.8
-3.6
-3.4
-3.2
-3.0
-2.8
-2.6
log ($dm_{Sr^{2+}}/dt$)
log ($m_{Sr^{2+}}{}_s - m_{Sr^{2+}}{}_t$)

Figure 13. Plot of log ($m_{Sr^{2+}_s} - m_{Sr^{2+}_t}$) versus t for strontianite dissolution under a 0.81 atmosphere P_{CO_2} at temperatures of 30, 40, and 50° C. This plot is based upon the assumption that the overall reaction is first order (n = 1.0) and obeys the first order rate law. Under the experimental conditions the integration constant, C, from equation (25) must equal the molality of Sr^{2+} at saturation, $m_{Sr^{2+}_s}$.

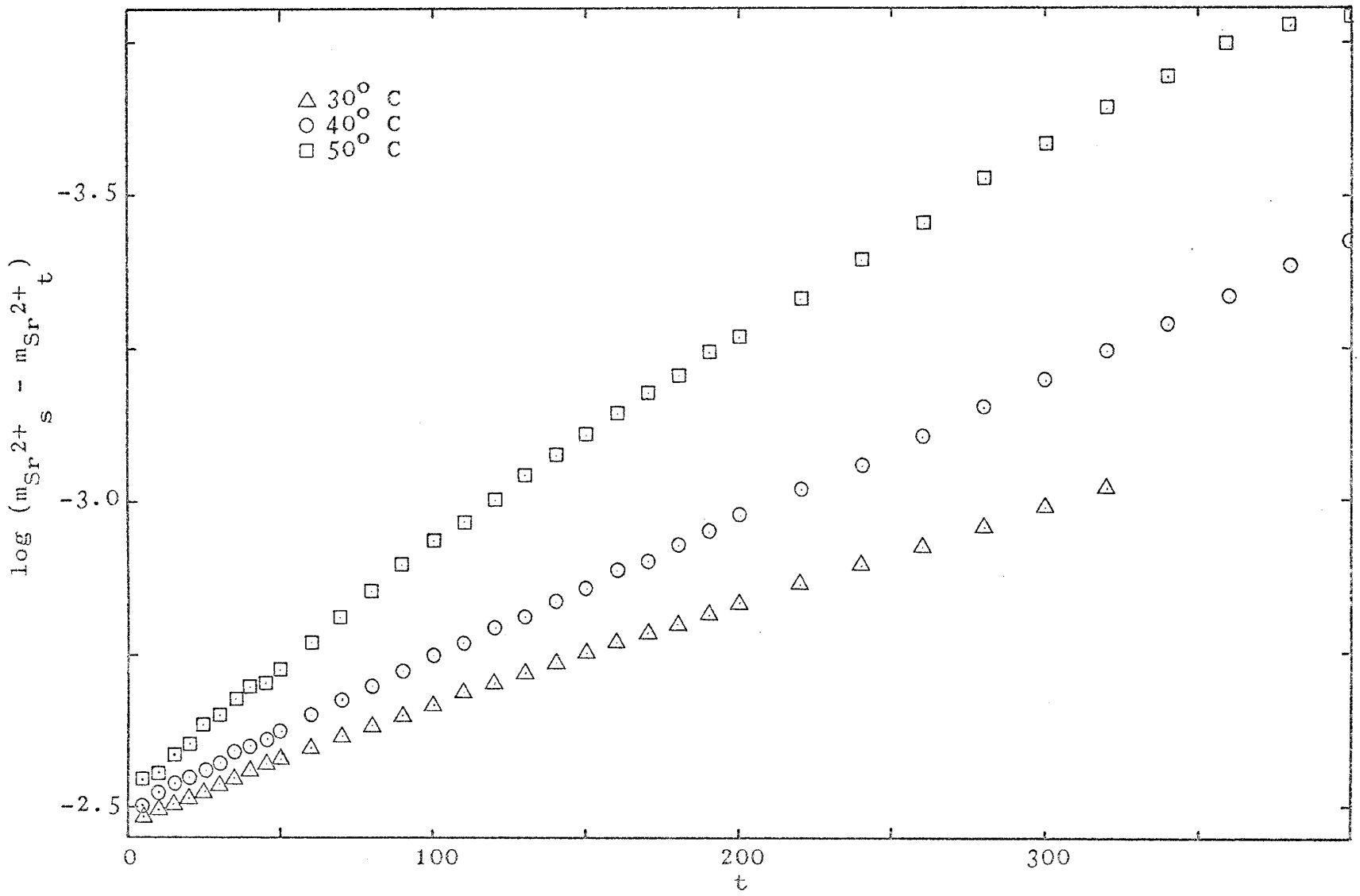
△ 30° C
○ 40° C
□ 50° C
-3.5
-3.0
-2.5
log ($m_{Sr^{2+}}$ s - $m_{Sr^{2+}}$ t)
0
100
200
300
t

rate controlling process which is dependent upon the concentration of the Sr^{2+} ion. The systematic curvature in the 50° C data may result from either an erroneous estimate of the solubility at this temperature or from a change of the rate limiting mechanism at later stages. The convex upper surface of the 50° C data plot could be altered by slightly decreasing the molality of Sr^{2+} at equilibrium. Nevertheless, the results shown in figure 13 constitute a good empirical fit.

Comparison of the molality of the Sr^{2+} ion predicted by the parabolic and first order rate laws provides a method of determining which of these rate laws best fits the experimental data. If the parabolic rate law applies, $m_{Sr^{2+}}$ should plot as a straight line as a function of $t^{\frac{1}{2}}$; the equation used to regress the data for the parabolic rate law was

$$m_{Sr^{2+}}{}_t = a + bt^{\frac{1}{2}} \qquad (52)$$

where a and b are empirical constants. These values were determined to be -0.27×10^{-3} and 0.153×10^{-3}, respectively. Regression of the 30° C data for the first order rate law used the equation

$$\log (m_{Sr^{2+}}{}_s - m_{Sr^{2+}}{}_t) = a + bt \qquad (53)$$

where the empirical coefficients a and b were determined to be -2.49 and -1.7×10^{-3}, respectively. Equations (52) and (53) were used to calculate values of $m_{Sr^{2+}}$ at various times as shown in Table 1. These calculated values show that the

TABLE I. CALCULATED VALUES OF $m_{Sr^{2+}}$ AT 30° C

Time in minutes	Experimental $m_{Sr^{2+}} \times 10^3$	First order rate law $m_{Sr^{2+}} \times 10^3$	$\Delta (m - m_{exp}) \times 10^3$	Parabolic rate law $m_{Sr^{2+}} \times 10^3$	$\Delta (m - m_{exp}) \times 10^3$
10	0.229	0.31	+0.08	0.21	-0.02
25	0.455	0.48	+0.03	0.49	+0.04
50	0.765	0.76	-0.01	0.81	+0.05
75	1.036	1.02	-0.02	1.05	+0.02
100	1.272	1.24	-0.03	1.26	-0.01
150	1.647	1.62	-0.03	1.61	-0.04
200	1.936	1.94	+0.00	1.89	-0.05
250	2.185	2.19	+0.01	2.15	-0.04
300	2.391	2.42	+0.03	2.38	-0.01

first order and parabolic rate laws provide equally valid equations to express the experimental dissolution of strontianite at 30° C. However, for reactions which approach equilibrium, the parabolic rate law alone cannot be expected to remain valid (cf. Helgeson, 1971, p. 432). This failure of the parabolic rate law is demonstrated in Table 2 by the m_{Sr}^{2+} values calculated for strontianite dissolution at 50° C; the departure from the parabolic rate law of the 40° C data is not as great. The parabolic rate law, fitted to the 50° C data for the first 200 minutes of reaction progress (line B, figure 10) with $a = -0.35 \times 10^{-3}$ and $b = 0.217 \times 10^{-3}$, provides a good predictive model for the early dissolution stage; but it is not applicable beyond t = 200 minutes. The regressed line for the entire experimental period (line C, figure 10), with $a = -0.07 \times 10^{-3}$ and $b = 0.166 \times 10^{-3}$, does not yield a satisfactory predictive model because of the large systematic errors which it introduces, up to 16% at 100 minutes. The first order rate law was chosen to represent strontianite dissolution because it provides a better fit over the investigated experimental conditions and allows for a molecular interpretation of the rate limiting step.

Witherite Dissolution

Witherite dissolution was investigated using the same experimental conditions and size fraction as employed for strontianite dissolution. The sample weights resulting

TABLE II. CALCULATED VALUES OF $m_{Sr^{2+}}$ AT 50° C

Time in minutes	Experimental $m_{Sr^{2+}} \times 10^3$	First order rate law $m_{Sr^{2+}} \times 10^3$	$\Delta (m - m_{exp}) \times 10^3$	Parabolic rate law (line B) $m_{Sr^{2+}} \times 10^3$	$\Delta (m - m_{exp}) \times 10^3$	Parabolic rate law (line C) $m_{Sr^{2+}} \times 10^3$	$\Delta (m - m_{exp}) \times 10^3$
10	0.313	0.45	+0.14	0.336	+0.02	0.455	+0.14
20	0.589	0.65	+0.06	0.625	+0.04	0.642	+0.05
40	1.016	1.01	-0.01	1.022	+0.01	0.980	-0.04
60	1.353	1.31	-0.04	1.331	-0.02	1.216	-0.14
100	1.885	1.79	-0.10	1.820	-0.05	1.590	-0.30
150	2.275	2.21	-0.07	2.308	+0.03	1.963	-0.31
200	2.510	2.49	-0.02	2.719	+0.21	2.278	-0.33
250	2.672	2.67	+0.00	3.081	+0.41	2.555	-0.12
300	2.790	2.80	+0.01	3.408	+0.62	2.805	+0.03
350	2.859	2.88	+0.02			3.036	+0.18
400	2.890	2.93	+0.04			3.250	+0.36

from the splitting procedure, ranging between 25.75 and 26.97 grams, were not as consistent as those for strontianite. However, for the experiments discussed, the maximum deviation from the mean weight was less than $2\frac{1}{2}\%$ and the effect is within the analytical tolerances of the pH determinations.

The experimentally determined parameters, pH and specific resistivity, were monitored to determine the reaction progress. Empirical resistivity values were obtained by titrating a 0.116 molal barium hydroxide solution into distilled water under a constant carbon dioxide partial pressure; the P_{CO_2} value was between 0.78 and 0.81 atmospheres at 40° C. A pH reversal and a resistivity break mark the saturation point at a pH of 6.075 with a total barium concentration of 6.62×10^{-3} moles per kilogram H_2O. A permanent precipitate was formed by further addition of the base (pH = 6.081).

The molalities of all aqueous species and the activities of all aqueous species other than H^+ were calculated using the computer program CATCALC as discussed on pages 29 and 30. Appendix B contains a listing of the equilibrium constants used in this study. Figure 14 is a plot of the calculated molality of Ba^{2+} against time for the dissolution of witherite at 30, 40, and 50° C. Stirred and unstirred reactions proceeded at the same rate.

Atomic absorption determinations of the barium concentration were not satisfactory. The sensitivity claimed for the Perkin-Elmer 403 could not be obtained (Billings, 1973,

Figure 14. Plot of the molality of Ba^{2+} in solution versus time for witherite dissolution under 0.81 atmosphere P_{CO_2} at temperatures of 30, 40, and 50° C. The time since the start of the reaction, t, is expressed in minutes. A reaction obeying the linear rate law would be represented by a straight line.

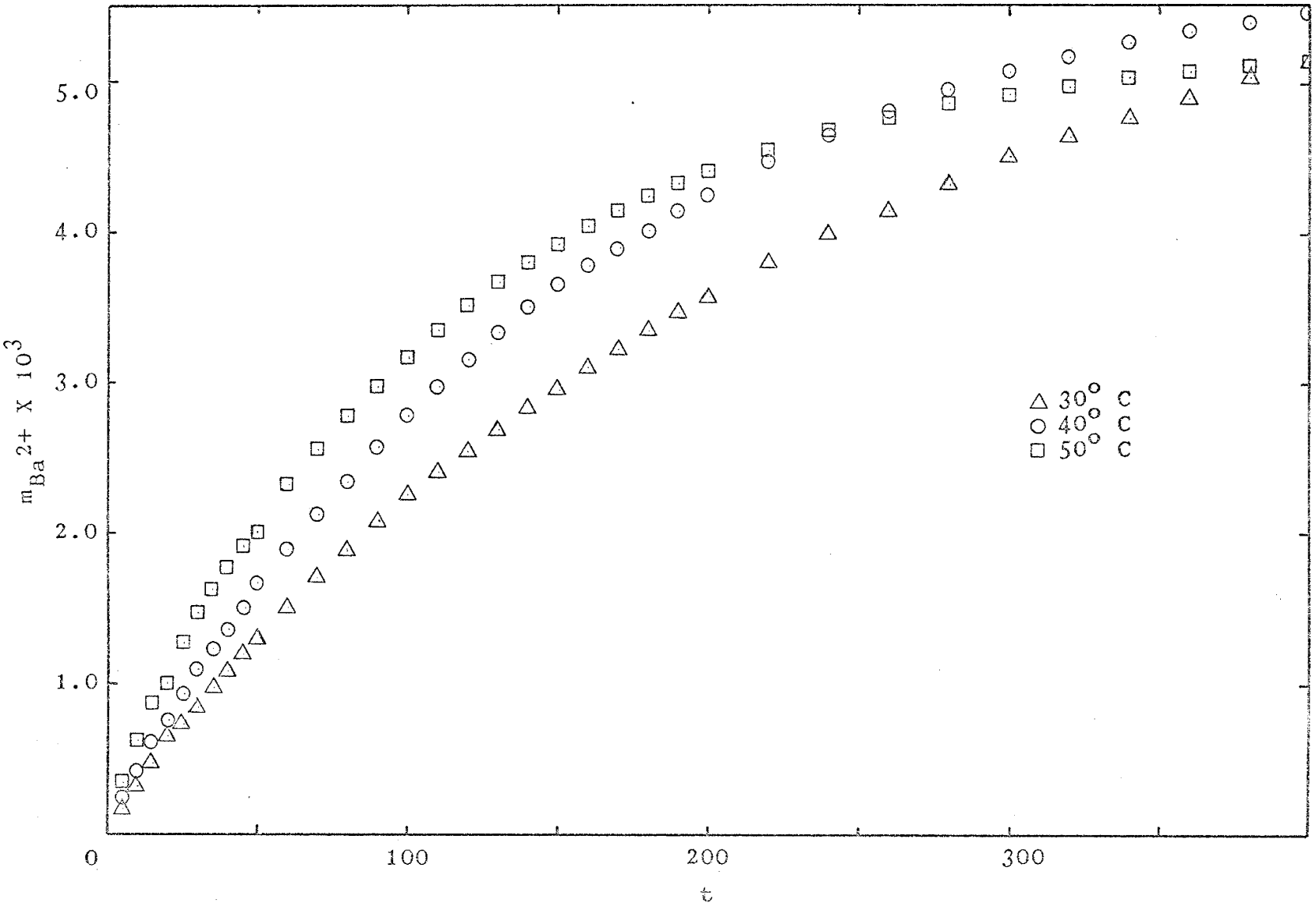
5.0
4.0
3.0
2.0
1.0
0
100
200
300
t
$m_{Ba^{2+}} \times 10^3$
△ 30° C
○ 40° C
□ 50° C

personal comm.). This problem of poor precision with barium is common with all atomic absorption equipment according to the U. S. Geological Survey Water Quality Laboratory in Atlanta, Georgia (Liefeste, 1974, personal comm.).

The molal solubility values used for subsequent calculations were estimated by the affinity method of Prigogine, Outer, and Herbo (1948) to be: 7.23×10^{-3} moles of Ba^{2+} per kilogram H_2O at 30° C ($pK_{sp} = 8.48$; equilibrium pH = 6.07); 6.03×10^{-3} moles of Ba^{2+} per kilogram H_2O at 40° C ($pK_{sp} = 8.55$; equilibrium pH = 6.07); and 5.24×10^{-3} moles of Ba^{2+} per kilogram H_2O at 50° C ($pK_{sp} = 8.62$; equilibrium pH = 6.07).

The linear, parabolic, and logarithmic rate laws were graphically tested by plotting the molality of Ba^{2+} against the appropriate function of time as shown in figures 14, 15, and 16. As was the case with strontianite dissolution, the linear and logarithmic rate laws do not provide a satisfactory fit for the witherite dissolution data. The parabolic rate law provides a good data fit at 30° C, but shows increased deviations from linearity at 40 and 50° C.

The data were next tested to determine if equation (26) could adequately represent the experimental data. Figure 17 is a plot of log $\underline{R}$ versus log $(m_{Ba^{2+}_s} - m_{Ba^{2+}_t})$ for witherite dissolution under a 0.81 atmosphere P_{CO_2} at temperatures of 30, 40, and 50° C. The linear portion of the plot is used to graphically determine the value of n in equation (26). The slopes decrease with increasing

Figure 15. Plot of the molality of Ba^{2+} in solution versus the square root of time for witherite dissolution under 0.81 atmosphere P_{CO_2} at temperatures of 30, 40, and 50° C. Time, t, is in minutes since the start of the reaction. A reaction obeying the parabolic rate law would be represented by a straight line. The lines marked A, B, and C result from regression of all of the 30° C data, the first 200 minutes of the 50° C data, and all of the 50° C data, respectively.

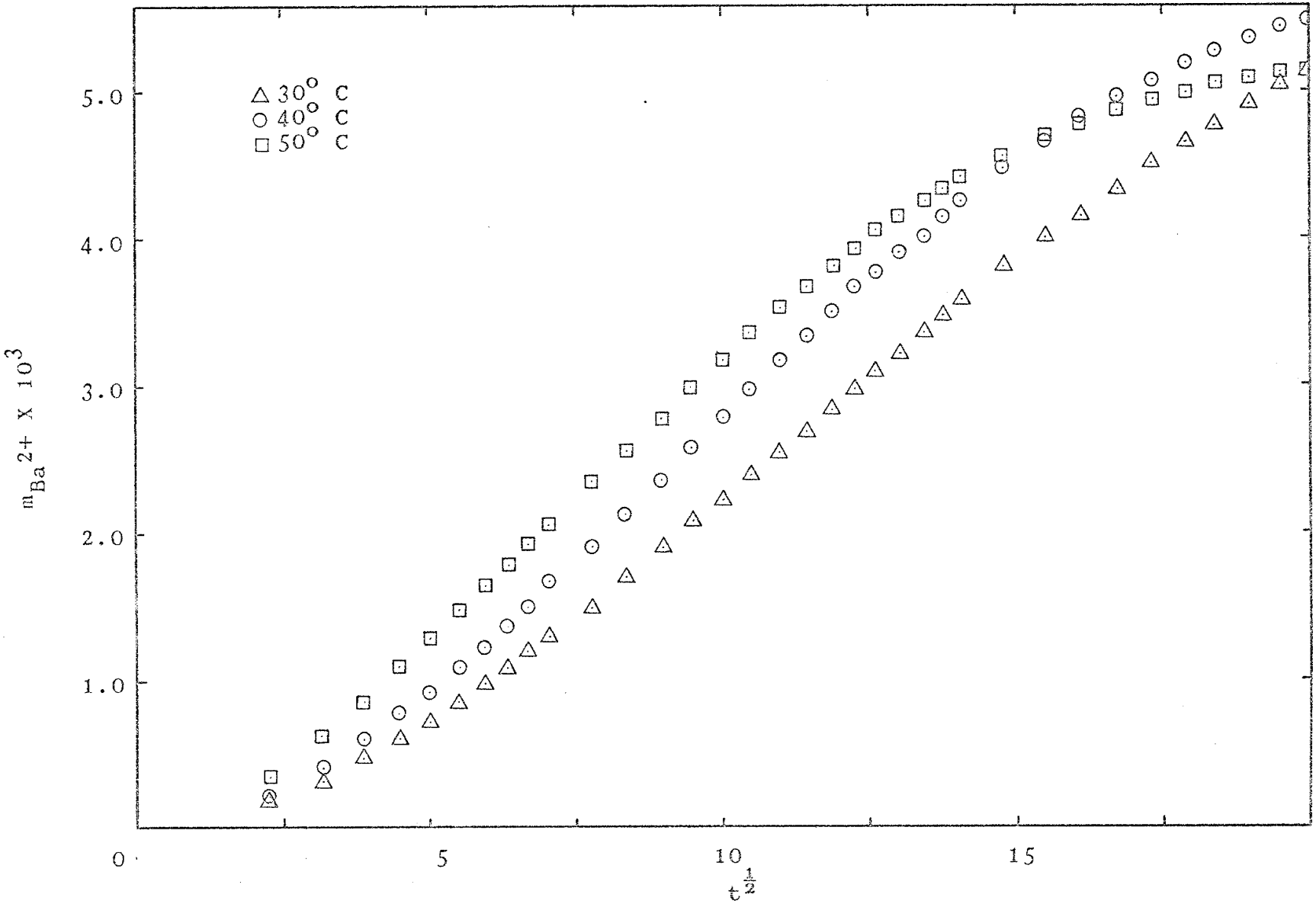
△ 30° C
○ 40° C
□ 50° C
5.0
4.0
3.0
2.0
1.0
0
5
10
15
$m_{Ba^{2+}} \times 10^3$
$t^{\frac{1}{2}}$

Figure 16. Semilog plot of the molality of Ba^{2+} in solution versus time, t, in minutes since the reaction started under 0.81 atmosphere of P_{CO_2} at temperatures of 30, 40, and 50° C. A dissolution reaction which obeys the logarithmic rate law would be represented by a straight line.

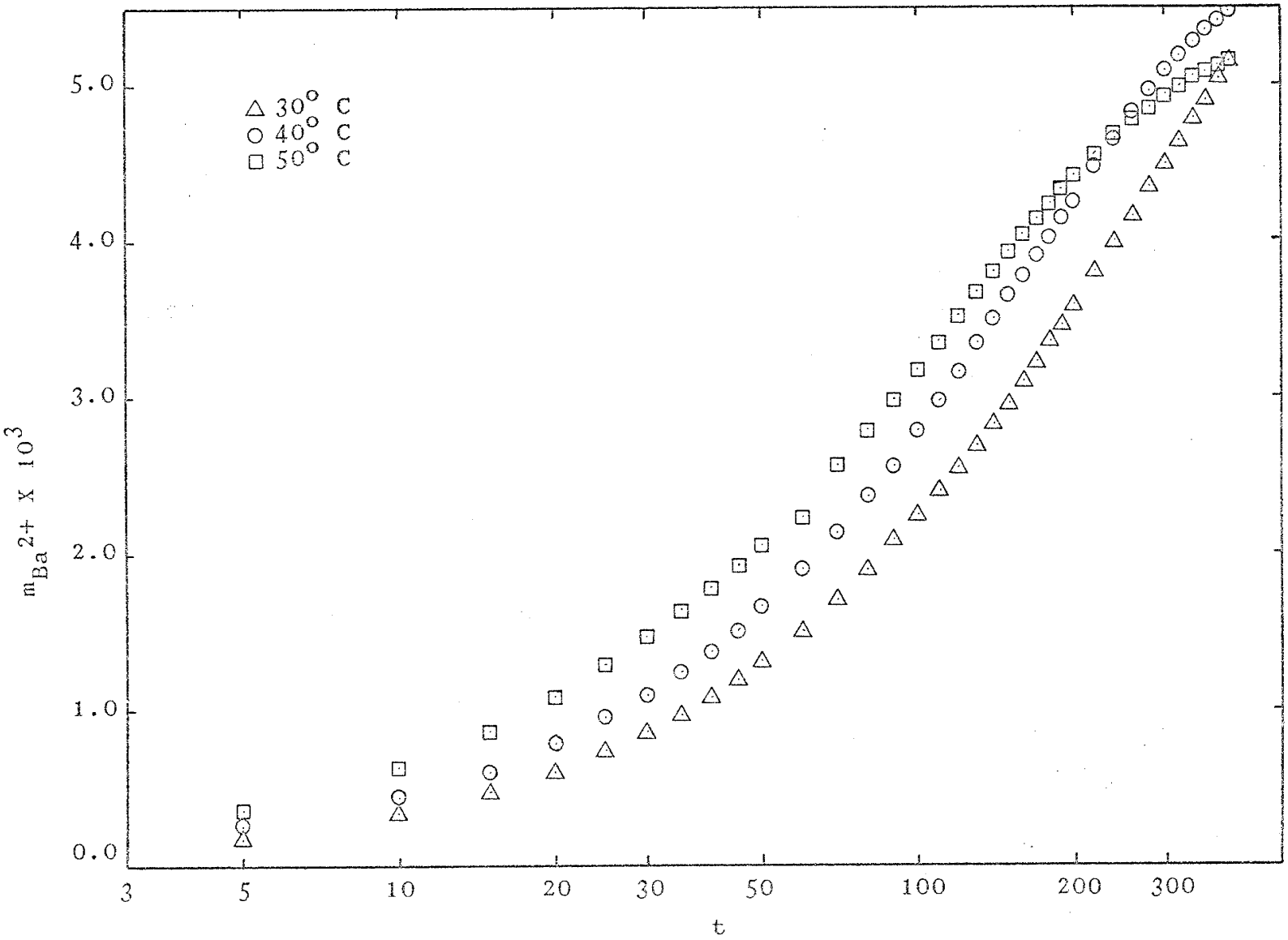
△ 30° C
○ 40° C
□ 50° C
5.0
4.0
3.0
2.0
1.0
0.0
$m_{Ba^{2+}} \times 10^3$
3
5
10
20
30
50
100
200
300
t

Figure 17. Plot of log R versus log ($m_{Ba^{2+}_s} - m_{Ba^{2+}_t}$) for witherite dissolution under 0.81 atmosphere P_{CO_2} at temperatures of 30, 40, and 50° C. This type of plot is used to graphically evaluate n in equation (18). The values of n are 1.3, 1.04, and 0.87 at 30, 40, and 50° C, respectively. There appears to be a systematic decrease in the value of n with increasing temperature.

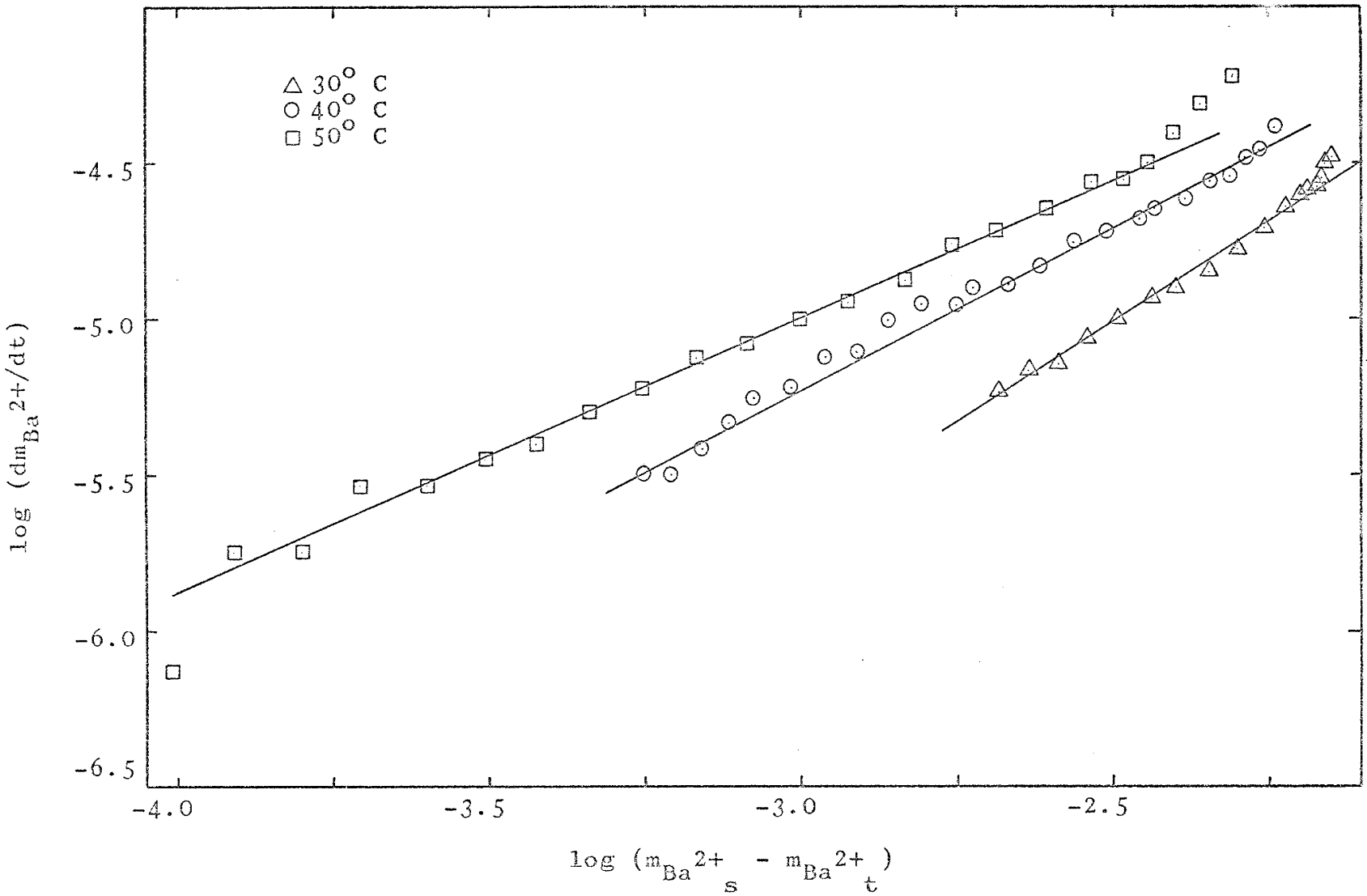
△ 30° C
○ 40° C
□ 50° C
-4.5
-5.0
-5.5
-6.0
-6.5
-4.0
-3.5
-3.0
-2.5
log (dm$_{Ba^{2+}}$/dt)
log ($m_{Ba^{2+}}{}_s$ - $m_{Ba^{2+}}{}_t$)

temperature, being 1.30, 1.04, and 0.87 at 30, 40, and 50° C, respectively. At all three temperatures, the witherite dissolution data for the first 5 minutes depart from the experimental slope. Since the experimental slopes are approximately 1.0, the data were plotted on a log ($m_{Ba^{2+}_s} - m_{Ba^{2+}_t}$) versus time diagram, figure 18. The linearity of the data points shows that the first order reaction, as expressed by equation (25), provides a good data fit.

The parabolic and first order rate laws were tested by predicting $m_{Ba^{2+}}$ as a function of time. As with strontianite dissolution, both rate laws yield adequate results at 30° C for witherite dissolution; however, at 40 and 50° C the first order rate law predicts values of $m_{Ba^{2+}}$ much closer to the experimental data than does the parabolic rate law. Consequently, the first order rate law was chosen to mathematically express witherite dissolution.

Discussion

Activation Energies

For reactions which obey the first order kinetic rate law, the activation energy of the reaction may be calculated by the time to half saturation method, i.e.

$$\ln (k_T) = \ln (A) - (E_a/RT) \qquad (33)$$

where k_T is the appropriate rate constant in sec^{-1}, A is an empirical constant, E_a is the activation energy, R is the gas constant, and T is the absolute temperature. The

Figure 18. Plot of log ($m_{Ba^{2+}_s} - m_{Ba^{2+}_t}$) versus t for witherite dissolution under 0.81 atmosphere P_{CO_2} at temperatures of 30, 40, and 50° C. This plot is based upon the assumption that the overall reaction obeys the first order rate law. Under the experimental conditions the integration constant, C, in equation (25) must equal the molality of Ba^{2+} at saturation, $m_{Ba^{2+}_s}$.

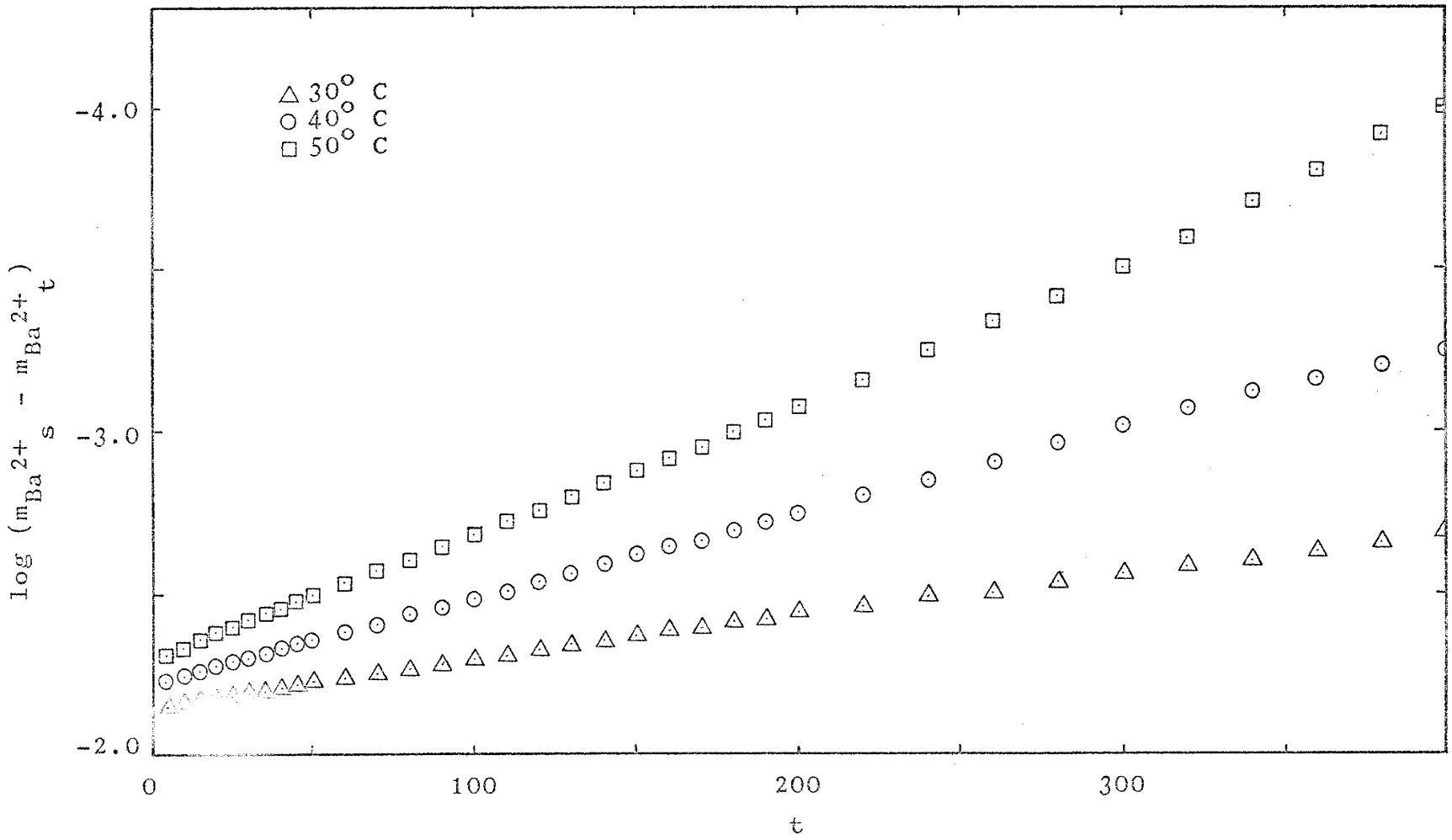
△ 30° C
○ 40° C
□ 50° C
-4.0
-3.0
-2.0
0
100
200
300
t
Log ($m_{Ba^{2+}}$ s - $m_{Ba^{2+}}$ t)

empirical reaction orders of strontianite and witherite dissolution are not precisely 1.0 as shown in figures 12 and 17. However, because the first order rate law provides a satisfactory data fit, the time to half saturation method may be employed with sufficient precision to determine whether or not the dissolution reactions are diffusion controlled [$E_a \cong 4.5$ kilocalories (Liu and Nancollas, 1971)].

Figure 19, a plot of ln (k_T) versus 1/T (discussed on pages 19 and 20), was constructed for the experimental temperatures of 303, 313, and 323° K. The calculated activation energies, using equation (33), are 8.4 kilocalories per mole for strontianite dissolution and 10.0 kilocalories per mole for witherite dissolution. These activation energies should be accurate to within 10% according to Benson's (1960) error estimating procedure; however, a confidence limit of 15% is preferred to account for any additional errors. This second value is approximately the same as that used by Liu and Nancollas (1971) for the dissolution of gypsum.

Controlling Process Far From Equilibrium

Strontianite dissolution was investigated far from equilibrium at various constant pH values and at various partial pressures of carbon dioxide at a fixed pH. The first series of experiments resulted in data which described the effect of a dissociated acid on the dissolution rate. Under the experimental conditions the dissolution

Figure 19. Plot of the natural logarithm of the overall rate constant versus 1/T. The rate constant, from equation (23) is expressed in reciprocal seconds and is temperature dependent. The temperature, T, is in degrees Kelvin. Use of the Arrhenius equation (33) permits evaluation of the activation energy, E_a, from the slope of the best fit lines for the experimental data. The slope, E_a/R, for witherite dissolution is 5.0×10^3 which yields an activation energy of 10.0 kilocalories. The slope for strontianite dissolution is 4.2×10^3 which yields an activation energy of 8.4 kilocalories.

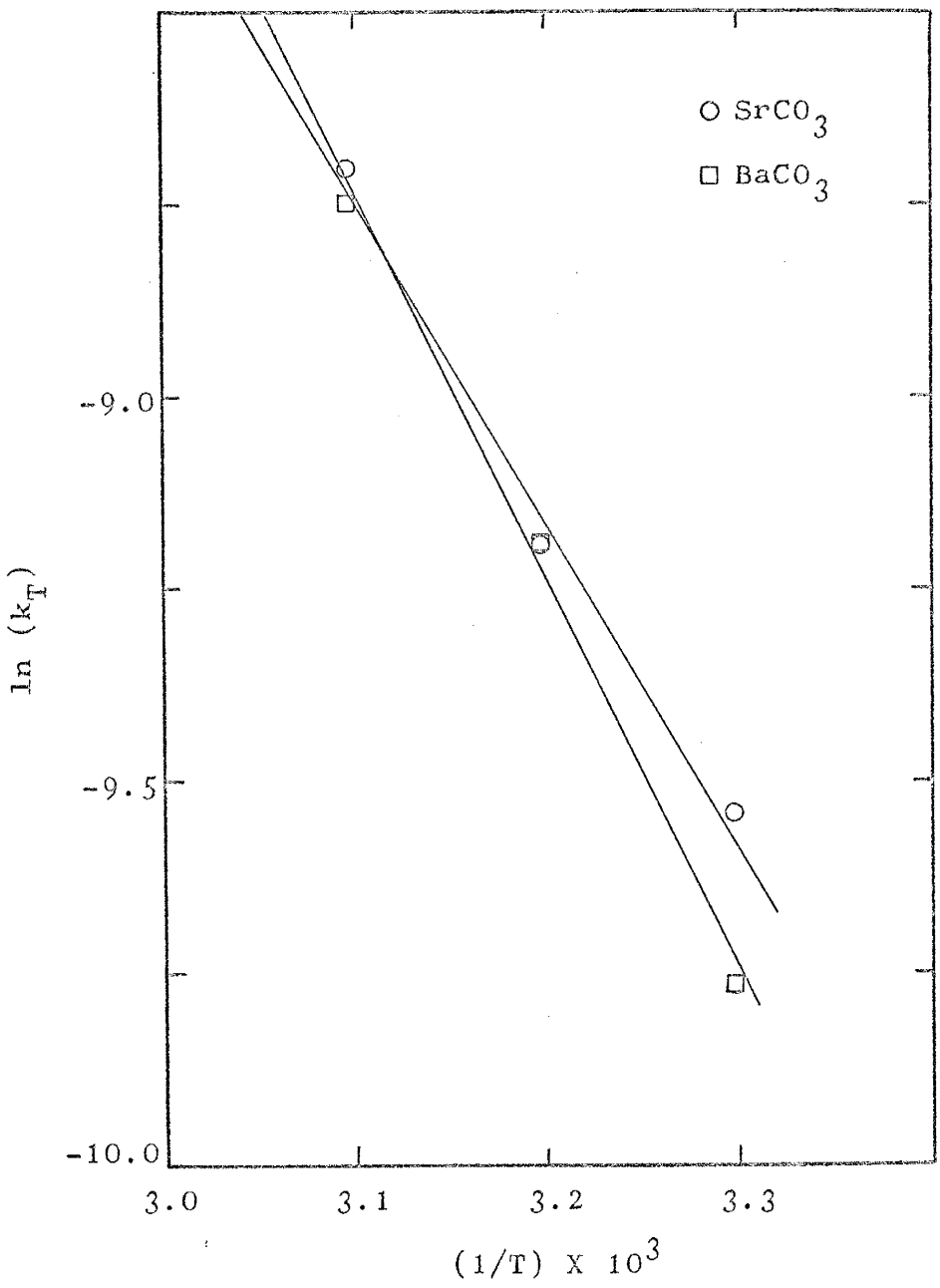
O SrCO3
□ BaCO3
-9.0
-9.5
-10.0
ln (kT)
3.0
3.1
3.2
3.3
(1/T) X 10^3

rate may be expressed as

$$\underline{R} = k_1(a_{H^+})^{0.92} + k_2(a_{H^+})^{0.13} \qquad (46)$$

The investigation of the effect of the partial pressure of carbon dioxide showed that the rate of reaction did not increase proportionally with the increase in associated acid (figure 6) and that the data were compatible with the Langmuir adsorption isotherm. The assumption necessary to reach the second conclusion was that the corrected reaction rate, $\underline{R}_T'$ in equation (51), could be attributed to the change in the partial pressure of carbon dioxide. Combining the separate experiments results in a rate equation of the form

$$\underline{R} = k_1(a_{H^+})^{0.92} + k_2(a_{H^+})^{0.13} + \frac{aP_{CO_2}}{1 + bP_{CO_2}} \qquad (54)$$

This equation is experimentally valid at 40° C, at pH values ranging from 1.5 to 6.5 when $P_{CO_2} = 0$, and at pH = 4.5 when P_{CO_2} ranges from 0.0 to 0.81 atmosphere.

The observed kinetic phenomena may be interpreted as the reactions of a dissociated acid, H^+, and an associated acid, H_2CO_3, at the mineral surface. The mineral surface must have alternating zones of opposite charge because the lattice is not complete at the surface. If the mineral surface is represented symbolically as

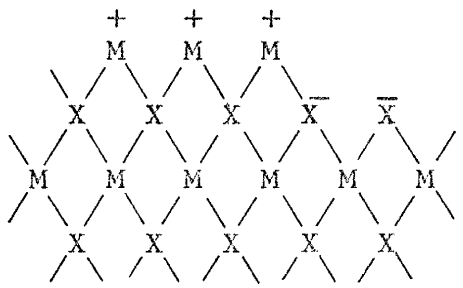

where a residual positive charge, +, is associated with the lattice cation, M, and a residual negative charge, -, is associated with the lattice anion group, X. For experiments run under a nitrogen atmosphere, the value of ($m_{Me}^{2+}{}_{s}$ - $m_{Me}^{2+}{}_{t}$) is infinite with respect to strontianite saturation if H_2CO_3 is removed from the system. Therefore, the rate limiting step is interpreted to be the interaction of a hydrogen ion at an anion position on the surface.

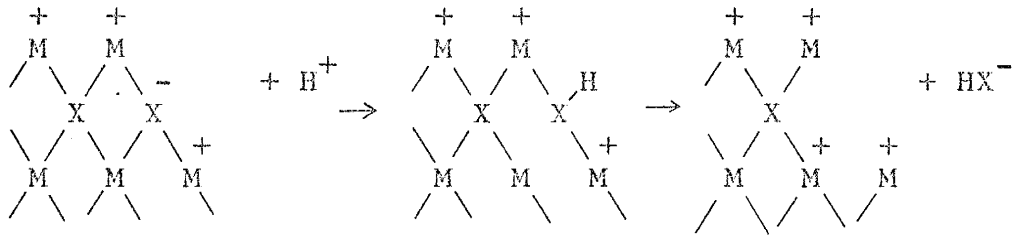

This process should result in a weakening of the ionic lattice bonds and should be followed by removal of the lattice cation, which would result in a layered or stepwise dissolution of the mineral surface. At pH values less than 4.0 hydrogen ion penetration beyond the surface layer probably occurs. Photomicrographs of calcite grains dissolved at varying pH values (Berner and Morse, 1974, p. 118-119) show rounding and pitting of calcite grains immersed in an aqueous solution with was maintained at a pH of 3.9. This hydrogen ion mechanism is associated with the linear region (low pH) of figure 4 which is a plot of reaction rate

reaction rate versus pH.

Similarly, the electrically neutral carbonic acid molecule may be attracted to the mineral surface because of the electrical assymmetry of the molecule. The deprotonation reaction would require the breaking of an O-H bond and the formation of a new O-H bond at the mineral surface, represented as

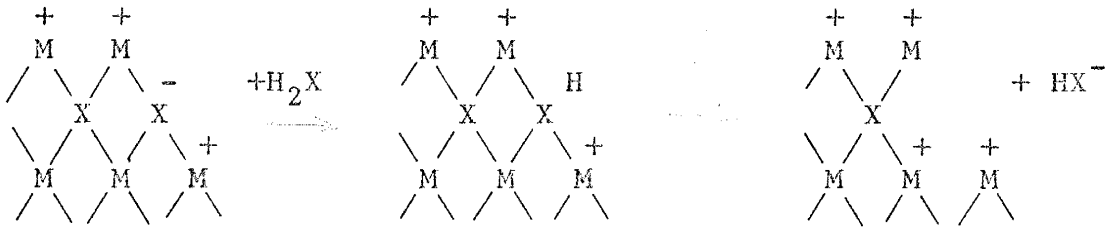

where H_2X is H_2CO_3 and HX^- is HCO_3^-. With the carbonate ion removed from the lattice, the lattice cation would be less strongly bonded to the mineral surface.

The relative effectiveness of free acid, H^+, and associated acid, H_2CO_3, can be compared in terms of reaction rate constants from the experimental data. The rate of acid addition at pH = 4.5 under a nitrogen atmosphere was 0.109 ml/min and with P_{CO_2} = 0.81 atmosphere was 0.869 ml/min. Assuming a first order reaction for hydrogen ion catalysis yields

$$0.109 \text{ ml/min} = k_1(a_{H^+})$$

for which $k_1 = 10^{+3.54}$ ml/min. Subtracting the contribution for this reaction and assuming a first order reaction for H_2CO_3 catalysis yields

$$0.76 \text{ ml/min} = k_2(a_{H_2CO_3})$$

for which $k_2 = 10^{+1.61}$ ml/min. Thus the ratio of k_1/k_2 is approximately 100 to 1 under these conditions.

The normal approach to general acid catalysis for reactions which do not consume the hydrogen ion suggests that the reaction rate shift should be proportional to the activity of the associated acid multiplied by its acid dissociation constant (Benson, 1960). This may be expressed as

$$\underline{R}_T' = G_{H_2CO_3}(K_{H_2CO_3})^{\alpha} a_{H_2CO_3} = k_a(a_{H_2CO_3}) \qquad (55)$$

where $G_{H_2CO_3}$ is a constant for acids with the H_2CO_3 structure, $K_{H_2CO_3}$ is the first dissociation constant for carbonic acid $a_{H_2CO_3}$ is the activity of carbonic acid, α is an empirical constant such that $0<\alpha<1$, and k_a is the general acid catalysis constant. This constant, k_a, is usually at least two orders of magnitude less than the unassociated acid catalysis rate constant (Laidler, 1950; Hammett, 1970). For H^+ and H_2CO_3, $k_1 \cong 100\ k_2$.

The structure constant, G, is usually close to unity, so for carbonic acid catalysis α is about 0.31. The standard interpretation of the α value is that it represents the fractional degree of proton transfer in the transition state. The transition state is thought to consist of the formation of an activated complex such as

$$CO_3^{2-}\cdots H^{+\delta}\cdots O^{-\delta}-C(=O)-OH$$

at the lattice anion position.

The available data imply that for dissolution far from

equilibrium adsorption reactions with two aqueous species, H^+ and H_2CO_3, limit the dissolution rate. Methods applicable for reactions which do not consume hydrogen ions, true catalytic reactions, suggest that the free hydrogen ion is about 100 times more effective than carbonic acid as a dissolution catalyst.

Controlling Process Approaching Equilibrium

Interpretation of the rate controlling processes from mathematical expressions is an inductive process (Gardiner, 1969). The model proposed to explain experimental data may be completely invalid yet its equation may describe the system investigated with good precision. The following discussion uses the principle of employing the least complicated model consistent with the available experimental data and uses data for the mean experimental temperature of 40° C. Kinetic expressions compatible with the observed overall reaction rate are discussed, tested against the calculated back reaction, and interpreted with respect to the dissolution mechanism.

Investigations by Plummer (1972) and Berner and Morse (1974) of calcite dissolution in the vicinity of equilibrium have shown that the dissolution rate can be expressed in terms of the activity of hydrogen ion at the time of interest minus the activity of hydrogen ion at saturation, $(a_{H^+_t} - a_{H^+_s})$. Figure 20 shows the relationship between hydrogen ion activity as log $(a_{H^+_t} - a_{H^+_s})$ and log $\underline{R}$ for

Figure 20. Plot of log $\underline{R}$ versus log $(a_{H^+_t} - a_{H^+_s})$ for strontianite dissolution at 40° C under 0.81 atmosphere P_{CO_2}. The slopes, which are interpreted to represent molecularities of 2/3, 1/3, and 1/6, are 0.71, 0.31, and 0.14 for lines A, B, and C respectively.

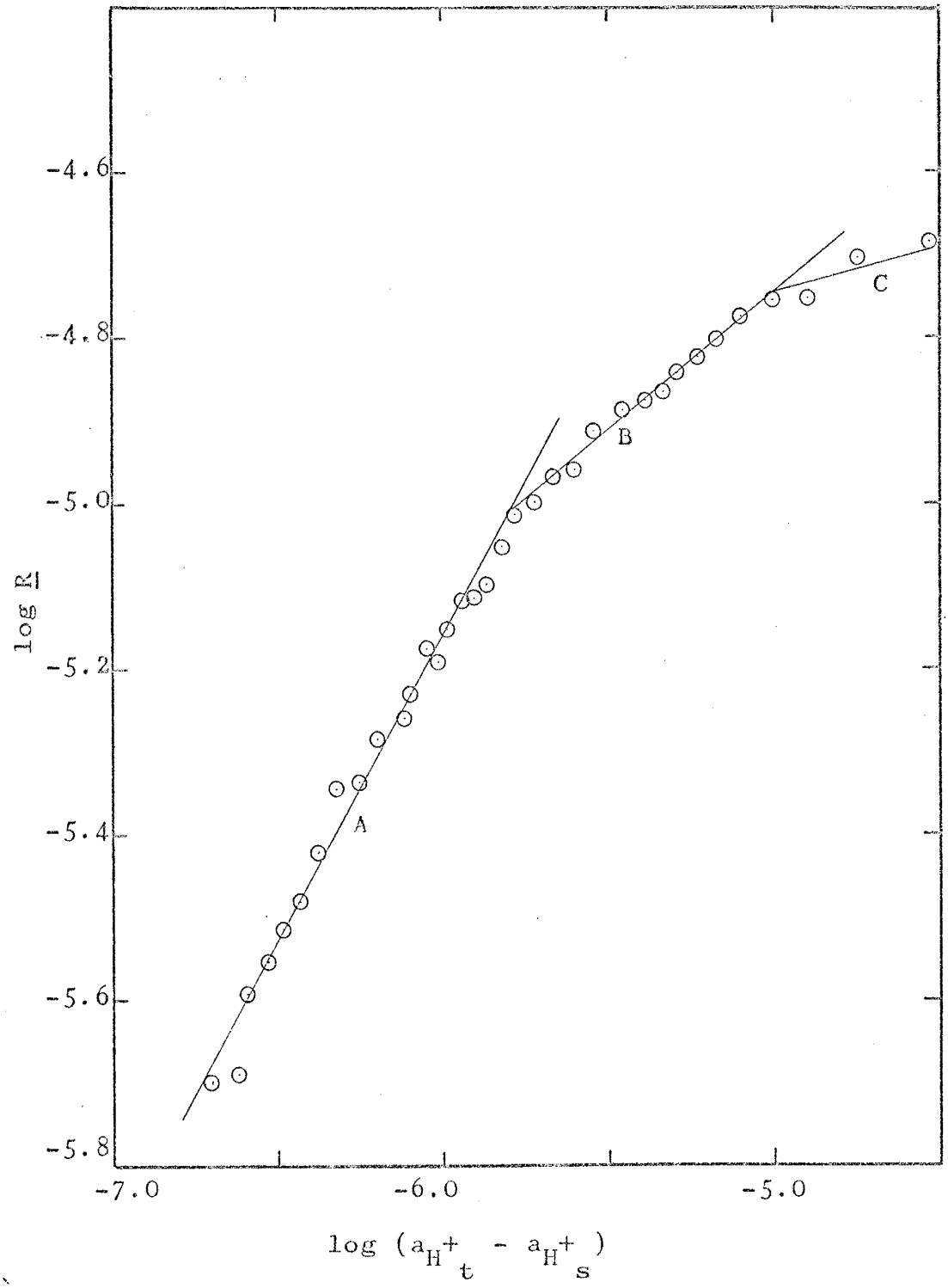
-4.6
-4.8
-5.0
-5.2
-5.4
-5.6
-5.8
log R
-7.0
-6.0
-5.0
log ($a_{H^+}{}_t$ - $a_{H^+}{}_s$)
A
B
C

strontianite dissolution. The first order rate law requires that the data as plotted behave linearly and have a slope of approximately one. The data for strontianite dissolution do not fulfill these requirements. By dividing the data into three groups, the linear relationships A, B, and C with slopes of 0.71, 0.31, and 0.14 may be defined. Line C, defined by only four data points, may not be necessary. Each of these linear relationships represent different stages of the reaction progress and are compatible with equation (26) which is used with reactions other than first order where the slope of the line, n, is the assumed molecularity. A plot of the witherite dissolution data, figure 21, lines A, B, and C have slopes of approximately 1, $\frac{1}{2}$, and $\frac{1}{4}$, respectively. The data for strontianite and witherite may be interpreted as having different stages, with different molecularities of the rate limiting mechanisms, related to the adsorption of H^+ at the mineral surface.

The linearity of the data and slope of approximately one shown in figures 22 and 23 indicate that the dissolution of strontianite and witherite can be more simply interpreted in terms of reactant removal from the mineral surface. Only one reaction mechanism is required to explain the kinetic behavior over most or all of the experimental range. Furthermore, plots of log ($m_{Me^{2+}_s} - m_{Me^{2+}_t}$) versus time, figures 24 and 25, show that the experimental data are compatible with equation (25) for first order kinetics.

Figure 21. Plot of log $\underline{R}$ versus log $(a_{H^+_t} - a_{H^+_s})$ for witherite dissolution at 40° C under 0.81 atmosphere P_{CO_2}. The slopes, which are interpreted to represent molecularities of 1, 1/2, and 1/4, are 1.01, 0.52, and 0.26 for lines A, B, and C, respectively.

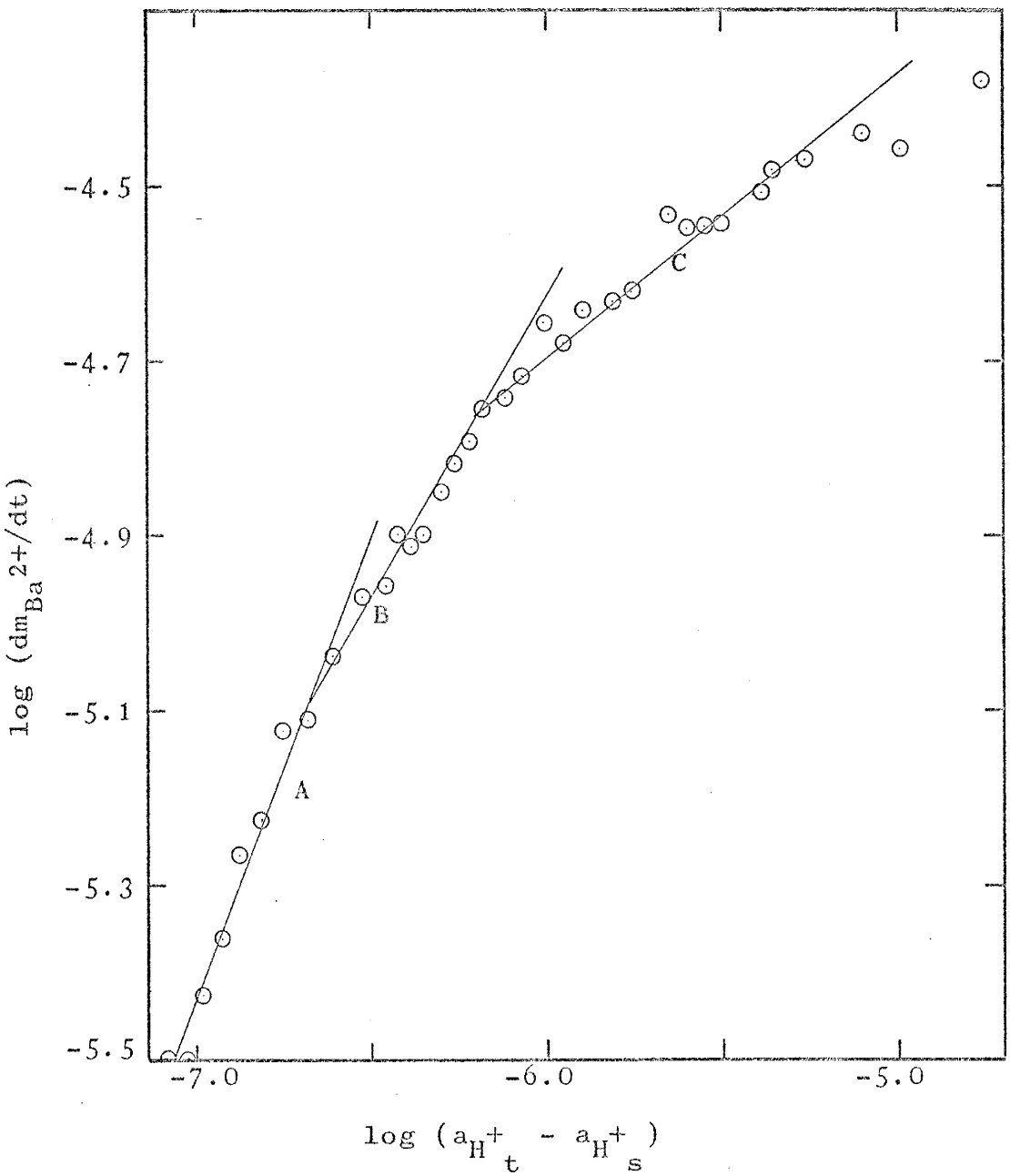
-4.5
-4.7
-4.9
-5.1
-5.3
-5.5
-7.0
-6.0
-5.0
A
B
C
log ($dm_{Ba^{2+}}/dt$)
log ($a_{H^+}{}_t - a_{H^+}{}_s$)

Figure 22. Plot of log R versus log ($m_{Sr^{2+}_s} - m_{Sr^{2+}_t}$) for strontianite dissolution at 40° C and P_{CO_2} = 0.81 atmosphere. The slope is 1.05.

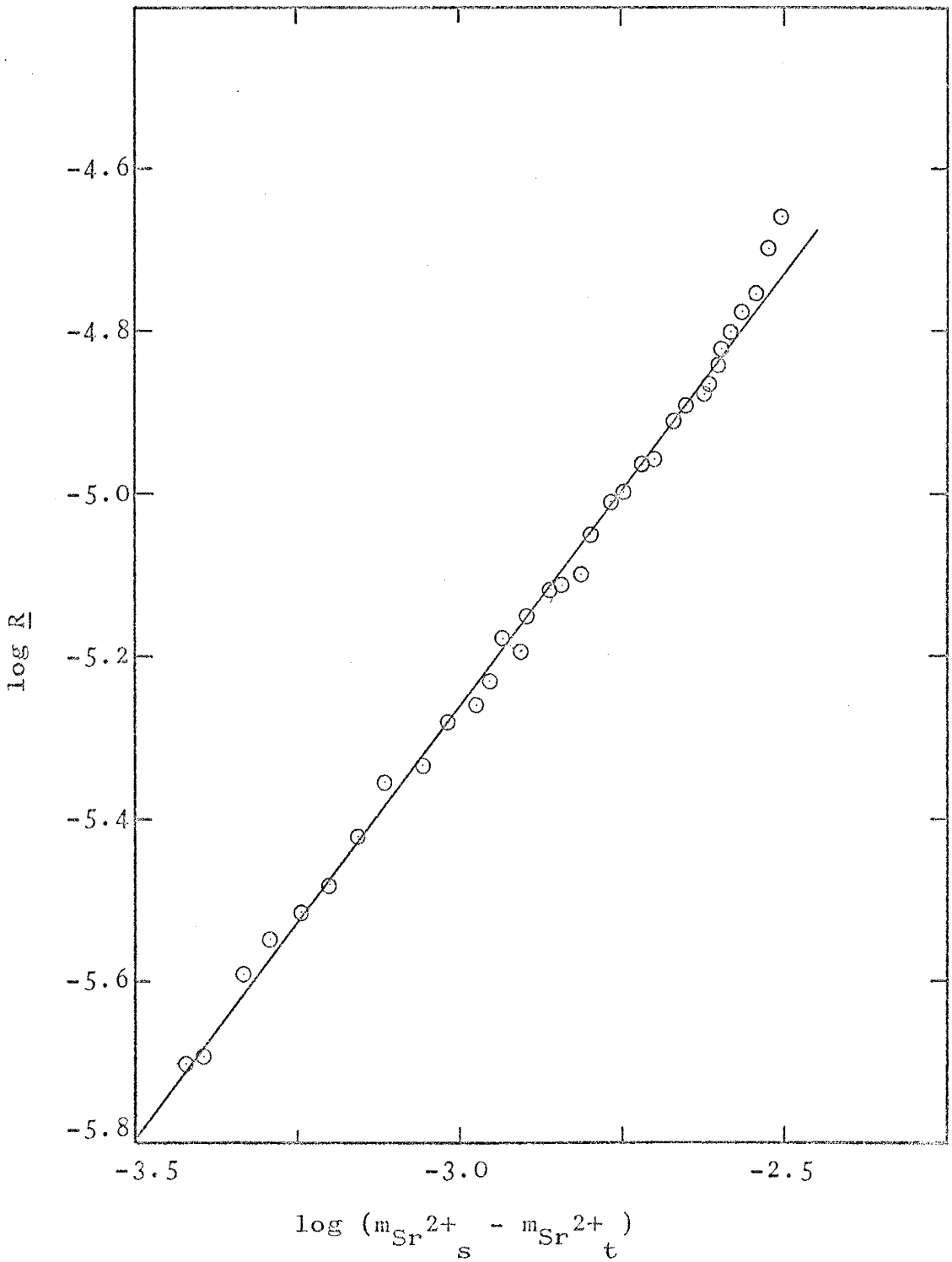
-4.6
-4.8
-5.0
-5.2
-5.4
-5.6
-5.8
log R
-3.5
-3.0
-2.5
log ($m_{Sr^{2+}}$ s - $m_{Sr^{2+}}$ t)

Figure 23. Plot of log R versus log ($m_{Ba^{2+}_s} - m_{Ba^{2+}_t}$) for witherite dissolution at 40° C and P_{CO_2} = 0.81 atmosphere. The slope is 1.0.

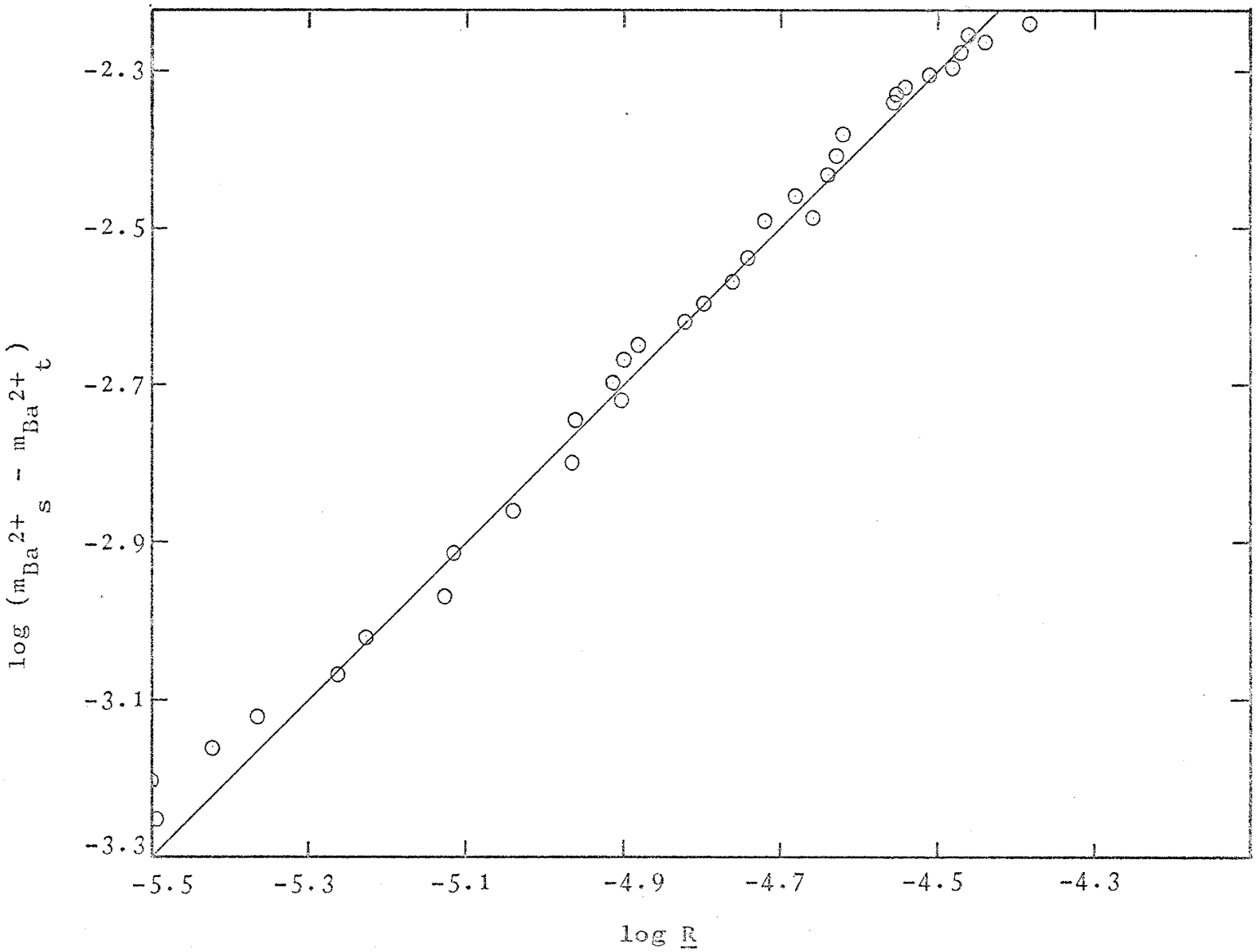
-2.3
-2.5
-2.7
-2.9
-3.1
-3.3
-5.5
-5.3
-5.1
-4.9
-4.7
-4.5
-4.3
log ($m_{Ba^{2+}}{}_s$ - $m_{Ba^{2+}}{}_t$)
log R

Figure 24. Plot of log ($m_{Sr^{2+}_s} - m_{Sr^{2+}_t}$) versus time in minutes for strontianite dissolution at 40° C and $P_{CO_2} = 0.81$ atmosphere. The slope of the line, 2.28×10^{-3}, is the rate constant, k, in min^{-1}.

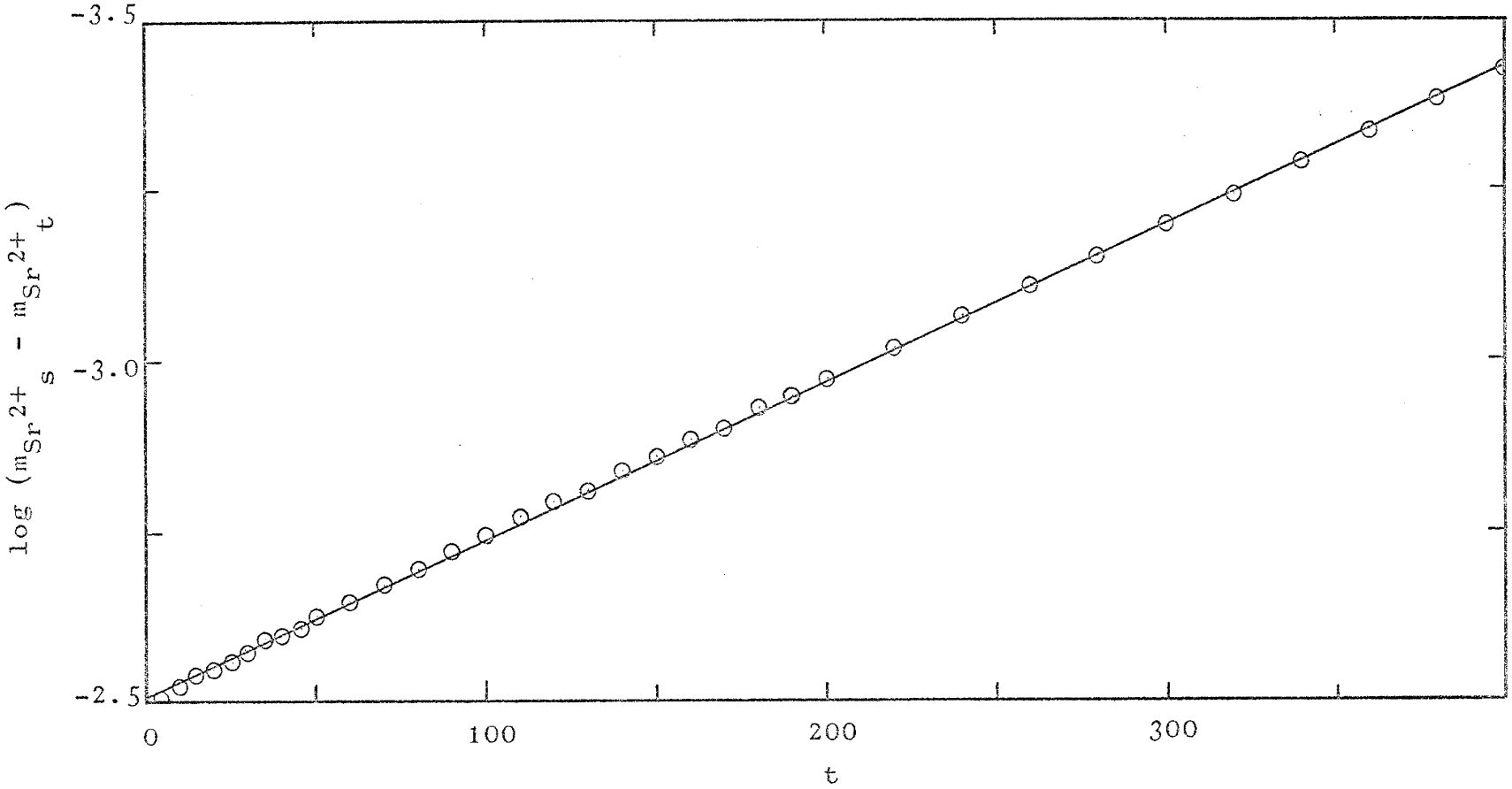
-3.5
-3.0
-2.5
0
100
200
300
t
log ($m_{Sr^{2+}}$ s - $m_{Sr^{2+}}$ t)

Figure 25. Plot of log ($m_{Ba^{2+}_s} - m_{Ba^{2+}_t}$) versus time in minutes for witherite dissolution at 40° C and P_{CO_2} = 0.81 atmosphere. The slope of the line, 2.65 x 10^{-3}, is the rate constant, k, in min^{-1}.

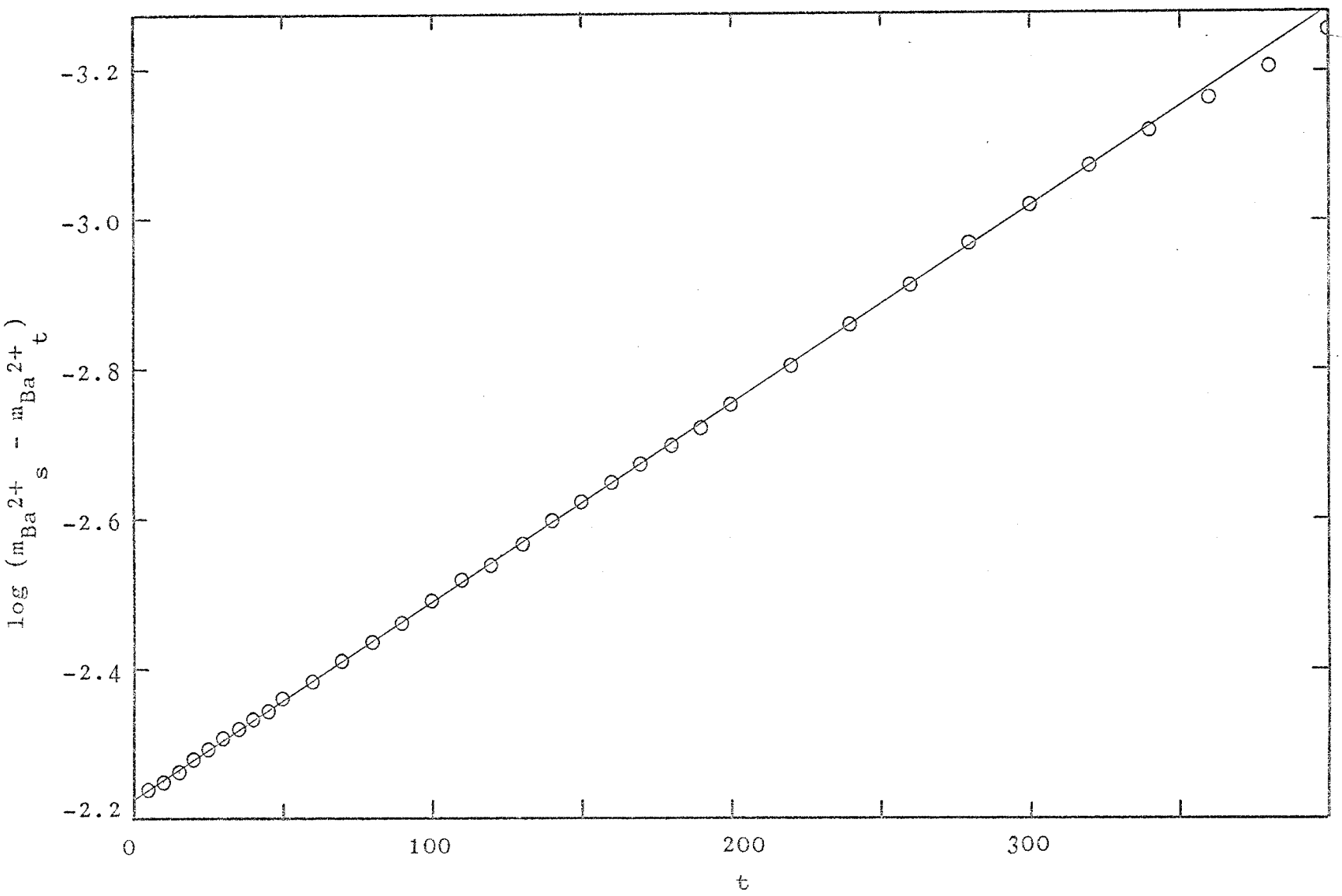
-3.2
-3.0
-2.8
-2.6
-2.4
-2.2
0
100
200
300
t
log ($m_{Ba^{2+}}{}_s - m_{Ba^{2+}} t$)

The first order relationship between $\underline{R}$ and ($m_{Me^{2+}_s} - m_{Me^{2+}_t}$) should also be valid using HCO_3^- as a variable; since, for the experiments which approach equilibrium, the dissolution reaction is

$$MeCO_{3(s)} + H_2CO_3 = Me^{2+} + 2HCO_3^- \qquad (56)$$

and electrical neutrality is largely maintained by increasing HCO_3^- concentrations. Figures 26 and 27 are plots of log $\underline{R}$ versus log ($m_{HCO_3^-_s} - m_{HCO_3^-_t}$) and ($m_{HCO_3^-_s} - m_{HCO_3^-_t}$) versus time for strontianite dissolution at 40° C. These figures show that there is essentially no difference in the quality of fit for a first order reaction controlled by ($m_{HCO_3^-_s} - m_{HCO_3^-_t}$) or ($m_{Sr^{2+}_s} - m_{Sr^{2+}_t}$). The same situation is true for witherite dissolution at 40° C. The dependence upon $m_{HCO_3^-}$ might be interpreted as either an adsorption reaction of an associated acid at the mineral surface or combined with $m_{Me^{2+}}$ dependence, as a precipitation (i.e. back) reaction at the mineral surface.

To test these mechanisms for precipitation control of the overall rate, certain preliminary assumptions were made. They are that the concentration of carbonic acid, H_2CO_3, is constant throughout the experimental runs and does not cause changes in the reaction rate during these runs. Aqueous diffusion is not considered to be the rate limiting step for the dissolution of strontianite and witherite because of the constant reaction rates under stirred and unstirred

Figure 26. Plot of log R versus log ($m_{HCO_3^-}{}_s$ - $m_{HCO_3^-}{}_t$) for strontianite dissolution at 40° C and P_{CO_2} = 0.81 atmosphere. The slope, 1.05, is the same as in figure 22, using the variable log ($m_{Sr^{2+}}{}_s$ - $m_{Sr^{2+}}{}_t$).

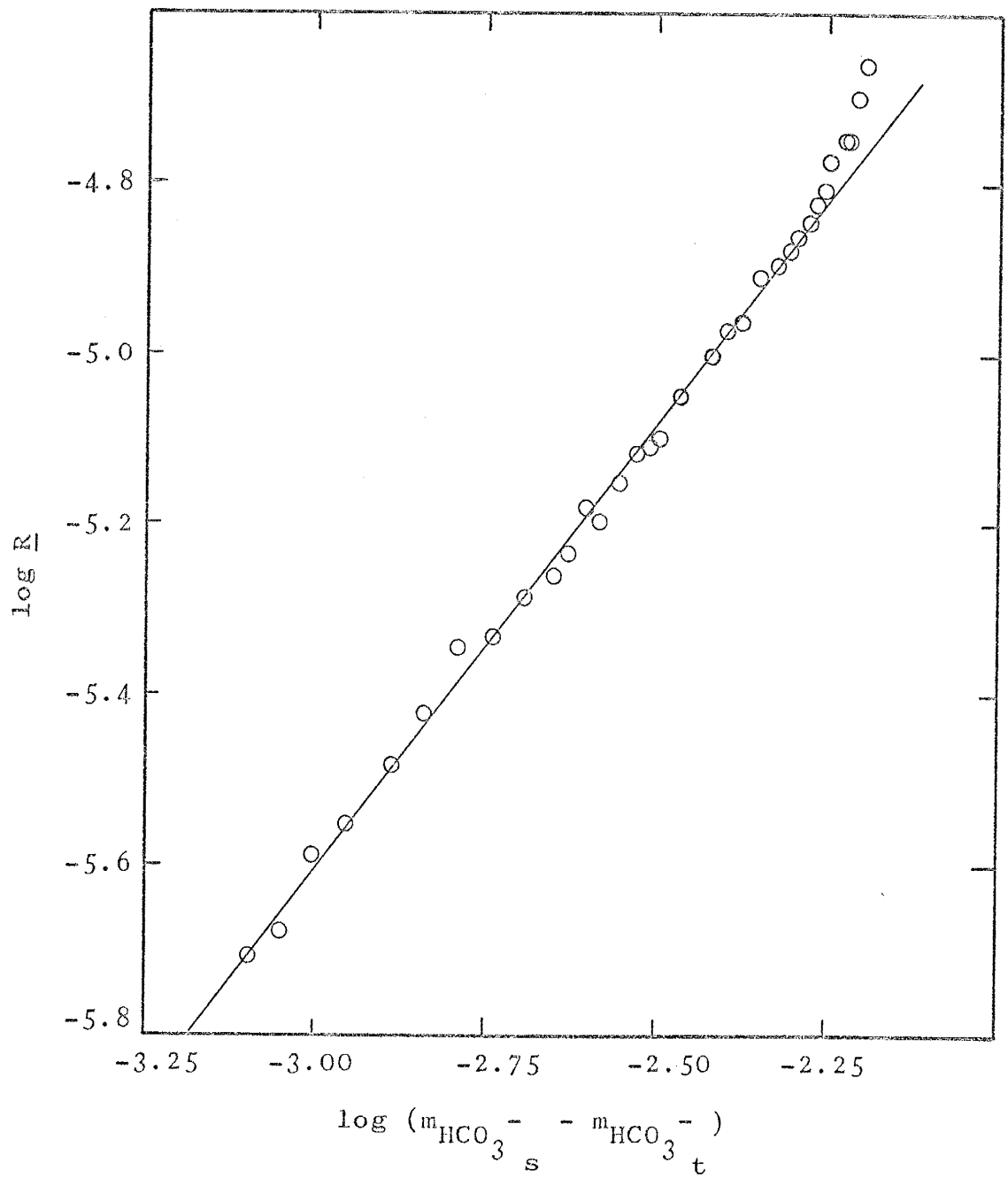
-4.8
-5.0
-5.2
-5.4
-5.6
-5.8
log R
-3.25
-3.00
-2.75
-2.50
-2.25
log ($m_{HCO_3^-}$ - $m_{HCO_3^-}$)
s
t

Figure 27. Plot of log ($m_{HCO_3^-}{}_s - m_{HCO_3^-}{}_t$) versus time in minutes for strontianite dissolution at 40° C and P_{CO_2} = 0.81 atmosphere. The slope of the line, 2.29×10^{-3}, is essentially the same as that determined using log ($m_{Sr^{2+}}{}_s - m_{Sr^{2+}}{}_t$).

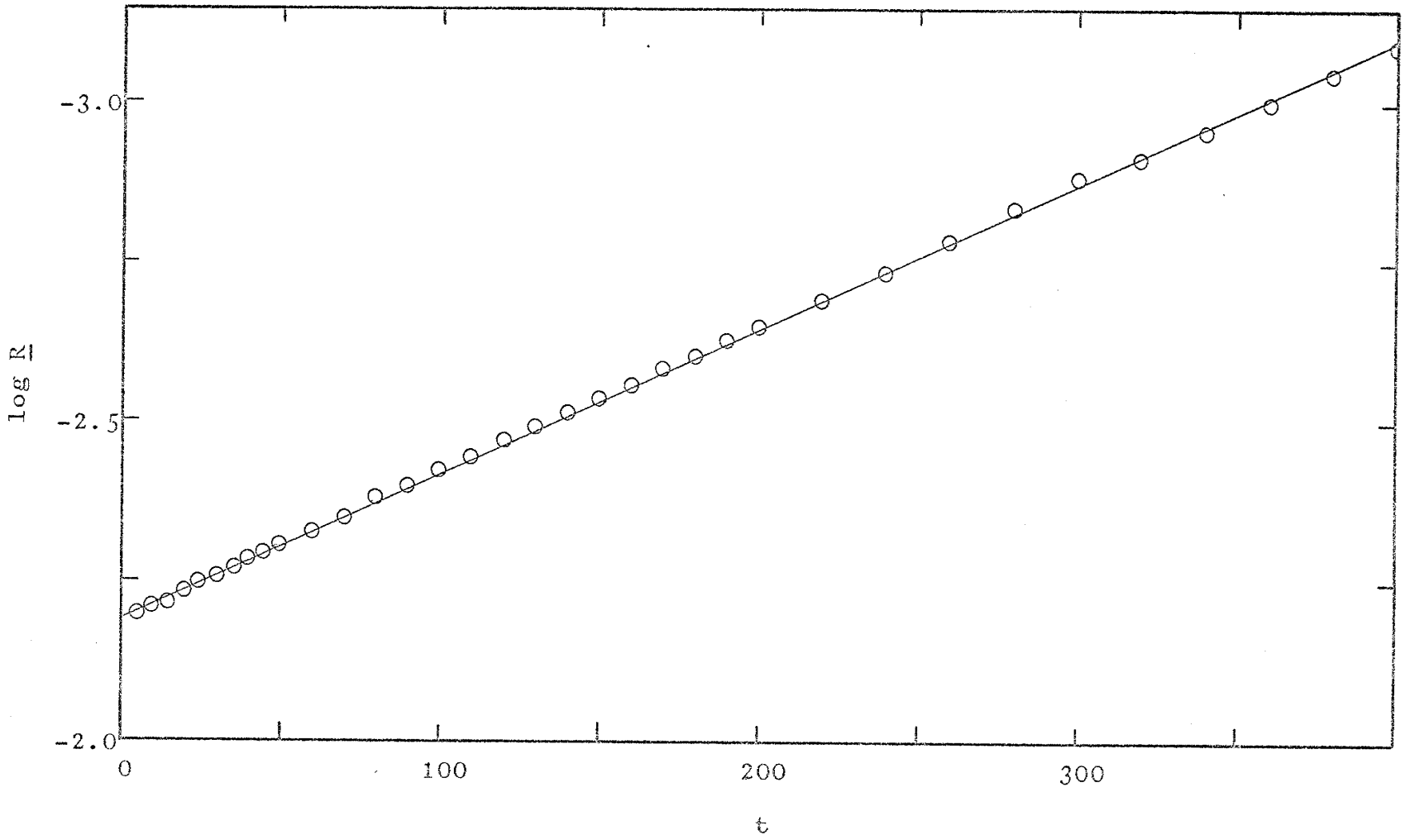
-3.0
-2.5
-2.0
log R
0
100
200
300
t

conditions and because the activation energies are considerably higher than 4.5 kilocalories per mole expected for aqueous diffusion.

The fact that n is approximately equal to 1 suggests that a back reaction is effecting the overall reaction rate. The hypothesis employed is that the mechanism for this surface reaction is the same for dissolution and precipitation (principle of microscopic reversibility). There is no experimental proof to support this hypothesis; but, it is the simplest possible assumption and in the absence of negative evidence is preferred to a more complicated one.

The overall reaction rate which is experimentally determined may be expressed as

$$\underline{R} = \underline{R}_f - \underline{R}_b \qquad (57)$$

where $\underline{R}$ is the overall reaction rate, $\underline{R}_f$ is the forward reaction rate, and $\underline{R}_b$ is the back reaction rate. Two approaches using the rate informtion determined far from equilibrium were employed to determine the forward reaction rate in order to calculate the back reaction rate. Because data far from equilibrium are available only for strontianite dissolution, the discussion of back reaction rates is restricted to strontianite.

One method of calculating the forward reaction rate is to use the data obtained far from equilibrium. Combining the first and third terms of equation (54) into one constant, the predicted forward rate is

$$\underline{R}_f = 3.08 \times 10^{-5} + 8.65 \times 10^{-6} \, (a_{H^+})^{0.13} \qquad (58)$$

if one assumes that the back reaction is not yet significant. A second option is to assume that the forward reaction rate is constant, which means that the forward reaction is zero order reaction. This would be the case if the adsorption of H_2CO_3 at the mineral surface were the rate limiting step for the forward reaction. Table 3 contains the calculated values of $\underline{R}_b$ resulting from the former approach. The back reaction rate was calculated by subtract- the observed reaction rate from the calculated forward reaction rate. Plots of $\underline{R}_b$ versus $(m_{HCO_3^-}{}_s - m_{HCO_3^-}{}_t)$, $m_{HCO_3^-}$, $(m_{Sr^{2+}}{}_s - m_{Sr^{2+}}{}_t)$, and $(a_{Sr^{2+}} \, a_{CO_3^{2-}})/K$ were constructed; the plot of $(a_{Sr^{2+}} \, a_{CO_3^{2-}})/K$ was included to determine if the principle of mass action, equation (14), might be applicable to the back reaction rate. Furthermore, a plot of log $\underline{R}_b$ versus log $(a_{H^+}{}_t - a_{H^+}{}_s)$ was made to determine if hydrogen ion activity might be related to the back reaction in a less complicated manner than log $\underline{R}$ versus log $(a_{H^+}{}_t - a_{H^+}{}_s)$. Both methods of calculating the forward reaction rate yield a non-linear plot for the first 25 minutes of the reaction; however, the calculated back reaction rate using equation (58) provides a better data fit of the variables tested for the period from 30 to 400 minutes. Figure 28, a plot of $\underline{R}_b$ versus $(a_{Sr^{2+}} \, a_{CO_3^{2-}})/K$, demonstrates that for $(a_{Sr^{2+}} \, a_{CO_3^{2-}})/K > 0.3$ a linear relation-

TABLE III. CALCULATED FORWARD AND BACK REACTION RATES

Time in minutes	pH	Calculated $R_f \times 10^5$	Observed $R \times 10^5$	Calculated $R_b \times 10^5$
5	4.513	2.493	2.185	.308
10	4.714	2.467	1.972	.495
15	4.842	2.450	1.778	.672
20	4.941	2.438	1.771	.667
25	5.018	2.428	1.682	.746
30	5.079	2.419	1.561	.858
35	5.130	2.413	1.485	.928
40	5.174	2.407	1.430	.977
45	5.212	2.403	1.359	1.044
50	5.246	2.398	1.322	1.076
60	5.305	2.390	1.279	1.111
70	5.355	2.384	1.231	1.153
80	5.395	2.378	1.094	1.284
90	5.431	2.374	1.076	1.298
100	5.462	2.370	1.002	1.368
110	5.490	2.366	0.970	1.396
120	5.514	2.363	0.883	1.480
130	5.535	2.360	0.814	1.546
140	5.554	2.358	0.772	1.586
150	5.572	2.355	0.764	1.591
160	5.588	2.353	0.706	1.647
170	5.602	2.352	0.640	1.712
180	5.616	2.350	0.662	1.688
190	5.628	2.348	0.585	1.763
200	5.639	2.346	0.550	1.796
220	5.659	2.344	0.519	1.825
240	5.676	2.342	0.460	1.882
260	5.692	2.340	0.450	1.890
280	5.705	2.339	0.379	1.960
300	5.716	2.337	0.329	2.008
320	5.726	2.335	0.307	2.028
340	5.735	2.334	0.282	2.052
360	5.743	2.333	0.256	2.077
380	5.750	2.332	0.228	2.104
400	5.756	2.332	0.198	2.134

Figure 28. Plot of $\underline{R}_b$ versus $(a_{Sr^{2+}} \; a_{CO_3^{2-}})/K$ for strontianite dissolution at 40° C and $P_{CO_2} = 0.81$ atmosphere. A linear relationship exists between the plotted variables once the reaction has proceeded beyond $(a_{Sr^{2+}} \; a_{CO_3^{2-}})/K = 0.3$.

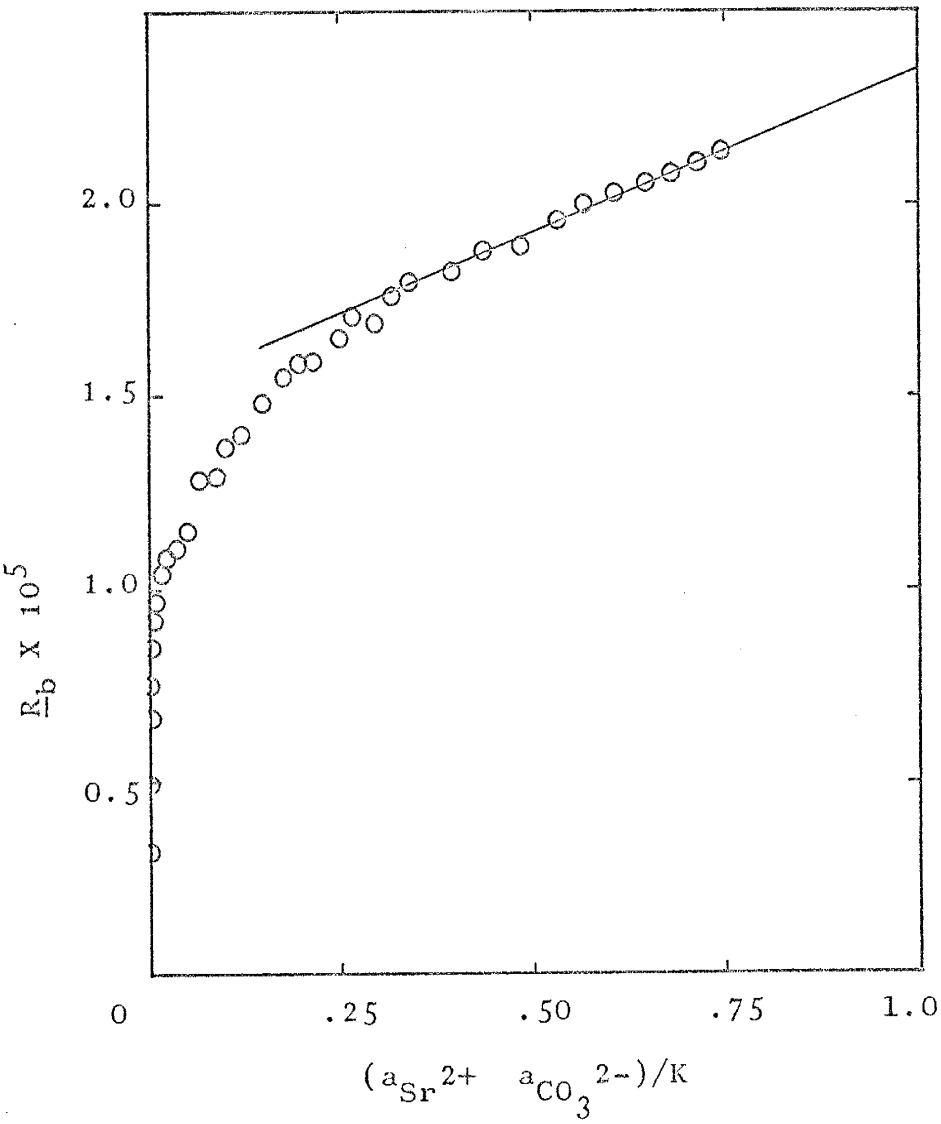
2.0
1.5
1.0
0.5
0
.25
.50
.75
1.0
$\underline{R}_b \times 10^5$
$(a_{Sr^{2+}} \quad a_{CO_3^{2-}})/K$

ship exists between three variables. Consequently, the principle of mass action may be applied to the back reaction as equilibrium is approached and be expressed as

$$\underline{R}_b = k(a_{Sr^{2+}} \quad a_{CO_3^{2-}}) \qquad (59)$$

where $k = 4.0 \times 10^5$. Figure 29, a plot of $\underline{R}_b$ versus $(m_{HCO_3^-}{}_s - m_{HCO_3^-}{}_t)$, represents the best data fit of the investigated variables. The intercept value, or rate at equilibrium, is slightly lower (7%) than predicted from the experimental values determined far from equilibrium, pH = 4.5. The maximum value that $(m_{HCO_3^-}{}_s - m_{HCO_3^-}{}_t)$ can attain is the value at t = 0 and is shown by an X at $\underline{R}_b = 0.0$. A better fit of the data obtained by approaching equilibrium might be possible if the constant and exponent in equation (58) were adjusted; however, this would negate the value of the rate experiments performed far from equilibrium. Figure 30, a plot of $\underline{R}_b$ versus $m_{HCO_3^{2-}}$, demonstrates that substituting $m_{HCO_3^{2-}}$ for $(m_{HCO_3^{2-}}{}_s - m_{HCO_3^{2-}}{}_t)$ does not improve the quality of the data fit.

Because the forward reaction rate appears to be controlled by proton adsorption at the mineral surface, it is logical to assume that the correspondence between the back reaction rate and $m_{HCO_3^-}$ represents a deprotonation reaction. In the following discussion, supporting evidence for this conclusion is provided by experiments conducted to determine

Figure 29. Plot of $\underline{R}_b$ versus $(m_{HCO_3^-}{}_s - m_{HCO_3^-}{}_t)$ for strontianite dissolution at 40° C and P_{CO_2} = 0.81 atmosphere. Projection of the data to saturation ($m_{HCO_3^-}{}_s = m_{HCO_3^-}{}_t$) yields a rate of 2.34×10^{-5} min^{-1}. $\underline{R}_b$ was calculated using equation (58) as discussed in the test; the calculated value at the equilibrium pH, 5.81, is 2.325×10^{-5} min^{-1}. This close agreement supports the internal consistency of the values used for m_{i_s} and m_{i_t}. The symbol X denotes the value of $(m_{HCO_3^-}{}_s - m_{HCO_3^-}{}_t)$ at time t = 0.

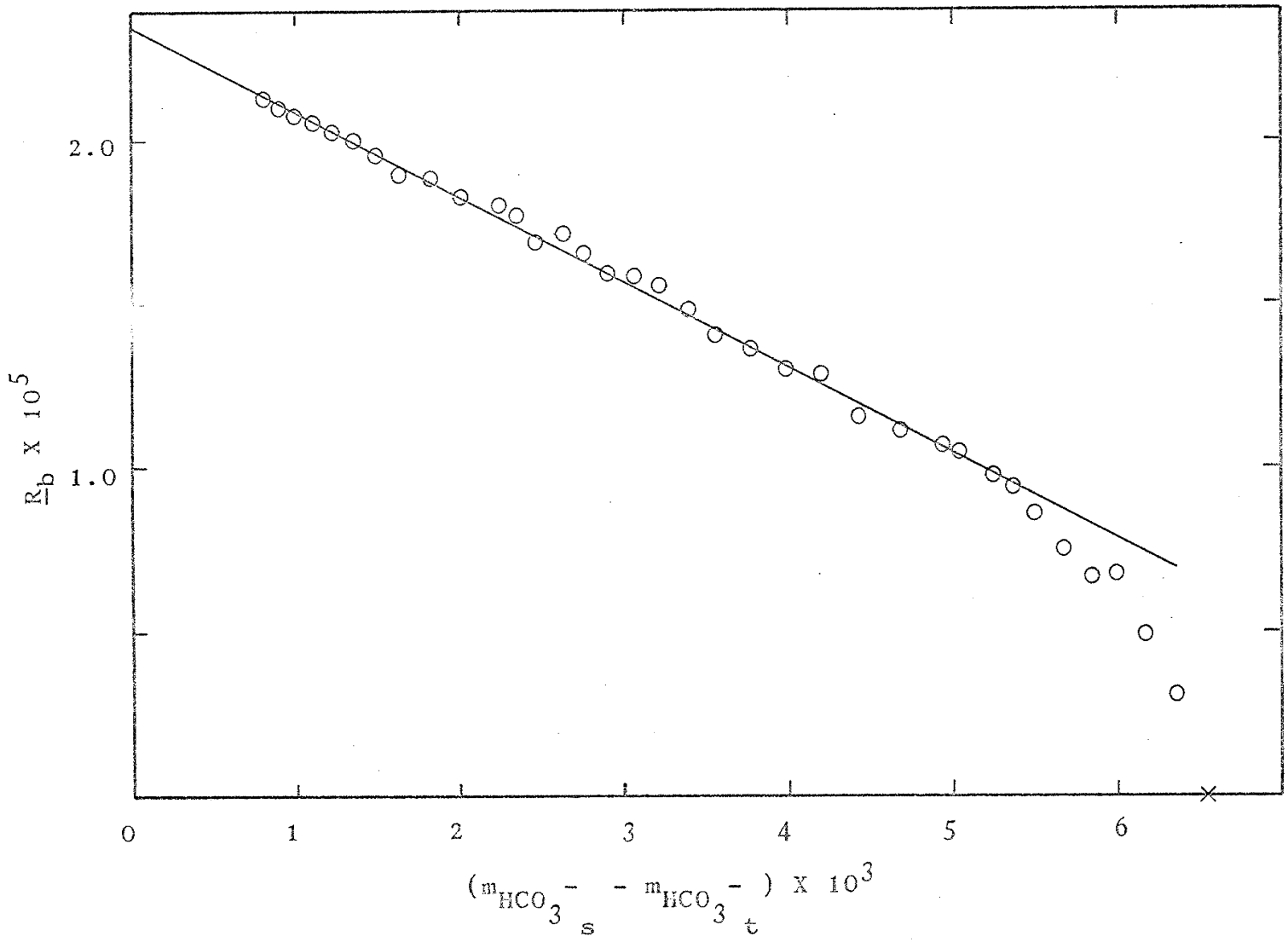
2.0
1.0
$\underline{R}_b \times 10^5$
0
1
2
3
4
5
6
$(m_{HCO_3^-}{}_s - m_{HCO_3^-}{}_t) \times 10^3$

Figure 30. Plot of $\underline{R}_b$ versus $m_{HCO_3^-}$ for strontianite dissolution at 40° C and P_{CO_2} = 0.81 atmosphere. Comparison with figure 29 shows that both $m_{HCO_3^-}$ and $(m_{HCO_3^-}{}_s - m_{HCO_3^-}{}_t)$ are non-linear with respect to $\underline{R}_b$ during the first 25 minutes of the dissolution reaction.

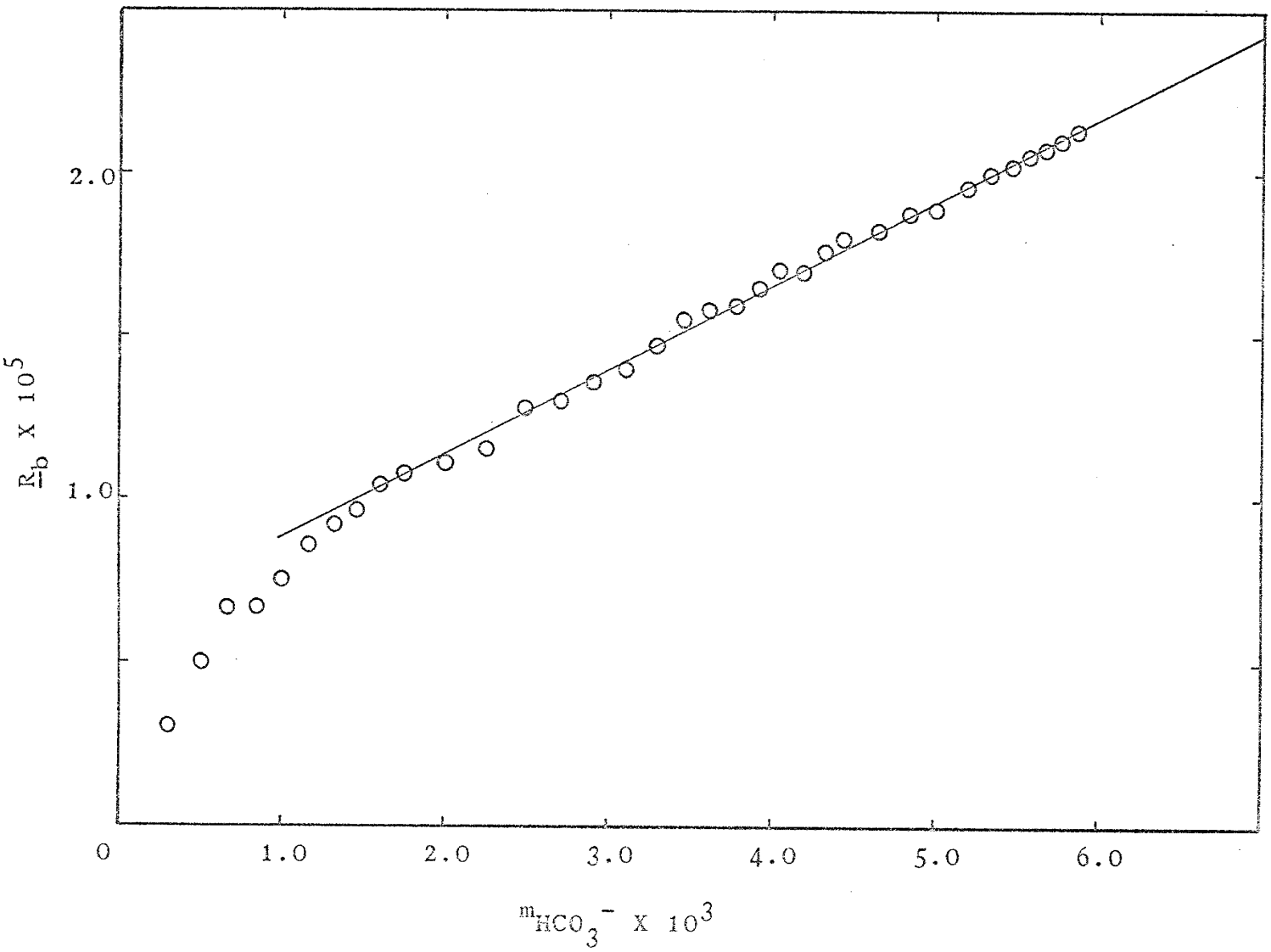
2.0
1.0
0
1.0
2.0
3.0
4.0
5.0
6.0
$\underline{R}_b \times 10^5$
$m_{HCO_3^-} \times 10^3$

the surface charge of calcite.

The zero point of charge, ZPC, of a mineral is the pH at which the mineral surface has an equal amount of positive and negative charges. At lower pH values the surface contains an excess of positive charges which are balanced by an excess of anions in the counter ion layer adjacent to the mineral surface. Theoretically, the ZPC should have as a value of the pH of minimum solubility for a mineral which dissolves congruently (Somasundaran and Agar, 1967). Using various techniques, Somasundaran and Agar (1967) determined that the ZPC for calcite was positive for pH's less than eight and interpreted the surface charge to be controlled by Ca species. The experimental changes in pH which they observed closely agree with those predicted from thermodynamic data. All alkaline earth carbonates would be expected to behave in a similar fashion, and as long as the pH increases during dissolution the surface charge should still be positive (cf. Parks, 1967; Stumm and Morgan, 1970, p. 479). Consequently, the strontianite and witherite mineral surfaces are believed to have been positively charged during the dissolution experiments which approached equilibrium.

Adsorbed ions in the fixed layer on the mineral surface effect the surface charge; however, the charge of the lattice ions which are most abundant on the mineral surface control the overall surface charge (cf. Parks, 1967). Therefore, it is reasonable to assume that Sr and Ba ions

predominate on the mineral surface (cf. Somasundaran and Agar, 1967). If the back reaction at the mineral surface is represented schematically as

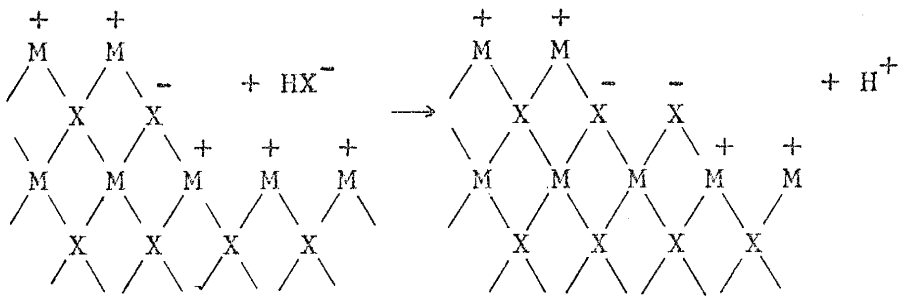

either the adsorption of the bicarbonate ion, HX^-, or the breaking of an O–H bond constitute the rate limiting process.

The positive surface charge suggested for strontianite and witherite under the experimental conditions is in agreement with the rate limiting steps proposed both for dissolution and precipitation. For dissolution, protonation of the CO_3^{2-} lattice ion and desorption as HCO_3^- would result in a stepwise removal of the surface layer and in a positive surface charge. Similarly, the precipitation mechanism would be dependent upon HCO_3^- ion adsorption and deprotonation. The positive surface charge implies that lattice cations are present in abundance and that precipitation is controlled by HCO_3^-.

SUMMARY AND SUGGESTIONS FOR FUTURE WORK

This study was undertaken to investigate the dissolution kinetics of barium and strontium carbonates. The major conclusions are:

1) Strontianite and witherite dissolution approaching equilibrium appears to be controlled by a surface reaction for the conditions investigated. Their dissolution rates were not effected by different stirring conditions and their calculated activation energies, 8.4 and 10.0 kilocalories respectively, are considerably greater than would be expected for an aqueous diffusion rate controlling mechanism.

2) Strontianite dissolution, far from equilibrium for pH values ranging from 1.5 to 6.5 and with a continuously renewed N_2 gas phase, may be expressed by the equation

$$dm_{Sr^{2+}}/dt = k_1(a_{H^+})^{0.92} + k_2(a_{H^+})^{0.13}$$

where $k_1 \cong 2.4 \times 10^3\ k_2$. The rate limiting step is believed to be protonation of the CO_3^{2-} lattice anion.

3) Strontianite dissolution, far from equilibrium at a pH of 4.5 and with a continuously renewed N_2-CO_2 gas phase, may be expressed by

the following equation employing the Langmuir adsorption isotherm

$$dm_{Sr^{2+}}/dt = k_3 + \frac{aP_{CO_2}}{1 + bP_{CO_2}}$$

where $k_3 = 2.35 \times 10^{-6}$, $a = 1.3 \times 10^{-4}$, and $b = 4.2$. The investigation showed that increasing the concentration of the reaction product, H_2CO_3, increased the dissolution rate. This indicates that carbonic acid or one of its ionization products, HCO_3^- and CO_3^{2-}, facilitates the dissolution process. If deprotonation of carbonic acid at the mineral surface is the mechanism which facilitates dissolution, then the effectiveness of carbonic acid is approximately 1/100 that of the hydrogen ion.

4) The back reaction rate for strontianite and witherite dissolution is believed to be controlled by adsorption and deprotonation of HCO_3^- at the mineral surface. The back reaction rate for strontianite dissolution approaching equilibrium was calculated using the dissolution rates obtained far from equilibrium. Both first order variables, $(m_{HCO_3^-}{}_s - m_{HCO_3^-}{}_t)$ and $(m_{Sr^{2+}}{}_s - m_{Sr^{2+}}{}_t)$, provided

satisfactory agreement with the calculated back reaction rate; however, the principle of microscopic reversibility and the postulated surface charge suggest that Sr^{2+} is not the rate limiting species for the back reaction.

Suggestions for future research resulting from this investigation are:

1) Future work should utilize material which has been aged in a saturated solution. This should result in the healing of surface defects and the dissolution and reprecipitation of the very fine material. Control of grain size in this study was not adequate to assign specific rate constants based upon calculated surface areas. Microscopic examination of the samples showed that there was significant retention of -200 mesh material which persisted despite the acid wash and distilled water rinses.

2) The role of H_2CO_3 as a general acid catalyst for carbonate mineral dissolution should be reinvestigated and compared with other acids having dissociation constants of about the same value.

3) The role of mineral crystallographic structure could be investigated using calcite and aragonite. The late stage shift to a high order mechanism observed by Plummer (1972) for calcite was not

noted for strontianite or witherite which have the aragonite lattice structure.

4) The kinetic expression

$$dm_{Me}2+/dt = k(a_{H}+_{t} - a_{H}+_{s})^{n}$$

should be investigated further for strontianite and witherite dissolution. Use of equipment similar to that described by Morse (1974) should permit experimental determination of the reaction rate at fixed pH values to within 0.05 units of the equilibrium pH. Such experiments could determine if a family of lines, as used with strontianite and witherite dissolution data, truely represent different dissolution stages with different molecularities or if these lines only represent approximations of the reaction rate.

REFERENCES CITED

Anderson, M. L., and Boyd, R. K., 1971, Nonequilibrium thermodynamics in chemical kinetics: Can. Jour. Chem., v. 49, p. 1001-1007.

Baily, A., and Reesman, A. L., 1971, A survey of the kinetics of wollastonite dissolution in H_2O-CO_2 and buffered systems at 25° C: Am. Jour. Sci., v. 271, p. 464-472.

Barton, P. L., Bethke, P. M., and Toulmin, P., 3rd, 1963, Equilibrium in ore deposits: Min. Soc. Am. Spec. Paper 1, p. 171-185.

Benson, S. W., 1960, The foundations of chemical kinetics: New York, McGraw-Hill, 703 p.

Berner, R. A., 1971, Principles of chemical sedimentology: New York, McGraw-Hill, 240 p.

Berner, R. A., and Morse, J. W., 1974, Dissolution kinetics of calcium carbonate in sea water. IV: Theory of calcite dissolution: Am. Jour. Sci., v. 274, p. 108-134.

Bovington, C. H., and Jones, A. L., 1970a, Tracer study of the kinetics of dissolution of barium sulfate: Trans. Faraday Soc., v. 66, p. 764-768.

_____ 1970b, Tracer study of the kinetics of the dissolution of lead sulfate: Trans. Faraday Soc., v. 66, p. 2088-2091.

Brown, T. H., ms, 1970, Theoretical predictions of equilibria and mass transfer in the system CaO-MgO-SiO_2-H_2O-CO_2-NaCl-HCl: Ph.D. thesis, Northwestern Univ., Evanston, Ill.

Campbell, J. R., and Nancollas, G. H., 1969, The crystallization and dissolution of strontium sulfate in aqueous solution: Jour. Phys. Chem., v. 73, p. 1735-1740.

Carpenter, A. B., and Miller, J. C., 1969, Geochemistry of saline subsurface water, Saline County (Missouri): Chem. Geol., v. 4, p. 135-167.

Denbigh, K., 1966, The principles of chemical equilibrium: Cambridge, Cambridge Univ. Press, 494 p.

Findlay, A., 1951, The phase rule, revised by A. N. Campbell, and N. O. Smith: New York, Dover, 494 p.

Frost, A. A., 1941, Effect of concentration on reaction rate and equilibrium: Jour. Chem. Ed., v. 18, p. 272-274.

Gaines, A. M., and Heffner, J. D., 1973, Dolomitization: A new experimental approach (abs): Geol. Soc. America Abs. with Program, v. 5, no. 7, p. 628.

Gardiner, W. C., Jr., 1969, Rates and mechanisms of chemical reactions: New York, W. A. Benjamin, 284 p.

Garrels, R. M., 1959, Rates of geochemical reactions at low temperatures and pressures: in Ableson, P. H., ed., Researches in geochemistry, v. 1: New York, John Wiley & Sons, p. 25-37.

Garrels, R. M., and Christ, C. L., 1965, Solutions, minerals and equilibria: New York, Harper and Row, 450 p.

Garrels, R. M., and Mackenzie, F. T., 1971, Evolution of sedimentary rocks: New York, W. W. Norton, 397 p.

Garrels, R. M., Thompson, M. E., and Siever, R., 1960, Stability of some carbonates at 25° C and one atmosphere total pressure: Am. Jour. Sci., v. 258, p. 402-418.

de Groot, S. R., and Mazur, P., 1961, Non-equilibrium thermodynamics: Amsterdam, North-Holland Pub. Co., 510 p.

Hammett, L. P., 1970, Physical organic chemistry; reaction rates, equilibria, and mechanisms, 2nd ed.: New York, McGraw-Hill, 420 p.

Helgeson, H. C., 1967, Solution chemistry and metamorphism, in Ableson, P. H., ed., Researches in geochemistry, v. 2: New York, John Wiley & Sons, p. 362-404.

_____ 1968, Evaluation of irreversible reactions in geochemical processes involving minerals and aqueous solutions: I. Thermodynamic relations: Geochim. et Cosmochem. Acta, v. 32, p. 853-877.

_____ 1969, Thermodynamics of hydrothermal systems at elevated temperatures and pressures: Am. Jour. Sci., v. 267, p. 729-804.

_____ 1971, Kinetics of mass transfer among silicates and aqueous solutions: Geochim. et Cosmochim. Acta, v. 35, p. 421-469.

Helgeson, H. C., Garrels, R. M., Mackenzie, F. T., 1969, Evaluation of irreversible reactions in geochemical processes involving minerals and aqueous solutions. II. Applications: Geochim. et Cosmochim. Acta, v. 33, p. 455-481.

Horn, M. K., and Adams, J. A. S., 1966, Computer-derived geochemical balances and element abundances: Geochim. et Cosmochim. Acta, v. 30, p. 279-297.

Klotz, I. M., Chemical thermodynamics: New York, W. A. Benjamin, 468 p.

Lagache, M., Contribution à l'étude de l'altération des feldspaths, dans l'eau, entre 100 et 200°C, sous diverses pressions de CO_2, et application à la synthèse de minéraux angileux: Bull. Soc. Fr. Min. Crystallogr., v. 88, p. 223-253.

Laidler, K. J., 1950, Chemical kinetics: New York, McGraw-Hill, 408 p.

Levenspiel, O., 1972, Chemical reaction engineering, 2nd ed.: New York, John Wiley & Sons, 578 p.

Lewis, G. N., and Randall, M., 1923, Thermodynamics: New York, McGraw-Hill, 653 p.

Little, D. M. S., and Nancollas, G. H., 1970, Kinetics of crystallization and dissolution of lead sulfate in aqueous solution: Trans. Faraday Soc., v. 66, p. 3103-3112.

Liu, S., and Nancollas, G. H., 1971, The kinetics of dissolution of calcium sulfate dihydrate: Jour. Inorg. Nuc. Chem., v. 33, p. 2311-2316.

Luce, R. W., ms, 1969, Dissolution of magnesium silicates: Ph.D. thesis, Stanford Univ., Stanford, Cal.

Maron, S. H., and Prutton, C. F., 1958, Principles of physical chemistry, 3rd ed.: New York, MacMillan, 789 p.

Mitterer, R. M., and Carter, P. W., 1973, Some analytical and experimental results bearing on the precipitation of $CaCO_3$ (abs): Geol. Soc. America Abs. with Programs, v. 5, no. 7, p. 741.

Moelwyn-Hughes, E. A., 1947, The kinetics of reactions in solution, 2nd ed.: Oxford, Oxford Press, 424 p.

Morse, J. W., 1974, Dissolution kinetics of calcium carbonate in sea water. III: A new method for study of carbonate reaction kinetics: Am. Jour. Sci., v. 274, p. 97-107.

Parks, G. A., 1967, Aqueous surface chemistry of oxides and complex oxide minerals. Isoelectric point and zero point of charge, in Gould, R. G., ed., Equilibrium concepts in natural water systems: Washington, D. C., Am. Chem. Soc. Pubs., p. 121-160.

Plummer, L. N., ms, 1972, Rates of mineral-aqueous solution reactions: Ph.D. thesis, Northwestern Univ., Evanston, Ill.

Plummer, L. N., and Mackenzie, F. T., 1974 Predicting mineral solubility from rate data: Application to the dissolution of magnesian calcites: Am. Jour. Sci., v. 274, p. 61-83.

Prigogine, I., 1967, Thermodynamics of irreversible processes, 3rd ed.: New York, Wiley Intersci., 147 p.

Prigogine, I., Outer, P., and Herbo, C., 1948, Affinity and reaction rate close to equilibrium: Jour. Phy. Chem., v. 52, p. 321-331.

Rankama, K., and Sahama, T. G., 1950, Geochemistry: Chicage, Univ. Chicago Press, 912 p.

Robinson, R. A., and Stokes, R. H., 1965, Electrolyte solutions, 2nd ed., revised: London, Butterworths, 571 p.

Sayles, F. L., and Fyfe, W. S., 1973, The crystallization of magnesite from aqueous solution: Geochim. et Cosmochim. Acta, v. 37, p. 87-99.

Sillen, L. G., and Martell, A. E., 1964, Stability constants of metal-ion complexes: London, Chem. Soc., 754 p.

Somasundaran, P., and Agar, G. E., 1967, The zero point of charge of calcite: Jour. Colloid and Interface Sci., v. 24, p. 433-440.

Stumm, W., and Morgan, J. J., 1970, Aquatic chemistry: New York, Wiley Intersci., 583 p.

Walls, R. A., 1973, Dissolution kinetics of incompatible strontium and magnesium in carbonate skeletal material (abs): Geol. Soc. America Abs. with Program, v. 5, nc. 7, p. 854.

Wollast, R., 1967, Kinetics of the alteration of K-feldspar in buffered solutions at low temperature: Geochim. et Cosmochim. Acta, v. 31, p. 635-648.

APPENDIX B. CONSTANTS USED IN PROGRAM CATCALC

Reaction	pK at 30° C	pK at 40° C	pK at 50° C	Reference
$H_2O \rightleftharpoons H^+ + OH^-$	13.883	13.535	13.262	a
$H_2O + CO_{2(g)} \rightleftharpoons H_2CO_3$	1.53	1.64	1.70	a
$H_2CO_3 \rightleftharpoons H^+ + HCO_3^-$	6.33	6.30	6.29	a
$HCO_3^- \rightleftharpoons H^+ + CO_3^{2-}$	10.29	10.22	10.17	a
$SrHCO_3^+ \rightleftharpoons Sr^{2+} + HCO_3^-$	1.20	1.20	1.20	b
$SrCO_3^0 \rightleftharpoons Sr^{2+} + CO_3^{2-}$	3.10	3.10	3.10	b
$SrCO_{3(s)} \rightleftharpoons Sr^{2+} + CO_3^{2-}$	9.37	9.32	9.28	c
$BaHCO_3^+ \rightleftharpoons Ba^{2+} + HCO_3^-$	1.10	1.10	1.10	b
$BaCO_3^0 \rightleftharpoons Ba^{2+} + CO_3^{2-}$	3.00	3.00	3.00	b
$BaCO_{3(s)} \rightleftharpoons Ba^{2+} + CO_3^{2-}$	8.48	8.55	8.62	c

Constant from equation (4) in text	T = 30° C	T = 40° C	T = 50° C	
A	0.5144	0.5244	0.5354	d
B	0.3292×10^{-8}	0.3310×10^{-8}	0.3329×10^{-8}	d
$a_{MeHCO_3^+}$	4.25	4.25	4.25	e

a - Garrels and Christ, 1965.
b - Estimated from data in Sillen and Martell, 1964.
c - Estimated from affinity plots.
d - Helgeson, 1967.
e - Estimated from mean value for HCO_3^- in Klotz, 1964. All other g_i values from Klotz, 1964.

This dissertation is accepted on behalf of the faculty of the Institute by the following committee:

Adviser

5/2/71
Date

```
//AG40FA08 JOB (451300200,W0001,1,4),'SONDEREGG',CLASS=F
//*  096  1840  JS E&WD     00200    CATION CALC          PRODUCTION    F
//  EXEC FORTGCG
//FORT.SYSIN DD *
C
C      PROGRAM CATCALC
C
C      PROGRAM CATCALC WRITTEN BY JOHN SONDEREGGER/NEW MEXICO TECH/1972-3
C      PROGRAM CATCALCIS DESIGNED TO CALCULATE ALL IMPORTANT SPECIES IN
C      SOLUTION FOR THE DISSOLUTION OF ALKALIAN EARTH CARBONATES.
C      THE MASTER VARIABLE FOR THESE CALCULATIONS IS PH
C
C      THIS PROGRAM ALSO CALCULATES CHEMICAL AFFINITY AND
C      THE RATE OF CHANGE OF CONCENTRATION, MOLALITY & ACTIVITY OF
C      THE ALKALAIN EARTH OF INTEREST
C
C      THE DOMINENT REACTION IS:  MECO3 + 2H+  =  ME+2 + H2CO3
C
       REAL*8 TITLE, INAME, KNAME, MNAME, PH
       REAL LGAI(3),LGCI(3),LGAK(4),LGCK(4),LGAM(2),LGCM(2),MECO3,LIAP
       DIMENSION TITLE(8),ACTVTI(3),ACTVTK(4),ACTVTM(2),CONCI(3,2),CONCK(
      14),CONCM(2,2),INAME(3,2),KNAME(4,2),MNAME(2,2),AZEROI(3),AZEROK(4)
      2,AZEROM(2),CHRGI(3),CHRGK(4),TIME(200),PH(200),ZSQI(3),ZSQK(4),
      3ABCHI(3),ABCHK(4),DENOMI(3),DENOMK(4),DECONI(3),CHRGM(2)
      4,ACTCFI(3),ACTCFK(4),ACTCFM(2),CHCONI(3),CHCONK(4),FLOGI(3),
      5FLOGK(4),AFFN(2),ALAMI(3),ALAMK(4),BLAMI(3),BLAMK(4),BLAMM(2)
      6,AML(200)
C
C      ***************************************************************
C
C      I___ OR ___I ARE CATIONIC SPECIES VARIABLES
C      K___ OR ___K ARE ANIONIC SPECIES VARIABLES
C      M___ OR ___M ARE NEUTRAL COMPLEX SPECIES VARIABLES
C      NUMA = NUMBER OF ITERATIONS EMPLOYED
C      NUMB = NUMBER OF DATA POINTS AS INPUT
C      MECO3 = INSTABILITY CONSTANT FOR DISSOCIATION OF THE NEUTRAL
C           SPECIES (ION PAIR) MECO3
C      BETAH = INSTABILITY CONSTANT FOR MEHCO3 COMPLEX
C      AMOL = MOLALITY OF HCL ACID
C      AML = NUMBER OF MILLILITERS OF HYDROCHLORIC ACID ADDED
C      PCO2 = PARTIAL PRESSURE OF CO2 GAS
C      DELTIM = TIME INCREMENT
C      LIAP = ALOG10(ION ACTIVITY PRODUCT)
C      ARG = ALOG10(Q/K)
C      QOK = (IAP/K(EQUILIB.))
C      MENOP = OPTION TO INCLUDE THE MEAN VALUE OF THE REACTION AFFINITY
C         OVER THE REACTION INTERVAL*** IF DESIRED SET MENOP = 1
C
C      ***************************************************************
       READ(5,100)TITLE
       WRITE(6,101)TITLE
       READ(5,131)T, PKW,PK0, PK1, PK2
       WRITE(6,130)T
       TK = T + 273.15
       RT  = (1.9872*TK)/1000.0
       E=0.100000E-30
       WRITE(6,99)
       READ(5,102)(INAME(I,1),INAME(I,2),AZEROI(I),CHRGI(I),BLAMI(I),I=1,
      13)
       WRITE(6,103)(INAME(I,1),INAME(I,2),AZEROI(I),CHRGI(I),BLAMI(I),I=1
      1,3)
       READ(5,102)(KNAME(K,1),KNAME(K,2),AZEROK(K),CHRGK(K),BLAMK(K),K=1,
      14)
       WRITE(6,103)(KNAME(K,1),KNAME(K,2),AZEROK(K),CHRGK(K),BLAMK(K),K=1
```

```
      14)
       WRITE(6,103)(KNAME(K,1),KNAME(K,2),AZEROK(K),CHRGK(K),BLAMK(K),K=1
      1,4)
       READ(5,102)(MNAME(M,1),MNAME(M,2),AZEROM(M),CHRGM(M),BLAMM(M),M=1,
      12)
       WRITE(6,103)(MNAME(M,1),MNAME(M,2),AZEROM(M),CHRGM(M),BLAMM(M),M=1
      1,2)
       WRITE(6,325)
       READ(5,105)AAHAT,ABHAT,XA,XB,MENOP,FUDGE
       WRITE(6,105)AAHAT,ABHAT,XA,XB,MENOP,FUDGE
       READ(5,104)NUMA,NUMB,MECO3,BETAH,PKSP
       READ(5,133)AMOL,PCO2
       WRITE(6,104)NUMA,NUMB,MECO3,BETAH,PKSP,AMOL,PCO2
       WRITE(6,131)T, PKW, PK0, PK1, PK2
C      ***ALL FIXED VARIABLES HAVE BEEN INPUT***
       WRITE(6,325)
       WRITE(6,107)
       DO 500 L=1,NUMB
       READ(5,124)PH(L),TIME(L),AML(L)
       WRITE(6,117)TIME(L),PH(L),AML(L)
  500 CONTINUE
       WRITE(6,325)
       ALCO2 = ALOG10(PCO2)
       DO 610 L=1,NUMB
       DO 501 I=1,3
  501 ACTCFI(I)=1.00000
       DO 502 K=1,4
  502 ACTCFK(K)=1.00000
       ACTCFM(1)=1.00000
       ACTCFM(2)=1.00000
       DO 600 N=1,NUMA
       LGAI(1)=-PH(L)
       LGAM(1)=-PK0+ALCO2
       LGAK(1)=-PKW+PH(L)
       LGAK(2)=LGAM(1)-PK1+PH(L)
       LGAK(3)=LGAK(2)-PK2+PH(L)
       DO 503 K=1,3
       ACTVTK(K)=10.00**LGAK(K)
       CONCK(K)=ACTVTK(K)/ACTCFK(K)
       LGCK(K)=ALOG10(CONCK(K))
  503 CONTINUE
       CONCK(4)=(AMOL*AML(L)*0.001)/(1.000+(AML(L)*0.001))
       CONCK(4)=CONCK(4)+E
       LGCK(4)=ALOG10(CONCK(4))
       ACTVTK(4)=CONCK(4)*ACTCFK(4)
       LGAK(4)=ALOG10(ACTVTK(4))
       SUMA=CONCK(1)+CONCK(2)+2*CONCK(3)+CONCK(4)
       ACTVTI(1)=10.00**LGAI(1)
       CONCI(1,2)=ACTVTI(1)/ACTCFI(1)
       SUMB=SUMA-CONCI(1,2)
       QBALL=LGAK(2)+BETAH
       PBALL=10.00**QBALL
       CRUD=(ACTCFI(2)/ACTCFI(3))*PBALL
       CONCI(2,2)=SUMB/(2.0+CRUD)
       CONCI(3,2)=CONCI(2,2)*CRUD
       ACTVTI(2)=CONCI(2,2)*ACTCFI(2)
       ACTVTI(3)=CONCI(3,2)*ACTCFI(3)
       DO 504 I=1,3
       LGAI(I)=ALOG10(ACTVTI(I))
       LGCI(I)=ALOG10(CONCI(I,2))
  504 CONTINUE
       ACTVTM(1)=10.00**LGAM(1)
       CONCM(1,2)=ACTVTM(1)/ACTCFM(1)
       LGCM(1)=ALOG10(CONCM(1,2))
       LGAM(2)=LGAI(2)+LGAK(3)+MECO3
       ACTVTM(2)=10.00**LGAM(2)
```

```
      ACTVTM(2)=10.00**LGAM(2)
      CONCM(2,2)=ACTVTM(2)/ACTCFM(2)
      LGCM(2)=ALOG10(CONCM(2,2))
      DSUM=0.0
      DO 508 I=1,3
      ZSQI(I)=CHRGI(I)**2
      CHCONI(I)=CONCI(I,2)*ZSQI(I)
  508 DSUM=DSUM+CHCONI(I)
      DO 509 K=1,4
      ZSQK(K)=CHRGK(K)**2
      CHCONK(K)=CONCK(K)*ZSQK(K)
  509 DSUM=DSUM+CHCONK(K)
      BARI=DSUM*0.50
      IF(N .EQ. NUMA) GO TO 600
  511 SQI=SQRT(BARI)
      DO 512 I=1,3
      ABCHI(I)=(-1.00)*AAHAT*ZSQI(I)*SQI
      DENOMI(I)=1.0+(ABHAT*AZEROI(I)*SQI)
      FLOGI(I)=(ABCHI(I)/DENOMI(I))+(0.1)*ZSQI(I)*BARI
      ACTCFI(I)=10.00**FLOGI(I)
  512 CONTINUE
      DO 513 K=1,4
      ABCHK(K)=(-1.00)*AAHAT*ZSQK(K)*SQI
      DENOMK(K)=1.0+(ABHAT*AZEROK(K)*SQI)
      FLOGK(K)=(ABCHK(K)/DENOMK(K))+(0.1)*ZSQK(K)*BARI
      ACTCFK(K)=10.00**FLOGK(K)
  513 CONTINUE
      STOICI=(CONCI(1,2)+4.0*(CONCI(2,2)+CONCI(3,2))+CONCK(1)+CONCI(3,2)
     1+CONCK(2)+4.0*CONCK(4))/2.0+4.0*CONCM(2,2)
      DO 514 M=1,2
      ACTCFM(M)=1.00+(XA*STOICI)+(XB*STOICI**2)
  514 CONTINUE
  600 CONTINUE
      WRITE(6,324)
  601 DELTIM=TIME(L)-TIME(L-1)
      WRITE(6,114)DELTIM
      WRITE(6,116)BARI
      LIAP=LGAI(2)+LGAK(3)
      WRITE(6,121)LIAP
C     KSP SET BELOW
      ARG=LGAI(2)+LGAK(3)+PKSP
      WRITE(6,115)ARG
      QOK=10.00**ARG
      WRITE(6,119)QOK
      AFF=-2.30258*RT*ARG
      WRITE(6,113)TIME(L),AFF
      AFFN(2) = AFF
      IF (MENOP .EQ. 0)GO TO 613
C     MEAN VALUE OF AFFINITY IS USED
      AFFM = (AFFN(2) + AFFN(1))/2.0
      WRITE(6,129)AFFM
  613 CONTINUE
      CONCA=CONCI(2,2)+CONCI(3,2)+CONCM(2,2)
      WRITE(6,118)TIME(L),CONCA
      DO 505 I=1,3
      WRITE(6,110)INAME(I,1),INAME(I,2),ACTCFI(I)
  505 CONTINUE
      DO 506 K=1,4
      WRITE(6,110)KNAME(K,1),KNAME(K,2),ACTCFK(K)
  506 CONTINUE
      DO 507 M=1,2
      WRITE(6,110)MNAME(M,1),MNAME(M,2),ACTCFM(M)
  507 CONTINUE
      WRITE(6,326)
      DO 550 I=1,3
      WRITE(6,109)INAME(I,1),INAME(I,2),CONCI(I,2),LGCI(I),ACTVTI(I),
```

```
      DO 550 I=1,3
      WRITE(6,109)INAME(I,1),INAME(I,2),CONCI(I,2),LGCI(I),ACTVTI(I),
     1LGAI(I)
  550 CONTINUE
      DO 551 K=1,4
      WRITE(6,109)KNAME(K,1),KNAME(K,2),CONCK(K),LGCK(K), ACTVTK(K),
     1LGAK(K)
  551 CONTINUE
      DO 552 M=1,2
      WRITE(6,109)MNAME(M,1),MNAME(M,2),CONCM(M,2),LGCM(M),ACTVTM(M),
     1LGAM(M)
  552 CONTINUE
      IF(L-1)610,610,609
  609 CONTINUE
      WRITE(6,326)
      DO 602 I=1,3
      DECONI(I)=CONCI(I,2)-CONCI(I,1)
      WRITE(6,111)INAME(I,1),INAME(I,2),DECONI(I)
      CONCI(I,1)=CONCI(I,2)
  602 CONTINUE
      DECONM=CONCM(2,2)-CONCM(2,1)
      WRITE(6,111)MNAME(2,1),MNAME(2,2),DECONM
      DECA=DECONI(2)+DECONI(3)+DECONM
      DERIV=DECA/DELTIM
      WRITE(6,112)DERIV
      ZAT = DECONI(2)/DELTIM
      WRITE(6,128)ZAT
      ZAP=DECONI(2)*ACTCFI(2)
      ZAB=ZAP/DELTIM
      WRITE(6,122)ZAB
      CONCM(2,1) = CONCM(2,2)
      AFFN(1) = AFFN(2)
  610 CONTINUE
C     ***FORMATS***
   99 FORMAT(//'0',33X,'COMPONENT',19X,'AZERO',15X,'CHRG',/)
  100 FORMAT(8A8)
  101 FORMAT(30X,8A8)
  102 FORMAT(A8,A7,2F10.2,F10.4)
  103 FORMAT(31X,A8,A7,10X,F10.2,10X,F10.2,10X,F10.4)
  104 FORMAT(2(7X,I3),2F10.2,3F10.4)
  105 FORMAT(4F10.4,I5,F10.3)
  106 FORMAT(F10.5,F5.0)
  107 FORMAT(' ',36X,'TIME',12X,'PH',9X,'AML',/,37X,'____',12X,'__',
     19X,'___',/)
  108 FORMAT(/'0','ITERATION NO.',I3,'  COMPLETED',/)
  109 FORMAT(' ',10X,A8,A7,'CONC=',E14.6,5X,'LOG=',E15.6,4X,'ACTIVITY=',
     1E14.6,5X,'LOG=',E14.6)
  110 FORMAT(' ',10X,A8,A7,5X,'ACTIVITY COEFFICIENT =',F8.5)
  111 FORMAT(' ',10X,A8,A7,5X,'DECONI =',E13.6)
  112 FORMAT(//,' ',30X,'DC CA/DT =',E13.6,'MOLES/MIN.')
  113 FORMAT(/ ' ',30X,'THE AFFINITY AT ',F7.1 , '  MINUTES IS',E13.6,
     1'  KILOCALORIES',/ )
  114 FORMAT(/' ',30X,'DELTA TIME =',F7.1 ,'  MINUTES',/)
  115 FORMAT(/' ',30X,'ARG =',E13.6,/)
  116 FORMAT(/' ',30X,'TRUE IONIC STRENGTH =',E13.6,/)
  117 FORMAT(' ',30X,F10.1,5X,F10.3,5X,F10.5)
  118 FORMAT(/' ',30X,'AT',F7.1 ,'  MINUTES, TOTAL ME =',E13.6,'  M/L',/
     1)
  119 FORMAT(/' ',30X,'QOK =',E13.6,/)
  121 FORMAT(/ ' ',30X,'LIAP =',E13.6,/)
  122 FORMAT(/,' ',30X,'DA(ME++)/DT =',E13.6,/)
  124 FORMAT(5X,F5.3,2X,F10.1,F10.2)
  128 FORMAT(/,' ',30X,'DM(ME++)/DT =',E13.6)
  129 FORMAT(' ',30X,'MEAN AFFINITY OVER TIME INTERVAL IS',E13.6,' KILOC
     1ALORIES',/)
  130 FORMAT(//' ',30X,'THE TEMPERATURE IS',F6.2,' DEGREES CENTIGRADE')
```

```
  325 FORMAT(/1X,100('+'),//)
  326 FORMAT(' ',100('+'),/)
      STOP
      END
/*
//GO.SYSIN DD *
```